Characterization of the association of Dbf4 and Cdc7 with Mcm2-7 and chromatin in *Saccharomyces cerevisiae*.

by

Matthew D. Ramer

A thesis

presented to the University of Waterloo

in fulfillment of the

thesis requirement for the degree of

Doctor of Philosophy

in

Biology

Waterloo, Ontario, Canada, 2011

Author’s Declaration

I hereby declare that I am the sole author of this thesis. This is a true copy of the thesis, including any required final revisions, as accepted by my examiners.

I understand that my thesis may be made electronically available to the public.

Abstract

Initiation of DNA replication requires the action of the Dbf4/Cdc7 kinase complex (DDK) which is also a phosphorylation target of Rad53 kinase in the S-phase checkpoint. DDK is thought to trigger DNA replication by phosphorylating members of the Mcm2-7 complex present at origins of replication. While DDK phosphorylation sites have been identified on Mcm2-7, the contributions made by Dbf4 and Cdc7 to the targeting of the complex have not been established. DDK has also been implicated in the S-phase checkpoint response since it is removed from chromatin in a Rad53-dependent manner.

The interaction of Dbf4 and Cdc7 with each of the Mcm2-7 subunits was assessed and showed an interaction between Dbf4 and Mcm2 and Mcm6, while interactions between Cdc7 and Mcm4 and Mcm5 were observed. Mutations in Mcm2 and Mcm4 that disrupt the interactions with Dbf4 or Cdc7 showed modest growth impairment and compromised DNA replication, while simultaneous abrogation of both interactions resulted in lethality. Strains overexpressing Mcm2 or Mcm4 were sensitive to genotoxic agents, while overexpression of Mcm2 in a Mcm4Δ175-333 strain background resulted in a severe growth impairment as well as sensitivity to genotoxic stress. ChIP analysis revealed the possibility of Dbf4/Cdc7 localization to origin flanking regions through most of S-phase, which may redistribute to origins at the time of firing.

Fluorescence microscopy of Mcm2 and Dbf4 in S-phase seem to show a punctate pattern of staining, consistent with these factors' localization to 'replication factories.' By using a Dbf4ΔN mutant, the N-motif was shown to be required for the Rad53-mediated removal of Dbf4 from chromatin under checkpoint conditions. Initial optimization of a

DNA combing protocol was also performed, which along with Dbf4ΔN mutant and the fluorescently-epitope tagged strains, will be useful tools for evaluating a role for DDK in the S-phase checkpoint response.

Altered levels of DNA replication factors have been implicated in many human cancers. The data presented in this study provide novel insight into the normal process of the initiation of DNA replication which can be applied to research involving higher eukaryotes, including humans, and can serve as a benchmark for comparison with the cancer phenotype.

Acknowledgments

I must begin by thanking my supervisor, Dr. Bernie Duncker. I have greatly appreciated the opportunity to work in your lab and your guidance over the course of my time here. I think I have come a long way since that quiet and nervous 1st-year undergrad more than 10 years ago, and that, I believe, is due to your supervision and direction. I have valued your advice and help in my many 'tours' on Duncker Island and I thank you for continuing to invite me back! Thank you also to Dr. Barb Moffatt and Dr. Trevor Charles for serving as my committee members; your support and encouragement over the years has been extremely helpful in navigating this project.

Thank you to Dr. Grant Brown for your interest and enthusiasm for the DNA combing collaboration and for being fun to hang out with at conferences. Special thanks to Jay Yang and Johnny Tkach for going out of your way to help with the combing experiments – you were always helpful and attentive no matter how busy you were. Thank you to Dr. Megan Davey for the original plasmid shuffle strains and vectors and a special thanks to Brent Stead for your help in making sense of the cloning involved in the shuffle vectors – you were always willing to answer my many emails!

Thank you to all the former members of the lab who have helped me throughout the years: Jeff, Lance, Ajai, and Michelle. Each of your expertise and advice saved me much time and headache and greatly appreciated my friendship with each of you – you each helped to make the lab a place that I wanted to come to each day in those first years. A special thank you to Jess – I greatly appreciated your help managing the timecourses and more importantly you became a good friend, thank you. A special thank you to 'The Germans' – Martina, Nicole, and Hagen and to Karen for your contributions to this

thesis. Of course Darryl and Rohan. What can I say? It's been a pleasure gentlemen. Darryl you were my go-to guy for technical questions thanks for helping make the science go smoother and for all the entertainment in the lab. Rohan...you are too school for cool. It's been fun travelling this journey with you. We'll always have Princeton.

Non-lab members have also played a key role in getting me through these last years. Laura Dindia, thank you for the brainstorming and our chats about other random stuff. I looked forward to our chats each day, and I will miss 'coffee with Laura.' And of course Erin Spicer, my friend, my sounding board. Thank you for your advice, your calmness, your deadlines, and your organization. I would like to think that some of your drive, discipline, and focus have rubbed off on me. I truly value our friendship.

My family. Thank you to my parents Mary Kay and Dave – you have supported me my entire life, taught me the value of education, and were there for all the exciting and trying times especially in the last few years. Thank you for your support (financially and emotionally!) You are my models for life and for parenting and I love you very much. To the Kuhlmann's and the Miller-Cushon's – thank you for taking care of me through the years. Guillaume, Isabelle, and Ian thank you for your friendship – we need to get together for beer and Settlers.

And finally, thank you to my wife Tanya and my wonderful children William and Emma for putting up with all the late nights and weekends, the stress and the frustration. Your patience, support, and love have been sustained me and I don't know where I would be without you. I love you very much.

Table of Contents

List of Tables

Chapter 2

List of Figures

Chapter 1

Chapter 3

Chapter 4

Chapter 5

List of Abbreviations and Acronyms

ACS – ARS Consensus Sequence

APC/C – Anaphase promoting complex

ARS – Autonomously Replicating Sequence

Cdc – Cell Division Cycle

CDK – Cyclin Dependent Kinase

ChIP – Chromatin Immunoprecipitation

CldU – 5-Chloro-2'-deoxyuridine

Co-IP – Coimmunoprecipitation

DDK – Dbf4-Dependent Kinase

dH_2O – distilled water

DNA – Deoxyribonucleic Acid

dNTP – deoxynucleotide phosphate

DTT – Dithiothreitol

eCFP – Enhanced Cyan Fluorescent Protein

EDTA – Ethylenediaminetetraacetic acid

eYFP – Enhanced Yellow Fluorescent Protein

For – Forward

FACS – Fluorescence Activated Cell Sorting

5' FOA – 5-Fluoroorotic Acid

GAL/RAF – Galactose/Raffinose

GINS – Go-Ichi-Ni-San

HA – Hemagglutinin

HU – Hydroxyurea

IdU – 5-Iodo-2’deoxyuridine

IPTG – Isopropyl β-D-1-thiogalactopyranoside

kb – kilobases

kDa – kilodalton

LEU - Leucine

MCM – Minichromosome Maintenance

MMS – Metheylmethane sulfonate

NLS – Nuclear Localization Signal

ONPG – 2-Nitrophenyl-β-D-galactopyranoside

ORC – Origin Recognition Complex

PCR – Polymerase Chain Reaction

PMSF – Phenylmethylsulphonyl fluoride

Pre-RC – Pre-replicative Complex

Rev – Reverse

RPA – Replication Protein A

SC – Synthetic Complete

SDS – Sodium Dodecyl Sulfate

URA – Uracil

WCE – Whole Cell Extract

WT – Wild-type

YPD – Yeast Extract/Peptone/Dextrose

Chapter 1: Literature Review and Project Goals

1.1 Why use yeast?

1.1.1 Yeast as a Model Organism

Yeasts are found throughout the world in many diverse habitats including aquatic, terrestrial as well as aerial environments. They are non-photosynthetic (since they lack chlorophyll) and are therefore chemoorganotrophic, meaning they require fixed organic carbon sources. Since carbon sources vary depending on the habitat – such as those on the surfaces of plants, in the digestive tracts of animals, or in soil – different yeasts have adapted to occupy distinct environmental niches (Walker, 1998). Yeast can be generally described as a single-celled fungus; but perhaps more usefully the yeasts are categorized into subdivisions based on characteristics of their capacity for sexual reproduction (in the case of *Ascomycotina* and *Basidiomycotina*) or lack thereof (in the case of *Deuteromycotina*, Walker, 1998). The budding yeast *Saccharomyces cerevisiae* – commonly known as baker's or brewer's yeast – is a member of the *Saccharomycetaceae* family of the *Ascomycotina* subdivision and is the organism in which the experiments presented in this thesis were carried out. The 'budding' denomination describes the asexual reproduction of these cells – namely by the formation of a small bud that grows in size and eventually pinches off from the mother cell forming the new daughter cell (see *The Cell Cycle* below). This is in contrast to fission yeast – such as *Schizosaccharomyces pombe* – which divides asexually by transverse binary fission (reviewed in Walker, 1998).

S. cerevisiae has been husbanded for more than 5000 years as a key fermenter in brewing and wine making. Molecular evidence places this yeast strain in pottery jars dating to one of the earliest Egyptian kings (Scorpion I circa 3150 BCE, Cavalieri *et al*.,

2003). More recently, nearly all laboratory stocks of *S. cerevisiae* have originated from stocks that early yeast researchers Øjvind Winge and Carl Lindegren distributed throughout the yeast research world. One of the most common strain backgrounds (and the one used for many of the experiments in my project) – S288C – was derived from an original strain called EM93, and was originally isolated from rotting figs (Mortimer and Johnston, 1986).

Typically ellipsoid in shape, *S. cerevisiae* diploid cells can vary from 2 to 50 µm in length and from 1 to 10 µm in diameter, although more commonly diploid cells measure 5 by 6 µm, while the more spherical haploid cells are 4 µm in diameter. Given these different dimensions, cell volumes are typically larger in diploid as compared to haploid cells (reviewed in Walker, 1998). Comprehensive descriptions of the cytology (cellular anatomy) of yeast cells have been compiled (Kockova-Kratochvilova, 1990; Rose and Harrison, 1991). Briefly, as with all eukaryotes, *S. cerevisiae* has a nucleus that contains the genomic content of the cell, as well as other membrane-bound organelles such as mitochondria, peroxisomes, endoplasmic reticulum, and vacuoles. There are two important features that distinguish *S. cerevisiae* from other typical eukaryotic cells. First, *S. cerevisiae* cells are encapsulated in a 100 to 200 nm thick cell wall that helps to maintain the cells' shape, offers protection, and is the site of interaction between the cell and its environment. Second, unlike most other eukaryotic cells, the nuclear membrane remains intact during mitosis as the nucleus pinches in half and one of the 'daughter nuclei' migrates to the bud (reviewed in Walker, 1998).

Model organisms are useful biological tools in elucidating the details of a pathway or process of interest when experimentation in more complex organisms – such as

humans – is logistically or ethically unfeasible. There are a number of practical advantages that *S. cerevisiae* offers as a model organism (reviewed in Ostergaard *et al.*, 2000; Sherman, 2002); first, *S. cerevisiae* is relatively non-pathogenic. It has 'generally recognized as safe' (GRAS) status and apart from the remote potential of it being an opportunistic pathogen, it is quite innocuous (Dickinson, 1999). Thus, few special precautions need be taken to prevent contamination or infection beyond aseptic technique and basic hygiene. Yeast cultures grow quickly (a shaking liquid culture at 30°C of wild-type cells doubling in approximately 90-100 minutes) meaning that over the course of a single day a culture can grow sufficiently to supply an adequate number of cells for an experiment. A third advantage is that *S. cerevisiae* has a versatile DNA transformation system. Yeast cells efficiently take up both circular plasmids (which can express a gene of interest), as well as linear DNA fragments and can be either maintained through the choice of selective media (in the case of plasmids) or incorporated into the genome (in the case of linear DNA) through a relatively simple single-step homologous recombination event (Longtine *et al.*, 1998). Genetic manipulation is also comparatively straightforward in *S. cerevisiae* and since the sequencing of its genome in 1996 researchers have this invaluable information when making changes to the genome. For example, the modification of a gene by the addition of the sequence for an epitope tag (such as myelocytomatosis [Myc] or hemagglutinin [HA]), creates a fusion protein. This is especially useful when trying to detect low abundance proteins or proteins for which there is no good commercially available antibody. Since the anti-Myc and –HA antibodies produce quite robust interactions with their corresponding epitope allowing for easier isolation of the protein through immunoprecipitation or its imaging on a western

blot. Another useful construct fuses the sequence coding for a fluorescent epitope to a gene of interest allowing proteins to be imaged in living cells using fluorescent microscopy.

It is sometimes desirable to be able to control the timing of a gene's expression and in *S. cerevisiae,* it is possible to replace an endogenous promoter through homologous recombination to do just that. A commonly used promoter is the *GAL1* promoter, which is a galactose inducible promoter, that allows the researcher to turn gene expression on or off by simply including or excluding, respectively, galactose from the growth medium. Due to the interest of researchers in using *S. cerevisiae* as a model organism, there are a variety of commercially available strains that have been genetically modified to allow easier exploration of gene products and cellular processes, including epitope-tagged proteins, deletion libraries (where a different single gene is deleted from each strain), promoter swaps (which allow genes of interest to be switched on or off), and strains containing temperature-sensitive mutations (where a gene product's function is compromised when the strain is grown at a restrictive temperature). Since much of the cellular machinery, DNA replication factors, and cell division mechanisms are similar between yeast and other eukaryotic organisms including humans, *S. cerevisiae* is perfectly placed to serve as a valuable tool for the exploration of DNA replication as it relates to human diseases including cancer (see section *1.5 Importance for cancer research* below).

1.1.2 Yeast Genetics

A haploid *S. cerevisiae* cell's DNA is organized into 16 chromosomes ranging from 230 to 1532 kilobase pairs (Kb) in size. The complete sequence of all 12,071 Kb chromosomal DNA was released in 1996 and was the first eukaryote to have its genome completely sequenced (Goffeau, *et al.*, 1996). Relative to other eukaryotes, the genome of *S. cerevisiae* is small and yet is highly compact with more than 70% of the genomic sequence coding for genes (Sherman, 2002). Currently, 6607 open reading frames (ORFs) have been proposed, of which 4941 (75%) have been verified as sequence encoding for a protein. Of the remaining ORFs, 857 (13%) have yet to be characterized while 809 (12%) are considered 'dubious' meaning that they may not be true ORFs (Saccharomyces Genome Database, 2011). Since only about 4% of genes contain introns, the cloning and manipulation of most genes is much less complicated than for other eukaryotes and can usually be accomplished in a single PCR amplification from a genomic DNA template.

An important, often overlooked, consideration is that most lab strains that are considered 'normal' in fact have mutations in or deletions of certain metabolic genes typically required for amino acid production. One such example is the mutation or deletion of the *URA3* gene. *URA3* encodes orotidine 5-phosphate decarboxylase (ODCase), which catalyzes the sixth step in the pathway of *de novo* synthesis of pyrimidine ribonucleotides (namely the decarboxylation of orotidine 5-phosphate to uridylic acid, Saccharomyces Genome Database, 2011). In a cell that is *ura3-1* or *ura3Δ0*, there is no functional copy of *URA3*, meaning that the cell cannot synthesize pyrimidines *de novo*; therefore, uracil must be supplied in the media in order for the cells

to grow and divide. This allows for the selection of cells that have been transformed with DNA containing the wild-type *URA3* gene by simply leaving uracil out of the growth medium.

In order to better understand the genetic modifications that have been made in the following experiments, a discussion of the conventional genetic nomenclature of *S. cerevisiae* is warranted. Unlike some other model organisms, such as *Drosophila*, genetic nomenclature in yeast usually reflects characteristics of the gene being described with the dominant allele being written as three capitalized italicized letters (for example *URA*). The three-letter gene designation is followed by a number that identifies the locus of that allele (e.g. *URA3*). In haploid strains where there is a single copy of a recessive allele, it is denoted by lower-case italics; for example *ura3*, indicates a uracil requirement. Specific alleles or allele-specific mutations, including temperature-sensitive mutations, are designated by a number separated from the locus number by a hyphen (e.g. *ura3-1*). Partial or complete deletion of a gene is indicated using the symbol Δ (e.g. *ura3*-Δ*1*). The insertion of one gene at the locus of another (causing inactivation of the second gene) is denoted by the symbol :: (e.g. *ura3*::*LEU2*, which indicates that a functional *LEU2* gene has been inserted at the *ura3* locus, which was or became nonfunctional).

1.2 The Cell Cycle

1.2.1 Overview

As alluded to above, *S. cerevisiae* can exist stably in both a haploid or diploid state and can maintain these states throughout mitosis. The life cycle of *S. cerevisiae* can be organized into two categories: growth and mitotic division producing identical daughter

cells, and a change in ploidy resulting from mating of haploid cells or sporulation of diploid cells (reviewed in Herskowitz, 1988). Growth and mitotic division will be considered first followed by the mating and sporulation aspects of yeast sexual reproduction.

The cell cycle is a highly conserved process in eukaryotic systems and the yeast mitotic cell cycle is no exception – it consists of the ongoing events of cell growth punctuated by the periodic events of DNA synthesis and mitosis. These events are organized into four phases: Gap1 (G1), Synthesis (S), Gap2 (G2), and Mitosis (which includes cytokinesis), each of which are discussed below. 'Landmarks' are tools for determining cell cycle progression and *S. cerevisiae* morphology offers useful markers to judge the cell cycle stage of a yeast cell. Hartwell (1974) first described this link between cell morphology and the cell cycle showing, for example, that cells with small buds correspond to early S-phase (Figure 1.1).

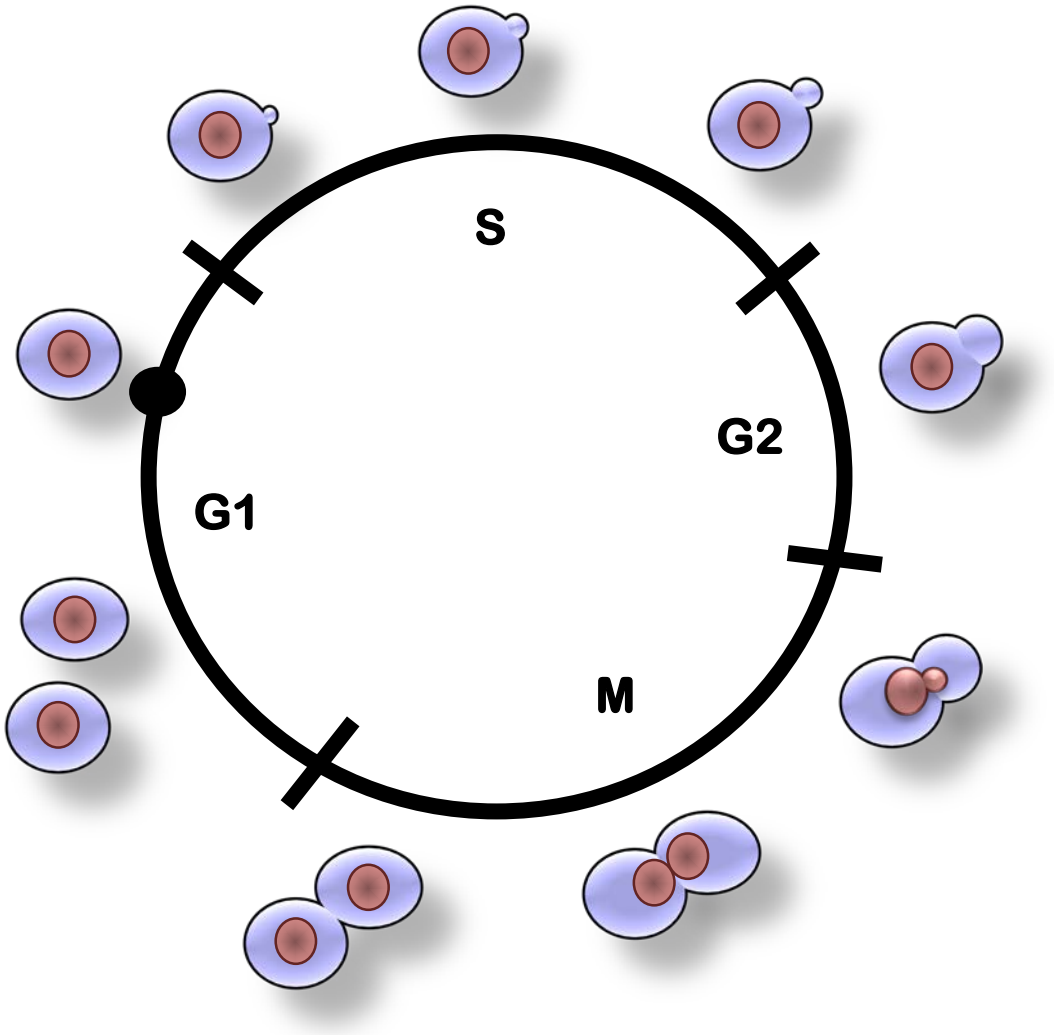

Figure 1.1: The *Saccharomycese cerevisiae* cell cycle. A schematic representation of the budding yeast cell cycle including the formation of a daughter bud. The red areas represent the nucleus while the black circle in G1-phase represents START (Adapted from Herskowitz, 1988).

1.2.2 G1-phase

Following cytokinesis, the cell enters a period of growth during which normal cellular processes are carried out including RNA synthesis and protein production. The longest of the *S. cerevisiae* cell cycle phases, G1 allows the cell time to grow large enough to proceed to the next phase of the cycle. Cell volume is linked to progression through G1-phase as only cells that have attained a 'threshold' size at the decision point called START can initiate DNA synthesis (Hartwell *et al.*, 1974). START is a crucial period in G1 phase where the cell 'decides' whether conditions are favourable for progression into S-phase and mitotic replication. Should external factors such as nutrient availability, temperature, or the presence of exogenous compounds favour growth, the cell can pass START and begin DNA replication. Thus growth is a limiting factor in the progression of the cell cycle. Once a cell has passed START it is irrevocably committed to completing the cell cycle, ultimately culminating in mitosis. Should a cell reach START and find that the external conditions do not favour division, it can enter a stationary phase (G0) where it remains viable, but no longer grows or divides. When conditions have once again become favourable, the cell can exit G0 and resume its progression through the cell cycle. A third 'decision' that a haploid cell can take prior to START is to undergo sexual reproduction by mating with a cell of the opposite mating type, if present. The resulting diploid cell can then either continue progressing through the cell cycle, or undergo meiosis and sporulate depending on the environmental conditions.

G1 phase is also the period when preparations are made on a molecular level for the beginning of DNA replication; namely, the assembly of the pre-replicative complex (pre-RC) at origins of DNA replication. The pre-RC is composed of a number of complexes

and factors that are required for the initiation of DNA replication. Once assembled, the origin is said to be 'licensed' for replication and awaits activation which begins DNA replication and signals the progression from G1- to S-phase. The details of the formation of the pre-RC as well as its role in the initiation of DNA replication will be discussed in detail in the *Initiation of DNA Replication* section of this chapter.

1.2.3 S-phase

In order for both the mother and the daughter cell to contain a complete genomic complement following mitosis, a cell must produce an accurate copy of its genome. It is during the synthesis phase (S-phase) of the cell cycle in which replication of the DNA takes place. The G1-S transition is marked morphologically by the appearance of a small bud and molecularly by the formation of active replication forks from the previously assembled pre-RCs. Following the activation of the replicative helicase at the origin of replication (Mcm2-7 complex, discussed in section *1.3 The Initiation of DNA Replication*), the DNA double helix is unwound bi-directionally generating two single strands of DNA bounded by two Y-shaped replication forks forming a replication bubble (reviewed in Sclafani and Holzen, 2007). In order to prevent re-annealing of the newly unwound strands, single-stranded DNA binding proteins (called RPA in yeast) bind to the exposed base pairs, preventing their re-association (discussed in Forsburg, 2008). A byproduct of helicase unwinding is the accumulation of tension downstream of the replication fork. If this tension is left unchecked, the DNA forms supercoiled structures, which are much more difficult for the replication machinery to process. Fortunately, the cell remedies this problem through the action of topoisomerases (specifically

topoisomerase II) which nick the DNA ahead of the replication fork thus relieving the tension (MacNeill, 2001).

As the DNA is unwound, the two complementary sequence strands are exposed and serve as the template for replication. Duplication of the DNA sequence takes place at the replication forks and relies on the action of a number of complexes and factors, including a number of DNA polymerases, to ensure fidelity in the duplication process. The first of these factors to bind is DNA polymerase α-primase. This enzyme binds to the exposed DNA sequence and synthesizes short complementary RNA sequences that act as primers or starting points for the addition of nucleotides; these primers are eventually elongated by the polymerase, effecting DNA replication.

DNA polymerase can only synthesize DNA in a 5' to 3' direction. Because only one of the strands is in the 5' to 3' orientation (the other one being in the 3' to 5' direction), there is a different method of DNA synthesis to effect replication of the other strand. Once the DNA polymerase α-primase has generated a primer on the leading strand, the term given to the 3' to 5' oriented strand, new DNA is typically synthesized by polymerase ε, which can continue uninterrupted in the direction that the fork is moving (Garg and Burgers, 2005).

DNA synthesis on the lagging strand (oriented 5' to 3') is somewhat more complicated. The polymerase α-primase must wait until the replication fork has progressed a sufficient distance from the origin before it can bind and synthesize the RNA primer. Once the primer has annealed, proliferating cell nuclear antigen (PCNA) is loaded onto the DNA. PCNA causes polymerase α-primase to dissociate and is involved in recruiting polymerase δ, which in turn, is responsible for elongating the primer.

Because nucleotides can only be added in a 5' to 3' direction, the direction of lagging strand elongation is in the opposite direction from which the fork is moving (i.e. back toward the origin of replication). As the replication fork advances and new stretches of single-stranded DNA are exposed, polymerase α-primase is required to generate a new primer before elongation can begin. This so called semi-discontinuous form of replication generates short 100-200 base pair fragments called Okazaki fragments. These fragments are eventually linked together to form a continuous DNA strand in a process called ligation. Prior to this ligation however, the RNA primer present in each Okazaki fragment must be removed; this is accomplished through the concerted action of the FEN1 complex and polymerase δ. The RNA primer is removed and replaced with nucleotides, and the strands are then ligated together by DNA ligase I forming a continuous DNA strand (reviewed in Garg and Burgers, 2005).

The fact that eukaryotic chromosomes are linear presents a problem for DNA synthesis of the lagging strand. Because the primer of the Okazaki fragment is removed following elongation and because DNA is only synthesized in the 5' to 3' direction, there would be no place to allow synthesis of the region corresponding to the primer. Therefore, an unreplicated sequence of the template strand may result at the end of a chromosome; this region would be quickly degraded resulting in loss of genetic information. Obviously this is an untenable situation for the cell, and Blackburn *et al.* (1985) elucidated the mechanism by which the cell solves this problem. Telomeres are highly repetitive sequences of non-coding DNA found at the ends of chromosomes. These telomeres act as caps, allowing the cell to recognize chromosome ends as distinct from double-stranded chromosome breaks, thus preventing one chromosome from being

ligated to another. Replication of telomeres is performed by a ribonucleoprotein reverse transcriptase called telomerase. This enzyme binds to the extreme ends of chromosomes where it adds extra sequence. The addition of this sequence allows polymerase α-primase to generate a primer, which is then elongated. The primer is then removed along with the added sequence, restoring the telomere to its original length (reviewed in Chan and Blackburn, 2003).

1.2.4 G2-phase

Following duplication of its genome, the yeast cell and the bud continue to grow in volume. Also during this period, the DNA is monitored for errors or mutations that, without correction, would be passed on to succeeding generations during mitosis. Due to the rapid progression from DNA replication to chromosome segregation it has been suggested that *S. cerevisiae* does not have a true G2-phase, however another landmark described by Hartwell (1974) marks the end of this phase, namely the migration of the nucleus to the bud neck where nuclear division will take place (Nurse, 1997).

1.2.5 Mitosis and Cytokinesis

As the cell cycle progresses, it becomes incumbent upon the cell to partition the duplicated DNA between the mother and the daughter cell, ensuring that both cells contain a complete copy of the genome. Mitosis is an ordered, continuous set of events typically divided into six phases: prophase, prometaphase, metaphase, early anaphase, anaphase, and telophase (Lebedeva *et al*., 2004).

The migration of the nucleus to the bud neck, where it will remain throughout mitosis, along with the organization of the chromosomes along the nuclear axis between the mother and daughter cells is accomplished through the action of microtubules. Microtubules are organized by the spindle pole bodies, which are the yeast equivalent of centrosomes. One of these spindle pole bodies remains in the mother cell, while the other migrates into the bud where it remains. A discrete region of each chromosome called the kinetochore, binds to the microtubules facilitating chromosome movement to the nuclear equator. Following the organization of the chromosomes in metaphase, the anaphase promoting complex/cyclosome (APC/C) mediates the progression into anaphase. APC/C is a multi-subunit complex involved in both the regulation of mitotic progression via proteolytic degradation of key cyclins (see section 1.2.6 *Control of the cell cycle* below), as well as indirectly in the separation of sister chromatids via an associated protein called Cdc20. Essentially, once APC/C is activated, Cdc20 ubiquitinates securin targeting it for APC/C-mediated degradation. This degradation leads to the activation of the protease Separase, which cleaves the cohesin complex ring that connects the sister chromatids to one another. Once separated, the sister chromatids migrate to the opposite spindle poles via elongation of the microtubules (reviewed in Pesin and Orr-Weaver, 2008). As these chromosomal events are taking place during anaphase, the nucleus begins a conformational change to a dumbbell configuration before it undergoes fission generating a separate nucleus (each containing the complete nuclear content) for each cell. As mentioned, unlike other eukaryotes, the nuclear membrane remains intact throughout this process in budding yeast (reviewed in Winey and O'Toole, 2001).

The final stage of cell division, called cytokinesis, is the complete separation of the mother and daughter cell. The main event in this process, again regulated by APC/C, is the formation of an actinomysin contractile ring and septum at the bud neck, which physically separates the mother and daughter cells (Corbett *et al*., 2006).

1.2.6 Control of the Cell Cycle

A cell must have the ability to control the progression of the cell cycle in order to ensure proper transition from one stage to another. This control is exerted through the action of protein factors called cyclins (reviewed in Kelly and Brown, 2000; Zou and Stillman, 2000, Nguyen *et al*., 2001). When present, cyclins activate specific kinases called cyclin-dependent kinases (CDKs), which regulate the cell cycle via specific phosphorylation events. Another type of kinase important for cell cycle control is Cdc7, which is regulated by an unstable protein called Dbf4. The model whereby Dbf4 acts as Cdc7's cyclin has been confirmed in many eukaryotes, and has led to Cdc7 being referred to as the DDK (Dbf4-dependent kinase; Nasmyth, 1996; Sclafani, 2000). While kinase levels are relatively constant, cyclin levels fluctuate throughout the cell cycle and different cyclins are expressed at different points; for example G1-phase cyclins as compared to S-phase cyclins. These cyclins ensure that cell cycle events take place at the proper time. Thus modulation of the concentration of the regulatory units (i.e. cyclins and Dbf4) is the mechanism by which control of CDKs and DDK is maintained. Gene transcription of the regulatory subunits is upregulated at the correct time in the cell cycle allowing appropriate levels of the active kinase to perform its phosphorylation function. When CDK or DDK action is no longer required, transcription is reduced and the subunit can be

degraded or compartmentalized away from the kinase, thus inactivating it. Specific inhibitors also play a role in the regulation of CDKs; for example, during early G1-phase Sic1 inhibits CDK activity preventing initiation of DNA replication at assembled pre-RCs (see section *1.3.3 Formation of the pre-replicative complex* below). In this case, for the cell to progress into S-phase, Sic1 must be degraded (Lengronne and Schwob, 2002).

1.2.7 Sexual Reproduction

The second aspect of the *S. cerevisiae* life cycle is its ability to change ploidy and stably maintain that ploidy through successive cell cycles (Figure 1.2). Under starvation conditions, diploid cells can undergo meiosis and sporulation resulting in a sac (ascus) containing four haploid spores; should growth conditions again become favourable, the spores can resume the normal cell cycle as haploid cells. Haploid cells can exist as one of two mating types – MATa or MATα and two cells of the opposite mating type can conjugate forming a diploid cell (reviewed in Landry *et al*., 2006). Cells of both mating types produce and secrete signaling molecules called pheromones, which bind to surface receptors found on cells of the opposite type. For example, MATα cells produce the pheromone α-factor, which binds to receptors on MATa cells leading to activation of the mating response pathway (reviewed in Bardwell, 2005). One consequence of this pathway is the arrest of the cell in late G1-phase just prior to the START decision point; this feature of the mating response is a useful tool in the lab and is discussed in section 1.2.8 below.

The mating response pathway also causes a morphological change in the cell that facilitates cell fusion during mating; the cells take on a distinctive pear shape often

referred to as a ‘shmoo’. When two shmoos fuse, conjugation takes place with the nuclei also fusing thus generating a zygote, which can then divide mitotically forming diploid cells.

1.2.8 Synchronizing Yeast Cultures

Because most experiments are performed on a large cell population, it is often important to ensure that all of the cells in a culture are at the same point in the cell cycle in order that a sample be representative of that specific point, rather than a mixture of different cell cycle intervals. A number of protocols and agents have been developed to arrest cells at different points in the cell cycle, but it is important to note that once the arresting agent has been removed, the culture will not remain synchronous for very long. This is because haploid mother cells tend to divide more quickly than daughter cells leading to a loss of the synchronicity of the culture after about two generations (Hartwell, 1974). In this project, the two arresting agents used for blocking cultures are α-factor and hydroxyurea (HU).

As mentioned, α-factor causes MATa cells to arrest in late G1-phase, prior to START. At this point in the cell cycle pre-RCs have formed with the Mcm2-7 complex being chromatin associated and the origins of replication licensed, awaiting CDK and DDK action for progression into S-phase. α-factor is an ideal arresting agent for exploring factors and interactions during S-phase, because once the pheromone is removed, cultures reliably and synchronously release from the block within 15-30 minutes.

Hydroxyurea (HU) reduces the pool of ribonucleotides that are available for incorporation during DNA elongation by inhibiting the action of ribonucleotide reductase, an enzyme that is crucial for the formation of dNTPs (Koc and Merril, 2007). Cultures treated with HU will begin S-phase as early origins will fire, but the cells will rapidly use up the pool of dNTPs causing the replication forks to stall. Recent evidence suggests that rather than a true S-phase arrest, HU actually causes an extremely slow progression since replication forks continue to migrate at a very slow rate. (Alvino *et al*., 2007). As with α-factor, cultures release from an HU block reliably and synchronously upon removal of the agent. HU arrests are useful for exploring replication events in mid- and late-S-phase and can also be used in checkpoint studies since stalled replication forks can trigger the intra-S-phase checkpoint (see section 1.4 Checkpoints below).

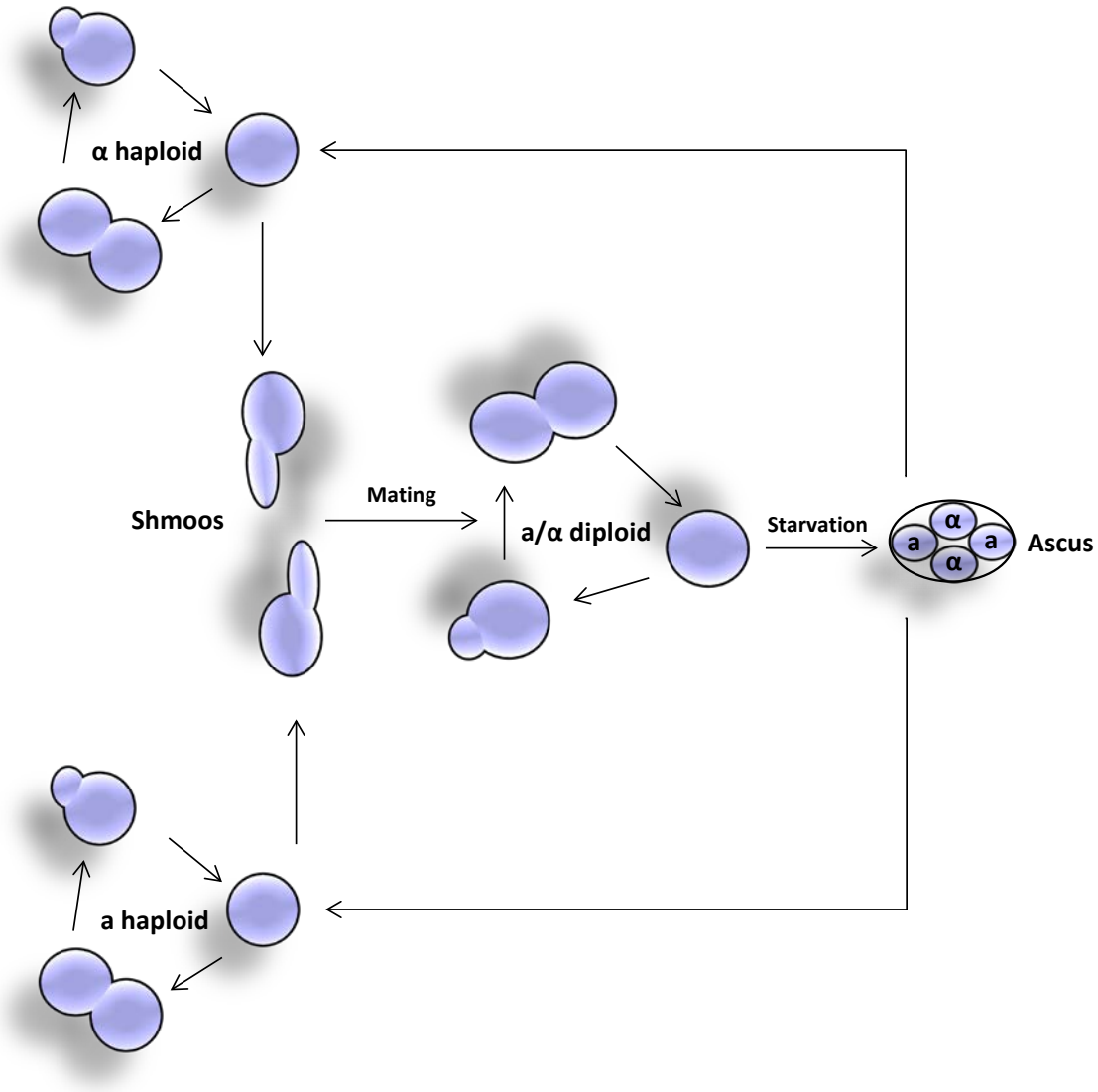

Figure 1.2: The *Saccharomycese cerevisiae* life cycle. Cells can reproduce asexually by budding in an haploid or diploid state. Haploid cells of the opposing mating type (a or α) can form shmoos and mate to form diploid cells. Under starvation conditions, diploid cells can sporulate forming four haploid spores. When conditions are favourable, the four spores can germinate to form four haploid cells (Adapted from Walker, 1998).

1.3 The Initiation of DNA Replication

1.3.1 Overview

While the initiation of DNA replication might be thought to begin at the G1-S transition, the process of complex formation that is required at origins for initiation to occur begins much earlier. This preparatory process, the initiation event itself, and the immediate consequences of initiation will be discussed with an emphasis on the DDK complex and the Mcm2-7 helicase complex, as these replication factors are central to this project.

1.3.2 Origins of Replication and the Timing of Firing

DNA replication begins at specific sites called origins of replication or simply 'origins'. Following the association of the necessary factors and initiation itself, replication proceeds bi-directionally away from the origin generating a replicon (all of the DNA replicated from a single origin). *S. cerevisiae* origins were first identified through a plasmid-based assay where fragments of the yeast genome were incorporated into bacterial plasmids lacking an eukaryotic origin. Any plasmid that could subsequently be replicated (as a mini-chromosome) in yeast must have contained a genomic sequence that could act as an origin. These sequences are called autonomously replicating sequences (ARSs, Brewer and Fangman, 1987). At around 150bp in length, the ARS consists of a 11bp highly conserved and essential consensus A-domain sequence (or autonomously replicating sequence consensus sequence, ACS) flanked by poorly conserved B domains. There are estimated to be more than 300 origins of replication found in intergenic regions throughout the yeast genome, most of which are very efficient (i.e. fire during every cell cycle; Raghuraman *et al*., 2001; Nieduszynski *et al*., 2006).

While origins fire throughout S-phase, some areas of the genome are replicated earlier in S-phase than others indicating that there is a temporal program to origin firing. Indeed eukaryotic origins can be classified as being early-, middle-, or late-firing origins depending on when during S-phase they are active. The reason for an origin firing when it does remains unclear, however one hypothesis advanced in other eukaryotes (*Drosophila* and human cells) – that origin activation is positively correlated with the level of transcription – has been disproved for budding yeast (Raghuraman *et al*., 2001; MacAlpine *et al*., 2004). Since both Cdk and DDK are active at the beginning of S-phase origin timing does not rely directly on these kinases, however it may be that late origin chromatin structure somehow makes it more difficult for Cdk or DDK to act. This idea is supported by evidence that the loading of Cdc45 (required for replisome loading, see below) is correlated with origin timing (Aparicio *et al*., 1997; Aparaicio *et al*., 1999; Zou and Stillman, 2000). In recent years evidence is emerging that the accumulation of a recyclable and limiting replication factor(s), attractive candidates include Sld2, Sld3, Dpb11, and Dbf4, may act stochastically to regulate origin timing (Goldar, *et al*., 2009). Evidence from fission yeast has also implicated heterochromatin-associated proteins in replication timing (Li *et al*., 2011). Relatedly, it is not known whether DDK is present at all origins at the beginning of S-phase or if the active kinase is redirected to later origins as S-phase progresses; one goal of this project is to address this question (see *Project Goals* below). The DNA damage and S-phase checkpoints (see below) may also play a role in origin timing since it has been shown that when the checkpoint kinase Rad53 (needed for normal checkpoint control) is inactivated (such as in a *mec2-1* mutant) later origins fire precociously (Santocanale and Diffley, 1998; Shirahige *et al*., 1998). The

action of Rad53 likely only contributes to regulation of origin firing and not fork progression as DNA combing experiments have shown that fork rates are normal in a *rad53-11* mutant, suggesting that Rad53 does not regulate fork progression (Versini *et al*., 2003).

1.3.3 Formation of the pre-Replicative Complex

The initiation of DNA replication requires the sequential binding of a number of proteins to origins of replication in order to 'license' or prepare them to fire; the culmination of this process is the loading of the Mcm2-7 helicase complex (Figure 1.3). The first factor to bind the origin is the origin recognition complex (ORC); in fact it has been shown that ORC is origin bound throughout the cell cycle in budding yeast (Liang and Stillman, 1997). ORC is a six-protein complex composed of subunits Orc1-6. ORC acts as a scaffold or 'landing pad' where the other members of the pre-RC congregate. The first factor to bind origin-bound ORC is the Cdc6 AAA^+ (ATPases Associated with various cellular Activities) -ATPase which is thought to act as a clamp loader to facilitate Mcm2-7 loading at origins. The inactive Mcm2-7 complex is transported to the origin by Cdt1 where it initially associates weakly in a Cdc6-dependent manner (Randell *et al*., 2006). Following ORC-dependent ATP hydrolysis by Cdc6, Mcm2-7 is stably loaded onto DNA; this results in a much more robust interaction than the initial weak association. Cdt1 and Cdc6 then dissociate from the origins and ORC ATP hydrolysis completes the Mcm2-7 loading reaction and allows the reiterative helicase loading necessary for bidirectional DNA unwinding (Randell, *et al*., 2006; Speck and Stillman, 2007). Once the MCM complex has been stably loaded, the origin is licensed and awaits

the activity of CDK and DDK in S-phase in order to fire and begin replication (Figure 1.3).

1.3.4 The Initiation of DNA Replication

As the cell makes the transition from G1 to S-phase, the levels of active CDK and DDK rise sharply. The major targets of CDK action seem to be factors that are necessary for initiation of replication but do not ultimately form part of the replisome; these factors include Sld2 and Sld3 (Figure 1.4). While the role of these factors is unknown, they are required for the recruitment and association of Cdc45 and the Go-Ichi-Ni-San (GINS) complex with Mcm2-7 (Figure 1.4). Stable loading of Cdc45 with Mcm2-7 is GINS-dependent and together these three factors form the CMG complex. This complex is integral to the helicase function of Mcm2-7, however the individual contributions of Cdc45 and GINS remains unclear (reviewed in Labib, 2010). Another major player in the recruitment of Cdc45 and GINS to Mcm2-7 is Dpb11 (DNA polymerase B 11), orthologs of which are required for DNA replication in all eukaryotes (Garcia *et al.*, 2005). Screens looking for synthetic lethality with a Dpb11 mutant (*dpb11-1*) isolated a number of *SLD* (synthetic lethal with Dpb11) genes including *SLD2* and *SLD3* which are major players in initiation (Kamimura *et al.*, 1998). The function of Sld2 is unknown, although its phosphorylation by CDK allows it to bind the C-terminus of Dpb11 (Tak *et al*., 2006). Sld3 is similarly required for replication initiation and both it and Cdc45 are recruited to early origins in a mutually dependant manner in G1-phase, even though stable association of Cdc45 with Mcm2-7 does not occur until S-phase with the recruitment of GINS (Labib, 2010). Sld3 binds to Dpb11 when phosphorylated by CDK, although unlike Sld2,

Sld3 binds to the N-terminus of Dpb11. All of this leads to the idea that Sld3 associates with the pre-RC (perhaps the Mcm2-7 complex) helping to recruit Cdc45. Dpb11 meanwhile, acts as a bridge between phosphorylated Sld3 and Sld2, and recruits GINS in S-phase (Figure 1.4; Araki, 2010). A recent study has revealed that the recruitment of GINS also requires DNA polymerase ε along with CDK, but that DDK and even the Mcm2-7 complex are dispensable (Muramatsu *et al*., 2010). DNA replication can proceed without CDK in yeast cells expressing a mutant allele of Cdc45 (*JET1*) or a phosphomimetic Sld2, so long as Sld3 is fused with Dpb11 in either case; this has led to the proposal that Sld2 and Sld3 are the 'minimal set' of CDK targets for initiation of replication in budding yeast (Zegerman and Diffley, 2007; Tanaka *et al*., 2007). While the order of CDK and DDK action has been controversial (Sclafani and Holzen, 2007), a recent study by Heller *et al*., (2011) using an *in vitro* assay that purports to recapitulate replication initiation events, demonstrated that DDK action in G1-phase is required for the initial recruitment of Cdc45 and Sld3. This study also showed that CDK activity is not required until S-phase for the recruitment of the GINS complex. This would seem to indicate that DDK acts prior to CDK even though DDK action is also necessary throughout S-phase (i.e. after CDK is activated).

While CDK can also phosphorylate the N-terminus of Mcm4, the Mcm2-7 complex is the major target of DDK (Devault *et al*., 2008; Labib, 2010). This phosphorylation leads to the stable loading of other replication factors including Cdc45, GINS, and Mcm10. While Cdc45 and GINS form part of the DNA helicase (see above), Mcm10 may act as a physical bridge between Mcm2-7 and DNA polymerase α-primase. This interaction that would be especially important for replication of the lagging strand since

the MCM proteins are 3' to 5' helicases (Bochman and Schwacha, 2009). The interaction between DDK and the Mcm2-7 complex will be considered in detail below. Once active, the helicase unwinds the DNA beginning at the origin and the newly exposed single-stranded DNA is stabilized by the binding of RPA. The polymerase α-primase complex is then recruited to the developing replication fork and begins synthesizing RNA primers. Following DNA synthesis the components of the pre-RC (other than ORC) dissociate from origins.

It is crucial that during the cell cycle exactly one copy of the DNA is synthesized. Re-replication occurs if parts of the genome are copied more than once per cell cycle, which can lead to compromised genomic integrity. In order to prevent re-replication from occurring, the cell has a number of tools at its disposal leading to a model for the block of re-initiation/re-replication; namely, that there are two mutually exclusive stages of initiation: the assembly at the origin of the pre-RC (licensing) in G1-phase followed by the activation of these licensed origins by CDK and DDK in S-phase (reviewed in Sclafani and Holzen, 2007; Labib, 2010). The low level of CDK activity in G1-phase prevents pre-RCs that have formed from firing until levels of the active CDK rise at the onset of S-phase. If origins could fire during G1, new pre-RCs could form leading to re-replication. Following origin firing and replication of the genome, CDK activity prevents some of the pre-RC components from reforming new pre-RCs in S- and G2-phases; for example, the phosphorylation of Cdc6 induces its proteolysis, phosphorylation of soluble Mcm2-7 promotes its export from the nucleus, and phosphorylation of Orc2 and Orc6 all work to prevent re-formation of the pre-RC until CDK levels drop in G1-phase (reviewed in Green *et al*., 2006).

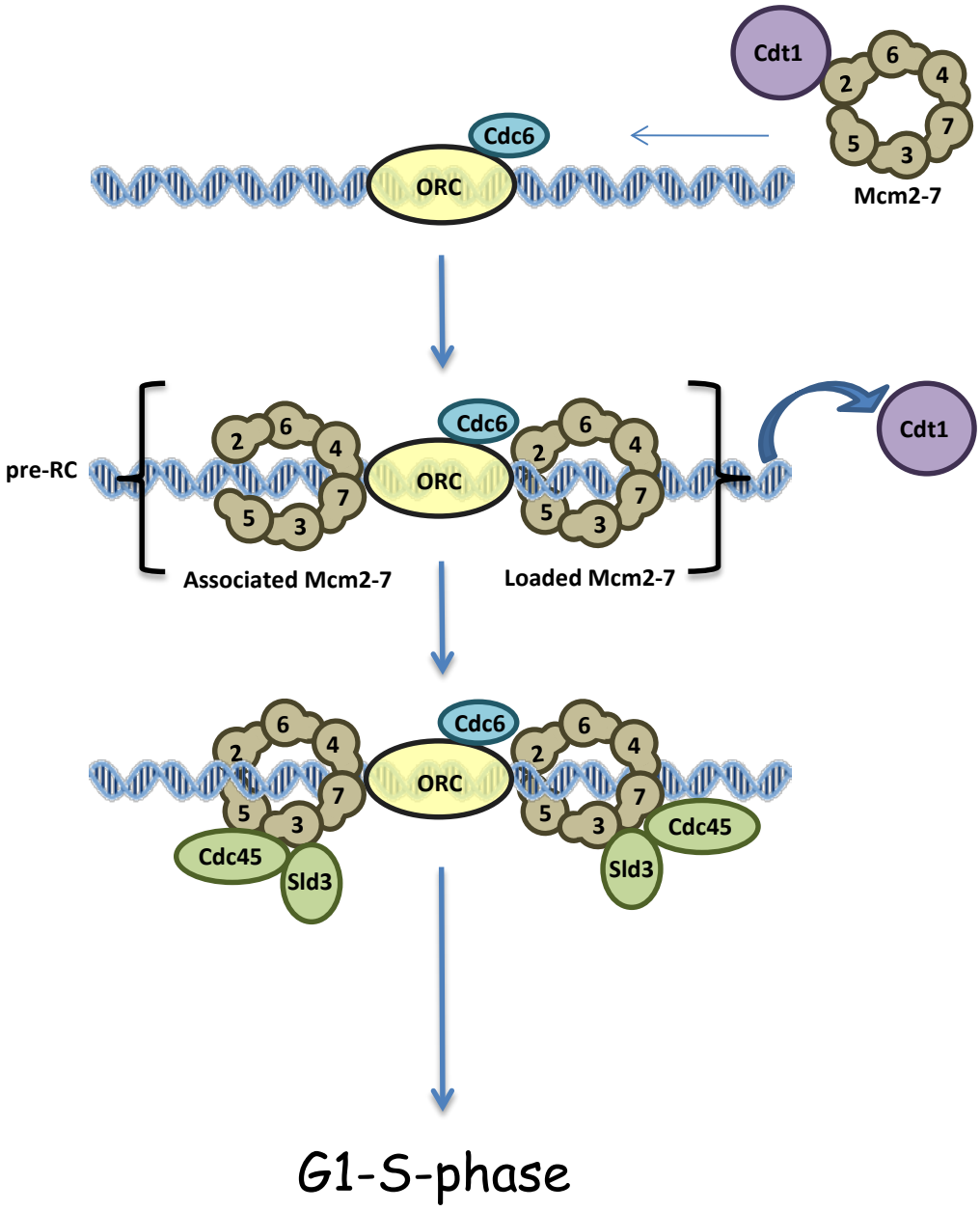

Figure 1.3: Events at origins of replication in G1-phase. The origin recognition complex assembles at origins of replication followed by Cdc6 and Cdt1 which effect the loading of the Mcm2-7 complex. Sld3 and Cdc45 are recruited to early origins in G1-phase, note that their specific interaction partners have yet to be identified (adapted from Labib, 2010).

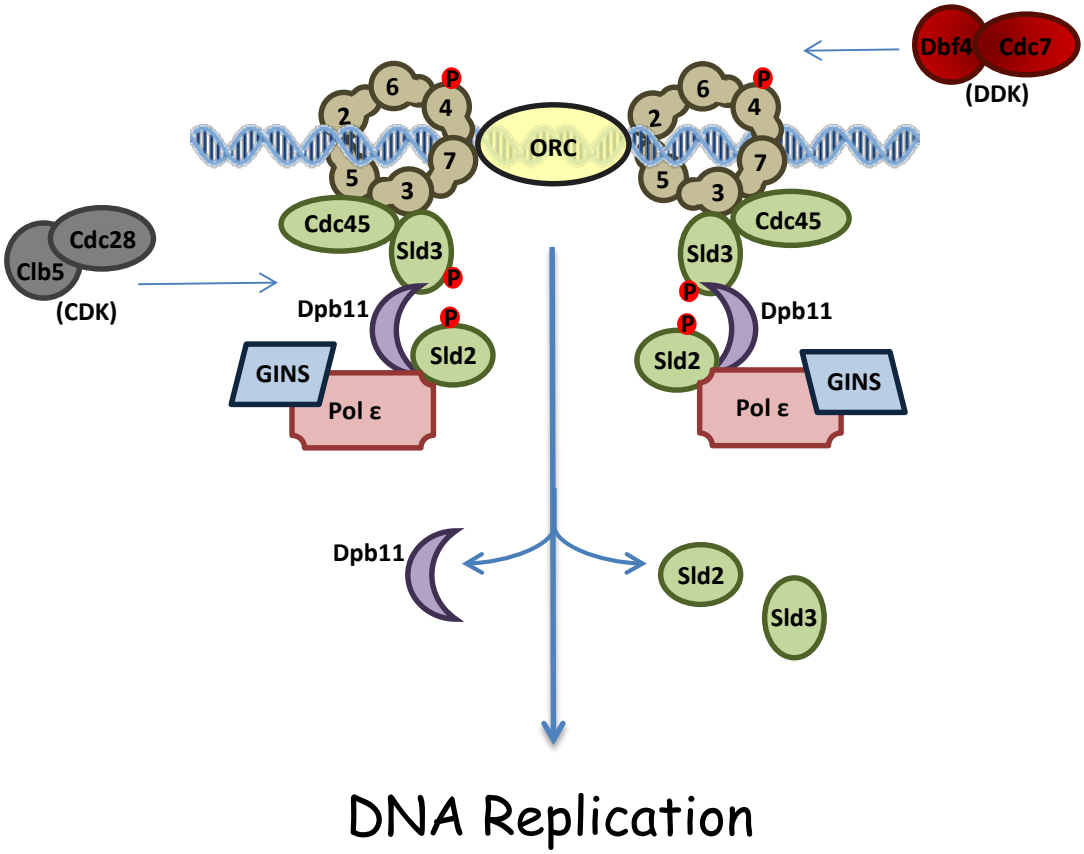

Figure 1.4: Events at origins of replication at the onset of S-phase. The Mcm2-7 complex (specifically the Mcm4 subunit) is phosphorylated by DDK. Sld2 and Sld3 are phosphorylated by CDK which allows their interaction with Dpb11 leading to the recruitment of Polε and the GINS complex. Following dissociation of Dpb11, Sld2, and Sld3, DNA replication proceeds bi-directionally (adapted from Labib, 2010).

1.3.5 Mcm2-7 helicase complex

The final step of pre-RC formation is the loading of the Mcm2-7 replicative helicase. *MCM* genes were first discovered in *S. cerevisiae* through mutations in *MCM2, MCM3,* and *MCM5* that resulted in faulty plasmid segregation in mitosis (hence minichromosome maintenance, Maine *et al*., 1984). *MCM4* and *MCM7* were identified as cell cycle division mutants and originally called *CDC54* and *CDC47* respectively (Moir *et al.*, 1982; Hennessy *et al.*, 1991). Finally, *MCM6* was identified in *S. pombe* as a chromosome segregation mutant (Takahashi *et al.*, 1994). For simplicity, these six paralogous genes were renamed *MCM2* through *MCM7* (Chong *et al*., 1996). *MCM* genes are found in both eukaryotes and archaea, but have so far not been isolated in bacteria. All known hexameric helicases are homohexamers composed of six copies of an identical subunit, except for the eukaryotic Mcm2-7, making this heterohexameric complex unique (Bochman and Schwacha, 2009). The six eukaryotic *MCM* genes (*MCM2-7*) are essential in budding and fission yeast and share significant sequence similarity particularly in a 250-amino acid region coding for an AAA^{+}-ATPase active site domain (Koonin, 1993; Sclafani and Holzen, 2007). These sites are formed in clefts between two adjacent subunits of the complex, with one contributing a P-loop domain and the other a lid domain. The P-loop domain contains ATP-binding motifs (Walker A box) and motifs involved in water molecule orientation (Walker B box and sensor 1). The lid domain is composed of motifs that interface with ATP (arginine finger and sensor 2; reviewed in Bochman and Schwacha, 2009).

In addition to the 'canonical' components of the ATPase active site just described, the Mcm proteins also have β-hairpin fingers, three of which extend into the central

channel of the complex. These fingers likely act to couple ATP hydrolysis to DNA unwinding. The binding and hydrolysis of ATP causes conformational changes in the helicase structure which allow it to physically manipulate (i.e. unwind) the DNA. While the Mcm2-7 complex has multiple ATPase sites, it is unclear in what order ATP binds these sites or if all the sites are bound simultaneously. The actual mechanism by which the helicase unwinds the DNA is not fully understood, but a number of models have been proposed, the most popular of which seem to be the dsDNA pump model and the 'ploughshare' model (discussed in Takahashi *et al.*, 2005).

The subunits of the Mcm2-7 complex are found in a 1:1:1:1:1:1 stoichiometry and electron microscopy analysis indicates that they form a ring-shaped structure similar to the archaeal Mcm complex (Ying and Gautier, 2005; Bochman and Schwacha, 2007). Within the ring, five dimeric subunit pairs have been identified: Mcm5/3, Mcm3/7, Mcm7/4, Mcm4/6, and Mcm6/2. These parings lead to the subunit organization of the MCM complex being: Mcm2-6-4-7-3-5 (Figure 1.3; Davey *et al*., 2003; Bochman *et al*., 2008). Studies of the helicase activity of the Mcm2-7 complex have been complicated by the lack of observable helicase activity *in vitro* (Ishimi, 1997; Davey *et al.*, 2003). A dimeric heterotrimer (Mcm4/6/7) has, however been isolated that has ATP-dependant DNA unwinding activity (Kaplan *et al*., 2003). It seems that only the Mcm7/4 active site is required for helicase activity and that addition of Mcm3 or a Mcm5/3 dimer actually inhibits Mcm4/6/7 helicase activity. This leads to a model whereby the ATPase activity of the Mcm2-7 complex can be divided into two groups: Mcm4, Mcm6, and Mcm7 active sites are required for helicase activity, while the active sites of Mcm2, Mcm3, and Mcm5 serve as negative regulators (Sato *et al*., 2000; Schwacha and Bell, 2001; Kanter *et al*.,

2008). Further analysis of individual active site dimers have revealed that the highest level of ATPase activity is found at the Mcm3/7 interface, similar to the level of the entire Mcm2-7 complex. The Mcm7/4 interface has moderate levels of ATPase activity, while the Mcm6/2 and Mcm5/3 interfaces have low and no ATPase activity, respectively (Davey, *et al*., 2003; Bochman *et al*., 2008). The active ATPase sites also seem to function inter-dependently as mutations in the Walker A motif of any one of the sites 'poisons' activity in the rest (Schwacha and Bell, 2001).

The Mcm5 subunit has proved particularly difficult to work with and even though an interaction between Mcm5 and Mcm2 would be predicted based on the order of the other subunits in the complex, no such interaction has yet been shown (Davey *et al*., 2003). This lack of interaction, along with evidence from studies of the DNA binding properties of the helicase using Mcm2 and Mcm5 ATP binding/hydrolysis mutants, suggest that these two subunits form a reversible ATP-dependent gap or 'gate', giving the ring a closed formation when the ATPase site is ATP bound and an open conformation when no ATP is bound (Bochman and Schwacha, 2007; 2008). This 'gate' model provides a mechanism through which the already-formed complex is able to encircle the DNA in order to perform its unwinding function.

1.3.6 Cdc7

Cdc7 (cell division cycle 7), also referred to as DDK, was first identified in cell division cycle genetic screens in budding yeast but is conserved in all eukaryotes studied so far, including human cells (Culotti and Hartwell, 1971; Sclafani, 2000). It is required throughout S-phase for the initiation of DNA replication at individual origins (Hartwell,

1976; reviewed in Weinreich and Stillman, 1999; Sclafani and Holzen, 2007). The levels of this 58 kDa protein have been show to be relatively constant throughout the cell cycle however its activity peaks at the G1-S transition (Jackson *et al*., 1993; Weinreich and Stillman, 1999). Strains lacking functional *CDC7* arrest prior to the initiation of DNA replication and it has been shown that replication is not initiated at late origins when Cdc7 is inactivated in mid-S-phase (using a *cdc7*-ts mutant). This suggests that Cdc7 acts locally to initiate replication, rather than in a global manner as once thought (Bousset and Diffley, 1998; Donaldson et al., 1998). Cdc7 is regulated in a similar manner to that of CDK; namely, the monomeric kinase subunit is inactive until it is bound by an unstable activating subunit (i.e. Dbf4 in the case of Cdc7). It is the cell cycle regulation of Dbf4 then, which imparts the cell cycle regulation of kinase activity.

1.3.7 Dbf4

As implied by its name, Dbf4 (dumbbell forming 4) was isolated in a screen for mutants that take on a dumbbell appearance upon cell cycle arrest. Because this morphology typically indicates defects in S-phase, Dbf4 was implicated in DNA replication early on (Johnston and Thomas, 1982a,b). Dbf4 is an 80 kDa protein whose levels have been shown to fluctuate throughout the cell cycle, being absent from the end of mitosis until late G1-phase when it accumulates (Cheng *et al*., 1999; Pasero *et al*., 1999; Weinreich and Stillman, 1999). Levels peak at the G1-S transition and Dbf4 is still present during G2 phase. At the onset of anaphase levels of Dbf4 drop rapidly as it is targeted for degradation by the APC/C as mitosis is completed (Ferreira *et al*., 2000). Dbf4 orthologs have been identified in all eukaryotes, including *S. pombe, Xenopus,* mice, and humans,

and sequence comparisons have revealed three well-conserved regions: the N, M, and C motifs (Landis and Tower, 1999; Masai and Arai, 2000). These motifs have been implicated in binding DNA replication factors. A region of Dbf4 including the M motif, as well as a region encompassing the C motif, both mediate the interaction with Cdc7 (Hardy and Pautz, 1996). The N motif is responsible for the interaction with Orc2 as well as the cell cycle checkpoint kinase Rad53. This motif is dispensable for viability and its deletion imparts hypersensitivity to genotoxic agents (Varrin *et al*., 2005). The M motif is required for cell viability and has been shown to mediate the interaction with Mcm2 (Varrin *et al*., 2005). The C motif is the most highly conserved of the three and has only recently been functionally characterized (Jones *et al*., 2010). Mutations in the C motif impair the ability of Dbf4 to phosphorylate Mcm2. Strains with C motif mutations are viable, but impaired for entry into and progression through S-phase, likely due to a weakened interaction with Mcm2. The C region may also play a role in the response to genotoxic stress (Jones *et al.,* 2010).

1.3.8 The Role of DDK in the Initiation of DNA Replication

Several lines of genetic and biochemical evidence indicate that the Mcm2-7 complex is a DDK target (reviewed in Masai and Arai, 2002; Sclafani, 2000). As is the case with ORC and MCM subunits, Dbf4 displays a punctate subnuclear foci pattern in fixed cells consistent with the idea that DDK functions in discrete replication factories to promote DNA replication (Pasero *et al*., 1999). Initially, Mcm2 was shown as the preferred substrate of DDK; however, Mcm3, Mcm4, Mcm6, and Mcm7 can also be phosphorylated by DDK (Lei *et al*., 1997; Weinreich and Stillman, 1999). Mcm5 has not

been shown to be phosphorylated by DDK however, interestingly, a P83L mutation in Mcm5 (*mcm5-bob1*) is able to bypass the requirement for DDK activity for DNA replication, although the exact mechanism is not well understood (Hardy *et al*., 1997). Because structural work with the eukaryotic Mcm2-7 has so far been difficult, this mutation was studied in the homohexameric archaeal equivalent of Mcm2-7 (MthMcm). The *bob-1* mutation causes a modest conformational change in the MthMcm N-terminal domain, leading to the 'domain-push' model whereby Mcm2-7 is activated via a DDK-mediated conformational change (Fletcher *et al*., 2003). Unfortunately, this model is difficult to test since Archaea do not contain a DDK homologue and, importantly, the homohexameric nature of MthMcm means that the mutation is present in all subunits of the complex. This is in contrast to the eukaryotic Mcm2-7 which would only contain the mutation in the Mcm5 subunit (Bochman and Schwacha, 2009).

DDK seems to act preferentially on Mcm2-7 complexes that have been loaded onto origin DNA as part of the pre-RC (Francis *et al*., 2009). Two recent studies have shown that the essential targets of DDK are the N-terminal tails of Mcm4 and Mcm6, and that the phosphorylation of one can compensate for that of the other (Sheu and Stillman, 2010; Randell *et al*., 2010). The Mcm4 N-terminal region is the best characterized with the identification of a DDK-docking domain (DDD) and a region called the NSD (N-terminal Ser/Thr-rich domain) which contains a number of sites that are progressively phosphorylated by DDK (Sheu and Stillman, 2006). In addition to its facilitating role in DNA replication, the NSD also contains a region (amino acid residues 74-174) that has been shown to have an inhibitory activity which is relieved when phosphorylated by DDK. Removal of N-terminal region of Mcm4 (encompassing the NSD) was also shown

to bypass the requirement for DDK activity. Thus the phosphorylation of the NSD of Mcm4 is thought to be the sole essential function of DDK (Sheu and Stillman, 2010). Furthermore, DDK phosphorylation of Mcm4 and Mcm6 requires prior or 'priming' phosphorylation via Mrc1-facilitated Mec1 activity (Randell *et al*., 2010). While traditionally thought of as checkpoint mediators, Mec1 and Rad53 also help to coordinate DNA replication by triggering the activation of ribonucleotide reductase. Therefore, the priming activity of Mec1 on the MCM subunits is an attractive regulatory mechanism for the activation of the Mcm2-7 complex (Zhao *et al*., 2001; Randell *et al*., 2010).

The N-terminal tails of Mcm2 and Mcm6 are less well characterized although removal of the tails of either protein is not sufficient to bypass the requirement of DDK activity for growth (Sheu and Stillman, 2010). There is evidence for a docking domain in the N-terminal region of Mcm2 (analogous to the DDD of Mcm4) and there is some controversy as to whether DDK phosphorylation at residue S170 is essential for DNA replication (Sheu and Stillman, 2006; Bruck and Kaplan, 2009). Although the sites of DDK phosphorylation have been mapped (Bruck and Kaplan, 2009; Randell *et al*., 2010; Stead *et al*., 2011), the way in which it is targeted to the Mcm2-7 complex remains unclear. While one model suggests that DDK is targeted to origins as an active complex either by Dbf4 alone or by the coordinated action of both subunits, a second model envisages Dbf4 activation of Cdc7 already present at replication origins. A goal of my project was to elucidate this mechanism (see section *1.6 Project Goals* below).

1.4 Checkpoints

1.4.1 Overview

The cell cycle is an orderly progression of events that lead to cell division; it is thus critical that these events occur in the proper order and that one event is completed before another begins. In order to ensure this orderly progression, special surveillance mechanisms called checkpoints are employed by the cell to monitor the completion of cell cycle events and respond to any problems detected with the DNA, including damage or errors during replication (reviewed in Sancar *et al*., 2004; Branzei and Foiani, 2006). In order to protect their genomic integrity, cells must detect and repair any damage to their DNA; checkpoints work by temporarily arresting the cell cycle to give the cell time to complete this repair before progressing to the next stage of the cell cycle. Genomic integrity is monitored before major events involving the DNA, namely at three intervals in the cell cycle: G1/S, intra-S, and G2/M. DNA damage in G1 is detected by the G1/S checkpoint which prevents the cell from entering S-phase (even if the cell has passed START) until the damage is resolved, thus preventing replication of damaged DNA. The G2/M checkpoint prevents cells with DNA damage from entering mitosis until it is repaired and also ensures proper microtubule-kinetochore attachments for chromosome segregation during anaphase (Sancar *et al*., 2004; Lew and Burke, 2003). An exploration of DNA damage and the intra-S phase checkpoint will be considered in greater detail below including the roles played by DDK and the Mcm2-7 complex.

1.4.2 The Intra-S-Phase Checkpoint

The intra-S-phase checkpoint functions to ensure accurate DNA replication as the cell moves through S-phase. Should DNA damage be detected, the checkpoint provides time for the cell to repair the damage by slowing the rate of replication by two mechanisms: 1) stabilizing stalled replication forks and 2) preventing late (unfired) origins from firing (Zegerman and Diffley, 2010; Duch *et al*., 2011).When DNA damage is encountered, the replication fork is impeded while the Mcm replicative helicase continues to unwind DNA ahead of the stalled fork. This generates ssDNA, which is then bound by RPA. RPA-coated ssDNA has been shown to physically interact with checkpoint factors and is required for checkpoint activation (reviewed in Forsburg, 2008; Xu *et al*., 2008; Branzei and Foiani, 2009). ssDNA-RPA independently recruits Mec1-Ddc2 and Rad24-RFC to the site of DNA damage. The Rad24-RFC complex acts as a clamp-loader and is responsible for loading the PCNA-related Rad17-Mec3-Ddc1 complex (9-1-1 complex in mammals, Majka *et al*., 2003). Mec1 phosphorylates the Rad17-Mec3-Ddc1 complex, but it is unclear what role this serves, although it may lead to the recruitment of other Mec1 substrates (Harrison and Haber, 2006; Branzei and Foiani, 2009). The checkpoint effector kinase Rad53 (radiation-repair protein 53) is phosphorylated in a Mec1-dependant manner in response to DNA damage as well as to replication stress (such as stalled replication forks due to HU treatment), although the pathways leading from Mec1 to Rad53 activation differ. In the DNA damage response, the checkpoint mediator Rad9 is hyperphosphorylated in a Mec1 and Tel1-dependant manner and this activated Rad9 is proposed to act as a scaffold to promote subsequent Rad53 autophosphorylation (Toh and Lowndes, 2003; Sweeney *et al*., 2005). Under replication stress conditions, Mec1

phosphorylation of Mrc1 leads to the hyperphosphorylation of Rad53, though Rad9 is able to act as a partial substitute in the absence of Mrc1, indicating that these two pathways are partially redundant (Alcasabas *et al*., 2001).

Following its autophosphorylation, Rad53 dissociates from the Rad9 complex and disperses throughout the cell leading to the amplification of the checkpoint signal. This signal generates a number of cellular responses, including cell cycle delay, DNA repair, inhibition of late origin firing, and replication fork stabilization (Branzei and Foiani, 2006). The preservation of late origins may be a safe-guard for the cell to be able to complete DNA replication should there be catastrophic replication fork collapse during the checkpoint. These origins would serve as a place to restart replication during checkpoint recovery (Santocanale and Diffley, 1998; Branzei and Foiani, 2005; 2009). Recently, a link has been established between the action of Rad53 and the inhibition of late origin firing; namely that Rad53 action inhibits both Cdk- and DDK-dependent pathways which in turn block further origin firing (Zegerman and Diffley, 2010). This study also showed that the phosphorylation of Sld3 (part of the CDK pathway) prevents its essential interaction with Cdc45 (thereby preventing replication) while allowing CDK itself to remain active. This activity is critical in preventing new pre-RCs from forming, thus preventing re-replication. Rad53 has also been shown to phosphorylate Dbf4 leading to DDK inactivation and its subsequent inability to activate the Mcm2-7 complex (Zegerman and Diffley, 2010). While in practice it seems that preservation of unfired origins contributes less to the viability/recovery from a checkpoint than does the stabilization and restart of stalled replication forks, this small contribution may offer cells a competitive advantage over a number of generations (Tercero *et al*., 2003; Duncker and

Brown, 2003; Zegerman and Diffley, 2010). Therefore, the stabilization of the replisome at stalled replication forks seems to be a main function of the intra-S-phase checkpoint (Lopes *et al*., 2001). This is supported by electron microscopy studies showing that the replisome dissociates from the fork and the fork itself degenerates and collapses in *rad53* mutants (reviewed in Branzei and Foiani, 2005; Sogo *et al*., 2002).

1.4.3 The Role of DDK and Mcm2-7 in the Intra-S-Phase Checkpoint

Given that 1) DDK activity is required throughout S-phase for origin activation; 2) that Dbf4 has been shown to interact with Rad53 via the N motif, and 3) that Rad53-dependent phosphorylation of Dbf4 reduces DDK activity, DDK is a likely player in the checkpoint response (Weinreich and Stillman, 1999; Varrin *et al*., 2005). Indeed, HU treatment results in the phosphorylation of Dbf4 and its removal from chromatin in a Rad53-dependent manner, while deletion of the N motif causes strains to be sensitive to genotoxic agents, presumably due to the lack of interaction with Rad53, and studies using mutants of either Dbf4 or Cdc7 show hypersensitivity to genotoxic agents (reviewed in Sclafani, 2000 and Pasero *et al*., 2003; Pasero *et al*., 1999; Varrin *et al*., 2005). DDK inactivation by Rad53 phosphorylation of Dbf4 has been linked to the preservation of unfired origins; however, the mechanism by which this phosphorylation leads to DDK inactivation remains unclear (Zegerman and Diffley, 2010). In vertebrates, the checkpoint mediator protein claspin (a Mrc1 ortholog) has been shown to be a phosphorylation target of DDK, and this phosphorylation is required for the activation of the ATR-Chk1 checkpoint pathway (Kim *et al*., 2008). Studies using *Xenopus* egg extracts have shown Cdc7 to be a downstream target in the ATR-Chk2 pathway following replication fork

stalling as a result of etoposide treatment (Chk2 is a Rad53 ortholog; Costanzo *et al.*, 2003). In human cells, the role of DDK in the checkpoint response may be less important as DDK activity is unchanged by replication fork arrest (Tenca *et al.*, 2007). Further work is required to elucidate the role of DDK in the checkpoint response in *S. cerevisiae.*

As described above, when replication forks stall, Mcm-dependent DNA unwinding is uncoupled from DNA synthesis leading to accumulation of RPA-bound ssDNA which is the signal for checkpoint activation. In *rad53* mutants, in which catastrophic replication fork collapse occurs, polymerases remain at the fork while MCMs seem to be lost, suggesting that DNA unwinding is regulated by Rad53 to allow enough ssDNA-RPA to signal the checkpoint, but not enough to completely decouple the replisome (Forsburg, 2008; Cobb *et al*., 2003). The MCM complex is required to maintain the integrity of stalled replication forks in *S. pombe* and loss of MCMs, using *mcm*-ts mutants at restrictive temperature, resulted in fork breakdown and extensive DNA double-strand breaks (Bailis *et al*., 2008). Interestingly, the same study also showed evidence that Mcm4 may be a Rad53 target, which is consistent with a role for checkpoint kinases in MCM regulation since MCM proteins are delocalized from the fork under HU conditions in *rad53* and *mrc1* mutants (Cobb *et al*., 2005; Bailis *et al*., 2008). Taken together this evidence points to a model whereby upon replication fork arrest, MCMs continue to unwind DNA in order to generate the RPA-ssDNA checkpoint signal, which in turn causes activation of Rad53. Subsequently, activated Rad53 phosphorylates the MCM complex preventing further DNA unwinding and promoting the stabilization of the replisome at the fork (Forsburg, 2008). Thus, the role of the MCM complex in the checkpoint response seems to be critical to the stabilization of the stalled replication fork.

1.4.4 A Role for DDK in Checkpoint Recovery?

While the role of the MCM complex in the checkpoint response is better understood than for DDK, several lines of evidence indicate a role for DDK in the recovery from a checkpoint arrest by aiding in the restart of stabilized stalled forks, rather than one in the stabilization process itself. First, as indicated above, Dbf4 is phosphorylated by Rad53 and removed from chromatin under checkpoint conditions. Rad53-dependent phosphorylation of Dbf4 reduces DDK activity, thereby reducing the likelihood that it plays an active role in fork stabilization. Varrin *et al* (2005) observed that a *dna52-1* allele (a Dbf4-ts point mutation) is more resistant to MMS treatment than wild type cells. They hypothesized that because this mutant retains its robust interaction with Rad53, Dbf4 is stabilized and that following checkpoint adaptation, DDK is able to help in the resumption of fork progression by interacting with other fork-associated substrates (e.g. Mcm2-7 complex). More recent work shows that mutations in the C motif of Dbf4 that weaken its interaction with Mcm2 impart a sensitivity to continuous exposure to HU and MMS, but do not result in any loss of viability following short term exposure to these compounds, consistent with a role in replication restart (Jones *et al*., 2010). Work in *S. pombe* corroborates this finding in that synthetic lethality was observed in a *hsk*1-ts (*CDC7* ortholog) mutant with a null mutation for *rqh1,* a RecQ-type helicase required for recovery from HU arrest (Snaith *et al*., 2000). In *Xenopus* egg extracts, DDK action works to attenuate the checkpoint signal and may trigger DNA replication resumption during recovery from the S-phase checkpoint (Tsuji *et al*., 2008). While it is not currently known what specific role DDK plays in fork restart it has been hypothesized that DDK

may phosphorylate the MCM complex leading to its stabilization at the fork and/or the re-activation of DNA helicase activity. Alternatively, DDK may activate Cdc45 or DNA polymerase α, which are known DDK targets *in vitro* (Jones *et al*., 2010); thus this is an attractive area for further study which is partially addressed in this dissertation.

1.5 Importance for Cancer Research

As the wealth of knowledge about cancer phenotypes continues to grow, it is becoming apparent that upregulation of many replication factors – including Mcm2, Mcm5, and Cdc6 – are a hallmark of many cancers, including some of the most common human types. This implies that these replication factors might be used as biomarkers for cancer pathology (Korkolopoulou *et al*., 2005; Murphy *et al*., 2005). Because DDK is associated with these replication factors and actually activates the MCM complex to promote DNA replication, it is logical to think that Cdc7 could be a reliable marker for human cancers as well. In fact studies have shown increased levels of Cdc7 mRNA and increased protein levels of both Cdc7 and Dbf4 in human cancer cell lines (Hess *et al*., 1998; Bonte *et al*., 2008). In addition to being a potentially valuable biomarker, Cdc7 is an ideal target for cancer therapy and there are currently a number of clinical trials testing the efficacy of Cdc7 inhibitors (reviewed in Swords *et al*., 2010). While this project does not deal directly with cancer or the deregulation of cellular mechanisms leading to the disease, it nevertheless contributes to the understanding of the normal function of some of these processes and factors, Dbf4 and Cdc7 being prominent among them. The knowledge garnered from this basic research can help to serve as a benchmark of what is 'normal' in the initiation of DNA replication for comparison with the disease state. Conceivably, this

information could be used to help isolate or develop better therapeutics with fewer side effects with the potential for better patient outcomes.

1.6 Project Goals

DDK acts at the level of individual origins and is required throughout S-phase in order for origins to be activated. While it has recently been shown that the essential DDK phosphorylation target for the initiation of DNA replication is the NSD of Mcm4, the way in which DDK is targeted to the origins to perform that essential modification remains unclear. Two models have been proposed for DDK recruitment: the first proposes that DDK is targeted to origins as an active complex (i.e. redistributing Cdc7 from non-origin regions to active origins, similar to the situation in *Xenopus;* Jares *et al.*, 2004). A second model envisages Dbf4 activation of Cdc7 already present at replication origins. Cdc7 is known to be chromatin bound throughout the cell cycle, but a distinction must be made between chromatin and origins; chromatin bound does not necessarily mean origin-bound (Weinreich and Stillman, 1999). Historically, models have posited that Dbf4 targets the complex to origins, but the contribution made by each subunit of DDK to the targeting of the complex remains an open question. The first objective of this project was to characterize how and through which subunits DDK is targeted to the MCM complex.

Since it was unclear which of the two aforementioned models accurately describe DDK targeting to origins, my second objective was to use chromatin immunoprecipitation to discriminate between the two. This technique allows for the exploration of individual origins, as opposed to bulk chromatin, and could therefore be a

useful tool not only to explore DDK targeting in general, but also the role this targeting might play in the timing of origin firing, as DDK association with early, middle, and late-firing origins could be examined (i.e. does DDK associate with all origins at the start of S-phase, or is there a sequential association with early, middle, and late as S-phase progresses?). As the S-phase checkpoint has been shown to have an impact on DDK activity, another avenue of exploration related to this second objective is to investigate the effect that this checkpoint has on Dbf4 and Cdc7 origin distribution, including the importance of the Dbf4-Rad53 interaction in the removal of Dbf4 from chromatin during the checkpoint response.

While a role for DDK in the inhibition of late origins under checkpoint conditions has been elucidated (Zegerman and Diffley, 2010), its role in fork recovery is less well understood. A third goal of this project is to lay the foundation for exploration of this potential role using a powerful technique called DNA combing whereby origin firing and stalled replication fork restart can be monitored. Part of this groundwork required the creation of a strain in which Dbf4 was able to be depleted in a specialized strain background modified for use in the combing procedure.

Finally, while it has been shown that Dbf4 and Cdc7 localize to discrete sub-nuclear foci in fixed cells, having the ability to monitor the temporal and spatial localization patterns of these proteins in live cells would be a valuable tool in understanding the mechanism of DDK action. In order to visualize these factors *in vivo*, it was necessary to generate strains in which the endogenous copy of Dbf4 and/or Cdc7 was tagged with the sequence for a fluorescent epitope, thus allowing visualization through fluorescence microscopy.

Chapter 2: Materials and Methods

2.1 Yeast Strains

DY-1 (*MAT***a** *ade2-1 can1-100 trp1-1 his3-11,-15 ura3-1 leu2-3,-112 pep4:LEU2*) was used for the two-hybrid analyses and coimmunoprecipitations. DY-262 (*MATα leu2Δ0 met15Δ ura3Δ0 lys2Δ0 mcm2*::*his3*) and DY-263 (*MATα his3Δ1 leu2Δ0 met15Δ ura3Δ0 mcm4*::*KanMX*) (supported for growth with wt *MCM2* or *MCM4* on a *URA3* CEN/ARS vector, Stead *et al.,* 2009) were used for the plasmid shuffle experiments. Mcm2 and Mcm4 plasmid shuffle strains were transformed with YCplac111-Mcm2WT, -Mcm2Δ2-4,10-63, -Mcm4WT, or –Mcm4Δ175-333 and grown on SC-ura-leu selective media. These were the 'shuffle in' strains. Colonies from these transformation plates were streaked on SC-leu +5'FOA plates to select for cells that had lost the *URA3* support plasmid. This resulted in the only copy of Mcm2 or Mcm4 being on the YCplac111 *LEU2*, CEN/ARS plasmid. These shuffle strains were then mated to DY-196 (*MAT***a**, *his3Δ1, leu2Δ0, ura3Δ0*) and the resulting diploids were sporulated and dissected to generate the haploid *MAT***a** shuffle strains. Genomic tagging of ORFs was performed by homologous recombination with linear PCR fragments amplified using plasmid templates, as described by Longtine et al., (1998). Epitope tagging cassettes were amplified from Longtine vectors which also contained selectable marker genes to allow for the selection of integrants. Specifically, pFA6a-eYFP-TRP1 was used to create DY-153 (MAT**a**, *ade2-1, can1-100, trp1-1, his3-11, his3-15, ura3-1, leu2-3, leu2-112, pep4::LEU2, cdc7::CDC7-eCFP-kanMX6, dbf4::DBF4-eYFP-TRP1).* The pFA6a-3HA-KanMX6 vector was used to create the DY-157 (MAT**a**, *ade2-1, can1-100, trp1-1, his3-11, his3-15, ura3-1, leu2-3, leu2-112, pep4::LEU2, orc2::ORC2myc13-TRP1, dbf4::DBF4-3HA-kanMX6*). pFA6a-TRP1-pGAL1-3HA was used to create DY-255

(MATa, *ura3::URA3[GPD-TK(7x)] ade2-1 trp1-1 can1-100 leu2-3,112 his3-11,15 GAL psi+, dbf4::Pgal1-3HA-DBF4-TRP1*), DY-256 (MATa, *ura3::URA3[GPD-TK(7x)] ade2-1 trp1-1 can1-100 leu2-3,112 his3-11,15 GAL psi+, dbf4::Dbf4-3HA-TRP1*), and DY-261 (MATa, *ura3::URA3[GPD-TK(7x)] ade2-1 trp1-1 can1-100 leu2-3,112 his3-11,15 GAL psi+ dbf4:dbf4ΔN-TRP1*). pFA6a-13Myc-TRP1 was used to create DY-124 (MATa, *ade2-1, can1-100, trp1-1, his3-11, his3-15, ura3-1, leu2-3, leu2-112, pep4::LEU2, cdc7::CDC7-Myc13-TRP1*). The cassette amplification was accomplished using primers that contained sequence complementary to that in the genome and thus allowed for homologous recombination. For the C-terminal-tagged strains, the forward PCR primer contained a sequence that allowed for recombination immediately upstream of the stop codon, while the reverse primer contained a sequence that allowed for recombination downstream of the ORF. This means that the tag was incorporated in-frame immediately after the last coding codon, resulting in a C-terminal fusion protein. In the case of DY-255, the forward PCR primer contained a sequence that allowed for recombination 50 bp upstream from the start codon, while the reverse primer contained sequence that allowed for recombination in the first 13 codons of the gene (Longtine *et al*., 1998). To generate the Dbf4ΔNTK+ strain, the Dbf4ΔN sequence was PCR amplified from DY-78 genomic DNA, along with 500bp of 5' upstream sequence. A two-PCR-fragment, single ligation scheme was employed whereby the forward and reverse primer contained Pac1 and Asc1 sites respectively (See Chapter 5, Figure 5.3). This allowed the Dbf4ΔN construct to be cloned into the pFA6a-TRP1 backbone creating a pFA6a-Dbf4ΔN-TRP1 vector. This was then used as the template for the PCR amplification of the tagging cassette. In this case, recombination needed to occur upstream of the deleted

N-motif (the 500bp of upstream sequence was included to increase the chance of this occurring) and in the complementary region provided in the primer, just as in the normal tagging procedure. Proper integration was confirmed by PCR using primers that flanked the region of recombination, and proper expression was confirmed by western blot.

Table 2.1: Yeast strains created/used in this project.

Strain	Genotype
DY-1	MATa, *ade2-1, can1-100, trp1-1, his3-11, his3-15, ura3-1, leu2-3, leu2-112, pep4::LEU2*
DY-5	MATa, *ade2-1, can1-100, his3-11,-15, leu2-3, -112, trp1-1, ura3, GAL, psi+, dbf4::DBF4-Myc18*
DY-26	MATa, *his3Δ200, leu2Δ0, met15Δ0, trp1Δ63, ura3Δ0*
DY-29	MATa, *ade2-1, can1-100, trp1-1, his3-11, his3-15, ura3-1, leu2-3, leu2-112, pep4::LEU2, cdc7::CDC7-eYFP-kanMX6*
DY-45	MATa, *ade2-1, can1-100, trp1-1, his3-11, his3-15, ura3-1, leu2-3, leu2-112, pep4::LEU2, nup49::NUP49-EYFP-kanMX6*
DY-78	MATa, *his3Δ1, leu2Δ0, lys2Δ0, met15Δ0, ura3Δ0, dbf4::dbf4ΔN*
DY-81	MATa, *ade2-1, can1-100, trp1-1, his3-11, his3-15, ura3-1, leu2-3, leu2-112, pep4::LEU2, orc2::ORC2myc13-TRP1*
DY-123	MATa, *ade2-1, can1-100, his3-11,-15, leu2-3, -112, trp1-1, GAL, psi+, dbf4::DBF4-Myc18, LEU2, mec2-1(rad53-11)*
DY-124	MATa, *ade2-1, can1-100, trp1-1, his3-11, his3-15, ura3-1, leu2-3, leu2-112, pep4::LEU2, cdc7::CDC7-Myc13-TRP1*
DY-137	MATa, *his3D200, leu2D0, met15?0, trpD63, ura3D0, orc6::ORC6-3HA-TRP1, mcm2::MCM2-eYFP-kanMX6*
DY-153	MATa, *ade2-1, can1-100, trp1-1, his3-11, his3-15, ura3-1, leu2-3, leu2-112, pep4::LEU2, cdc7::CDC7-eCFP-kanMX6, dbf4::DBF4-eYFP-TRP1*
DY-157	MATa, *ade2-1, can1-100, trp1-1, his3-11, his3-15, ura3-1, leu2-3, leu2-112, pep4::LEU2, orc2::ORC2myc13-TRP1, dbf4::DBF4-3HA-kanMX6*
DY-215	(DY228 background) MATa, *his3D200, leu2D0, met15D0, trp1D63, ura3D0, mcm2::PGal1-3HA-TRP1-MCM2*
DY-216	(DY228 background) MATa, *his3D200, leu2D0, met15D0, trp1D63, ura3D0, mcm3::PGal1-3HA-TRP1-MCM3*
DY-217	(DY228 background) MATa, *his3D200, leu2D0, met15D0, trp1D63, ura3D0, mcm6::PGal1-3HA-TRP-MCM6*
DY-218	(DY228 background) MATa, *his3D200, leu2D0, met15D0, trp1D63, ura3D0, mcm7::PGal1-3HA-TRP1-MCM7*
DY-221	(DY228 background) MATa, *his3D200, leu2D0, met15D0, trp1D63, ura3D0, mcm5::PGal1-3HA-TRP1-MCM5*
DY-230	(DY228 background) MATa, *his3D200, leu2D0, met15D0, trp1D63, ura3D0, mcm4::PGal1-3HA-TRP1-MCM4*
DY-255	MATa, *ura3::URA3[GPD-TK(7x)] ade2-1 trp1-1 can1-100 leu2-3,112 his3-11,15 GAL psi+, dbf4::Pgal1-3HA-DBF4-TRP1*
DY-256	MATa, *ura3::URA3[GPD-TK(7x)] ade2-1 trp1-1 can1-100 leu2-3,112 his3-11,15 GAL psi+, dbf4::Dbf4-3HA-TRP1*
DY-261	MATa, *ura3::URA3[GPD-TK(7x)] ade2-1 trp1-1 can1-100 leu2-3,112 his3-11,15 GAL psi+ dbf4:dbf4ΔN-TRP1*

2.2 Plasmid Construction

pEG-Dbf4-FL and pJG4-6-Mcm2 FL have been previously described (Varrin et al, 2005). pJG4-6-Mcm3, pJG4-6-Mcm5, and pJG4-6-Mcm6 were generated by PCR amplification of genomic *MCM3, MCM5,* and *MCM6,* respectively, from DY-26 with the forward and reverse primers containing Apa1 and Xho1 restriction sites, respectively. pJG4-6-Mcm4 was generated by PCR amplification of genomic *MCM4* from DY-26 with the forward and reverse primers containing Nco1 and Xho1 restriction sites, respectively. pJG4-6-Mcm7 was generated by PCR amplification of genomic *MCM7* from DY-26 with the forward and reverse primers containing Nco1 and EcoR1 sites, respectively. pJG4-6-Mcm2Δ63 was generated by PCR amplification of genomic *MCM2* from DY-26 with the forward and reverse primers corresponding to sequence encoding amino acids 64-868, containing NcoI and XhoI sitesrespectively. pJG4-6-Mcm2 1-63 was generated by PCR amplification of genomic *MCM2* from DY-26 with the forward and reverse primers corresponding to DNA sequence encoding amino acids 1-63, containing BglII and EcoRI sites, respectively. Both pJG4-6-Mcm2 505-868 and pJG4-6-Mcmd2 1-504 were generated by PCR amplification of genomic *MCM2* from DY-1 with the forward and reverse primers corresponding to DNA encoding either amino acids 1-504 or 505-868, containing NcoI and XhoI, respectively. In all cases, the PCR products were kit-purified (GE Healthcare) and then ligated into the appropriately digested vector, followed by transformation of the entire ligation mix into DH5α competent cells. pEG-Cdc7-WT was generated by PCR amplification of the entire *CDC7* from DY-26 genomic DNA with the forward and reverse primers containing EcoRI and BglII, respectively. pEG-202 (Ansubel *et* al., 1995) was then cut with EcoRI and BamHI with the fragment and vector

then ligated thus generating an in-frame fusion with the LexA coding sequence. Both pCM190-Mcm2WT and pCM190-Mcm2Δ63 were generated by PCR amplification of *MCM2* and *mcm2Δ63* from pJG4-6-Mcm2WT and pJG4-6-Mcm2Δ63 with the forward primers corresponding to the gene coding sequence, containing NotI and BamHI respectively. pJG4-6-Mcm2Δ2-4,10-63 was generated by PCR amplification of genomic *MCM2* from DY-26 with a forward primer containing both Nco1 and Nde1 sites followed by the sequence encoding amino acids five through nine and 64-75. The reverse primer corresponded to the C-terminal coding sequence of *MCM2* containing BamH1 and Xho1. pJG4-6-Mcm4Δ175-333 was generated by PCR amplification of two fragments of *MCM4* from DY-26 genomic DNA (encoding amino acids 1-174 and 334-878) which were joined by an Nco1 site that was engineered into the reverse primer of the first fragment and the forward primer of the second fragment. The two cut and purified fragments were cloned together into the pJG vector using Apa1 and Xho1. The plasmid shuffle vector (YCplac111) is a CEN/ARS vector with a *LEU2* selectable marker. The YCplac111-Mcm2WT and YCplac111-Mcm4WT plasmid shuffle vectors were obtained from Megan Davey (Stead et al, 2009; unpublished). The YCplac111-Mcm2WT vector along with pJG4-6-Mcm2Δ2-4,10-63 were cut with Nde1 and BamH1 and the resulting Mcm2Δ2-4,10-63 fragment was cloned into the cut YCplac111 vector in order to generate the mutant plasmid shuffle vector. Mcm4Δ175-333 was PCR amplified using pJG-4-6-Mcm4Δ175-333 as template using a forward primer corresponding to the *MCM4* N-terminal coding sequence and containing Nde1 and a reverse primer corresponding to the C-terminal region of *MCM4*. This PCR product was then cut with Nde1 and Mlu1 (an internal site in Mcm4) and then cloned into the Mcm4FL plasmid shuffle vector which

was also cut with Nde1 and Mlu1 to generate the mutant plasmid shuffle vector. All plasmid constructs were sequenced in order to confirm that no additional mutations had been generated.

2.3 Genomic DNA Isolation

Cells were resuspended in 0.2 ml of DNA isolation mix (2% Triton X-100, 1% SDS, 100 ml NaCl, 10 mM Tris-HCl (pH8), 1 mM EDTA). 0.2 ml of phenol:chloroform (25:24) and 0.3 g of acid-washed glass beads were added and the samples were vortexed for 4 min. 0.2 ml of TE was added and each sample was then centrifuged at 13,000 rpm for 5 min. The top layer was transferred to a new tube and 1 ml of 100% ethanol was added to the samples. After 2 min of centrifugation at 13,000 rpm, the supernatant was discarded and the pellet was resuspended in 0.4 ml TE. RNase A (125 µl/ml) was added to each sample and incubated for 15 min at 37°C. Following incubation, ammonium acetate (0.1 M) was added, followed by 1 ml of 100% ethanol to each tube. The DNA was pelleted by centrifugation for 2 min at 13,000 rpm and the supernatant was discarded. Finally, the pellets were air-dried and resuspended in 50 µl of TE.

2.4 Yeast Two-hybrid Assay

Liquid culture two-hybrid assays were performed as previously described (Ausubel et al, 1995). The lacZ reporter plasmid pSH18-34, pEG-202-derived bait, and pJG4-6-derived prey plasmids were transformed into DY-1. Cultures were grown to an initial concentration of 1 x 10^7 cells/ml in 10 ml of SC medium (Amberg *et al*., 2005) lacking

uracil, histidine, and tryptophan. Cells were then washed in water and induced for 6 h in 20 ml of 2% galactose-1% raffinose medium lacking uracil, hisitidine, and tryptophan. The interactions between the fusion proteins were detected by the quantitative β-galactosidase (β-gal) assay on 5 x 10^6 permeabilized cells. The β-gal activity was determined by the following formula: β-gal activity = 1,000 x A_{420} / (t x V x A_{600}), where t = time of the reaction (in minutes), and V = volume of culture used in the assay (in millitres). Whole cell extracts (WCEs) were obtained from the remaining samples as described in the following section. Protein concentrations were determined by Bradford assays and protein expression was examined by western blot. The LexA-tagged bait proteins were detected using a rabbit polyclonal anti-LexA antibody (ABR), while the HA-tagged prey proteins were detected using a mouse monoclonal anti-HA antibody (Sigma). Alexa Fluor 647 goat anti-rabbit and Alexa Fluor 488 goat anti-mouse polyclonal secondary antibodies (Invitrogen) were used. Detections were performed on a Typhoon 9400 laser scanning system.

2.5 Whole Cell Extract Preparation and Western Blotting

Proteins were isolated using the following method unless otherwise noted. Cells were pelleted at 4000 rpm for 3.5 min and resuspended in 400 ul of ice-cold lysis buffer (10 mM Tris-HCl, pH 8; 140 mM NaCl; 1% Triton X-100; 1 mM EDTA; PMSF and protease inhibitor tablet from Roche, Germany). The suspension was transferred to a 2 ml screw-cap tube containing 0.3 g of 0.5 mm glass beads, on ice. Samples were lysed by 6 cycles of bead beating (Biospec) with 30 sec on/30 sec on ice. The slurry was then spun at 13,000 rpm for 30 sec and the supernatant transferred to a fresh tube. Protein

concentration was assayed immediately (BioRad Protein Assay, BioRad), followed by the addition of a half-volume of sample buffer (60% 4x buffer [15% SDS; 40% glycerol, 166 mM tris-base]; 0.26 M DTT; 7% bromophenol blue) to the sample and boiling for 7 min. The sample was then stored at -20°C until it was run on a 7.5% SDS polyacrylamide gel. The proteins in the polyacrylamide gel were transferred to a nitrocellulose membrane by sandwiching the gel and the membrane between two pieces of Watman paper and sponges in a cassette that was then transferred using an OWL transfer apparatus containing transfer buffer (200 mM glycine; 25 mM tris-base; 20% MeOH; 0.05% SDS). The transfer was carried out at 30-50 volts at 4°C for 2-16 h. The membranes were stained with 0.1% Ponceau S, and imaged. The membranes were then destained with TEN+T (20 mM Tris-HCl; 1mM EDTA; 0.14 M NaCl; 0.05% Tween 20). Detections were carried out by first blocking the membrane in TEN+T with 5% skim milk powder for 45 min at room temperature (RT) or overnight at 4°C. The membrane was then incubated with primary antibody in TEN+T with 5% skim milk powder for 1-2 h at RT with gentle rocking. Following 2-3 washes in TEN+T, the membrane was incubated in secondary antibody in TEN+T for 45 min-1 h at RT with gentle rocking; for Alexaflour antibodies this incubation was carried out in the dark. The membrane was then washed twice in TEN+T and once in dH_2O. Secondary antibodies requiring ECL detection were incubated for 5min with the substrate (Amersham ECL Plus, GE Healthcare) before detection, while Alexaflour secondary antibodies were imaged directly. Imaging was done on a Typhoon 9400 (GE Healthcare) or a Pharos FX Plus (BioRad). Quantifications were carried out using Alpha Imager HP sofware.

Table 2.2: Antibodies used in this study for western blot analysis.

Antibody	Source	Dilution
AlexaFluor 488 donkey anti-goat	Invitrogen	1:2500
AlexaFluor 488 goat anti-mouse	Invitrogen	1:2500
AlexaFluor 647 goat anti-rabbit	Invitrogen	1:2500
HRPO swine anti-goat	CedarLane	1:5000
anti-HA (mouse monoclonal)	Sigma	1:5000
anti-LexA (rabbit polyclonal)	ABR	1:3000
anti-MYC (mouse monoclonal)	Sigma	1:5000
anti-Orc2 (rabbit polyclonal)	S. Gasser	1:1000
anti-Dbf4 (yN-15) (goat polyclonal IgG)	Santa Cruz	1:100
anti-Cdc7 (yN-18) (goat polyclonal IgG)	Santa Cruz	1:100

2.6 Coimmunopreciptation

DY-1 cells were transformed with pCM190- and pJG4-6-derived expression vectors and were initially grown to 1 x 10^7 cells/ml in 10 ml SC medium lacking uracil and tryptophan. Cells were then centrifuged (2,000 x *g*, 3.5 min), after washing with 20 ml dH_2O, the pellet was resuspended in 20 ml of 2% galactose-1% raffinose medium (Sigma) lacking uracil and tryptophan, grown for 6 h, and centrifuged (2,000 x *g*, 3.5 min). All subsequent steps were carried out at 4ºC. Pellets were resuspended in 400 µl ice-cold lysis buffer (50 mM Hepes, pH 7.5; 140 mM NaCl; 1 mM Na-EDTA; 1% Triton X-100) supplemented with protease inhibitor cocktail (Roche) and lysed with a bead beater by using 0.5 g glass beads per sample as described in the previous section. The lysate was centrifuged (13,000 x *g*, 30 s) and the supernatant collected. Supernatant was incubated on a rotating wheel (o/n, 4ºC) with 15 µl protein A sepharose beads saturated with rabbit-α-Myc monoclonal antibody (Sigma). Following incubation, the unbound supernatant was removed and saved and the beads were washed twice in 600 µl of lysis buffer with a final resuspension in 30 µl of lysis buffer.

2.7 Plasmid Shuffle Growth Assays

Spot plate growth assays were performed by growing cells to a concentration of $2x10^7$cells/ml in SC-leu medium. Cultures were then serial diluted and 5 μl aliquots were spotted onto SC-leu plates which were incubated at 30ºC for 2-4 days. Spotting assays for genotoxic sensitivity were performed in the same manner, except that for the Mcm subunit over-expression assay the aliquots were plated on YPD plates supplemented with 20-100 mM HU (Sigma) or 0.01%-0.02% MMS (Sigma), and for the plasmid shuffle genotoxic assay the aliquots were plated on SC-leu supplemented with 20-100mM HU (Sigma), or 0.01%-0.02% MMS (Sigma). Growth curves were generated by growing cultures to a concentration of $5x10^6$cells/ml in SC-leu medium and then diluting the culture to a final starting concentration of $1.67x10^6$cells/ml in SC-leu medium. OD_{600} readings were taken at the indicated timepoints and converted to a cell concentration using the conversion factor of $0.36/1x10^7$cells/ml. The final growth curve is an average of three independent experiments.

2.8 Chromatin Immunoprecipitation (Classic and Modified)

2.8.1 Classic ChIP

50 ml cultures (~$5x10^6$cells/ml) were arrested in YPD with 30 μg/ml α-factor (New England Peptide) for 2.5 h followed by release into YPD lacking the pheromone but containing 50 μg/ml of Pronase E. In experiments requiring it, HU was added to a final concentration of 0.2 M for 1 h, followed by release in drug-free medium. In all cases, proteins were cross-linked with 1% formaldehyde for 30 min at 30ºC with gentle shaking.

The reaction was quenched by the addition of 2.5 ml of 2.5 M glycine and incubation for 5 min at 30ºC. Cultures were centrifuged (4000 x *g*, 4 min) and washed with 40 ml of ice-cold PBS. Cells were pelleted and frozen at -80°C. Cells were resuspended in 400 µl of lysis buffer (50 mM HEPES-KOH, pH 7.5; 140 mM NaCl; 1 mM EDTA; 1% Triton X-100) with protease inhibitor cocktail (Roche) supplemented with fresh PMSF. The cell suspension was transferred to a 2 ml screwcap tube filled ~1/3 full with 0.5 mm glass beads and lysed in a Mini Beadbeater in the cold room (6 rounds of 30 sec), with 30 sec rest on ice between each round. The bottom of the tube was punctured with a heated 25G needle and centrifuged (2000 rpm, 30 sec) into a 2 ml tube placed beneath the screwcap tube in a 14 ml snap-cap tube to separate the cell slurry from the glass beads. The cell slurry was transferred to a 1.5 ml tube and sonicated (5-6 rounds, 20 sec) with a 2 min rest on ice between each round on an Ultrasonix sonicator set for 5-6 watts. Tubes were centrifuged (7000 rpm, 2 min) and the supernatant transferred to a fresh 1.5 ml tube labeled WCE. 25 µl was removed and stored at -20°C as the INPUT. WCE was added to 30 µl previously prepared sepharose beads. 30 µl (per sample) of Protein A sepharose beads (Sigma) were washed 3 times in 200 µl of lysis buffer. Beads were centrifuged (1000 x *g*, 30 sec) and the supernatant removed with a 1cc insulin syringe (BD). Beads were resuspended in 15 µl of lysis buffer to create a 50% slurry. 3 µl of anti-myc antibody (Sigma) was added to the bead slurry and rotated end-over-end overnight at 4°C in parafilm-sealed 1.5 ml tubes. Following the incubation, the supernatant was removed from the beads and the WCE was added to the beads and incubated rotating overnight at 4°C. Following the incubation, the mixture was centrifuged (1000 x *g*, 30 sec). The supernatant was saved and stored at -20°C. The beads were washed twice in 600 µl of

lysis buffer and once in 600 µl of TE. The final TE wash was discarded and the beads resuspended in 60 µl of elution buffer (10 mM Tris-HCl, pH 8; 1 mM EDTA; 1% SDS) and incubated for 10 min at 65°C with mixing every 2 min. Samples were centrifuged (1000 x g, 30 sec) and the supernatant removed and saved as the IP. This elution step was repeated and the supernatant was pooled to generate the final IP sample. 130 µl of elution buffer was added to the IP samples, 100 µl of elution buffer added to the INPUT samples and both were incubated for 6 h at 65°C. Following the incubation, 240 µl TE, 4 µl glycogen (10 mg/ml in dH_2O), and 10 µl Proteinase K (20 mg/ml in dH_2O, Sigma) was added to the IP samples and half of each volume added to the INPUT samples. Samples were incubated for 2 h at 37°C. Following the incubation, 50 µl and 25 µl of 5 M LiCl were added to the IP samples and the INPUT samples, respectively, and the tubes inverted to mix. Equal volumes of phenol:chloroform were added and mixed well before centrifugation (13,000 rpm, 2 min). The top layer was transferred to a fresh tube and 2x volume of 100% EtOH was added. DNA was precipitated overnight at -20°C. Samples were then centrifuged (13,000 rpm, 10 min) and the supernatant discarded. The pellet was washed with a half volume of cold 70% EtOH. Both the IP and INPUT pellets were resuspended in 60 µl of TE and used as template for ChIP PCR. General ChIP PCR reaction mix: 14.6 µl water; 2 µl PCR buffer; 1.2 µl 25 mM $MgCl_2$; 0.2 µl 10 mM dNTP; 0.2 µl 5’ upstream ARS1 primer (50 pmol/µl); 0.2 µl 3’ upstream ARS1 primer; 0.6 µl 5’ ARS1-specific primer; 0.6 µl 3’ ARS1-specific primer; 0.1 µl 5’ downstream ARS1 primer; 0.1 µl 3’ downstream ARS1 primer; 0.2 µl LoFi Taq Polymerase (Fermentas, 5 U/µl). 0.5 µl of INPUT and 2 µl of IP was used as template, and the water volume was adjusted to compensate for the difference in template volume. 5 µl of the resulting PCR

product was run on a 0.8% agarose gel. DNA that was isolated for the classic ChIP as described above was subjected to qPCR analysis. Ingredients for the qPCR reaction were as follows: 2 µl of the isolated DNA; 2 µl Fwd primer (10 µM stock); 2 µl Rev primer (10 µM stock); 40 µl SYBR GREEN mix (BioRad); 34 µl water. The primer pairs were for either the origin-specific sequence or the upstream region. The reaction program was as follows: 95°C, 3 min; 40 x (95°C, 30 sec; 60°C, 20 sec); 95°C, 1 min; 55°C, 1 min; 80 x (55°C, 10 sec) and was run on a BioRad iCycler. Following the reaction, the following equation was used to generate a value for the origin:flanking ratio where Ct is the threshold cycle.

$$2^{(Ct(In)-Ct(IP))}$$

2.8.2 Modified ChIP

The same procedure was followed as for the classic ChIP up to the overnight incubation of the WCE with the beads. For the modified ChIP, following this overnight incubation, the mixture was centrifuged (1000 x g, 30 sec). The supernatant was saved and stored at -20°C. The beads were washed twice in 600 ul of lysis buffer and then resuspended in 40 µl of lysis buffer to which half the sample volume of protein sample buffer was added. The samples were then boiled for 7 min and stored at -20°C until run on a SDS-polyacrylamide gel and immunoblotted.

2.9 Fluorescence Microscopy

All images were taken with live cells. Prior to imaging, cells were grown to ~5 x 10^6 cells/ml in SC medium (2% glucose, 0.02% adenine), washed in ddH_20 and

resuspended in fresh medium. Cultures were diluted with fresh medium to ~1 x 10^6 cells/ml, with 10 μl added to growth chambers for imaging. Chambers were created using depression slides (VWR) filled with SC medium (2% glucose, 0.02% adenine) with 2.4% agar. Once the cells were added to the medium, a glass coverslip was secured using clear nail polish to seal the edges of the coverslip to the slide. Cells were imaged on a Zeiss LSM 510 Meta microscope with a 63X, 1.4 N/A objective lens. To image eYFP, filter sets consisted of exciter HQ500/20x; dichroic 515LP; emitter 520LP. Images were collected with Zeiss AIM software and processed in ImageJ 1.38v (NIH, Bethesda). To obtain a higher signal, 10 fluorescent images were taken in succession and subsequently summed using ImageJ software. Camera gain was adjusted to maximize signal to noise ratios in individual frames.

2.10 DNA Combing

50 ml cultures were grown to a concentration of ~5x10^6 cells/ml at 30ºC and then centrifuged (4000 rpm, 4 min) and resuspended in 2% Gal/1% Raf medium containing 30 μg/ml α-factor for 3.5 h. At the 3 h mark of the incubation, 400 μg/ml of the base analogue CldU was added. Following the incubation, the cultures were washed once in dH_2O and resuspended in 50 ml of fresh Gal/Raf medium with 50 μg/ml Pronase E and 0.2 M hydroxyurea (HU) and 400 μg/ml CldU and incubated for 1 h. Cultures were then washed once in dH_2O and resuspended in 50 ml of fresh YPD with 0.2 M HU and 400 μg/ml CldU and incubated for 3 h. At the 2.5 h mark of this incubation 400 μg/ml of IdU was added. Following this incubation, cells were washed once in dH_2O and resuspended in 50 ml fresh YPD with 400 μg/ml of IdU and 15 ml samples (for plug creation) were

collected at 15 min intervals. 1 ml FACS samples were also taken. The OD_{600} of each collected sample was determined and the cells were pelleted (4000 rpm, 4 min) and resuspended in 1 mL cold 10 mM Tris-HCl, 50 mM EDTA, pH8 and pelleted (13,000 rpm, 1 min) in a microcentrofuge. SCE buffer (1 M Sorbitol, 100 mM sodium citrate, pH8.5, 10 mM EDTA pH8, 0.126% beta mercaptoethanol, 10 U/mL zymolyase) was added to the cells followed by LMP buffer (1.0% low melt agarose, 50 mM EDTA, pH8). The volume of each buffer was calculated as follows: Volume of LMP: (cell density*culture volume)/($2x10^8$); Volume of SCE: 80% of LMP volume. Samples were mixed and 90 µl cast into a BioRad plug cast. Plugs were incubated for 45 min at 4°C to allow the agarose to set. Using a pasteur pipette bulb, the plugs were ejected from the cast into 14 ml snap cap tubes with 0.5 ml of SCE per plug. Typically three plugs were made for each sample. Tubes were stored at 4°C and sent to the Brown Lab at the University of Toronto for downstream processing and imaging as previously described (Versini *et al*., 2003).

2.11 Mating Yeast Strains and Picking Zygotes

Fresh cultures of cells of opposite mating types were grown to ~$5x10^6$ cells/ml. 5 µl of each culture was dropped adjacent to one another on a YPD plate and the drops were then mixed well using a sterile toothpick making a circle about 5 mm in diameter. Once the spot was dry, the plate was incubated at 30°C for 3 h. Following the incubation, a toothpick was used to streak a sample of the mating mixture across the edge of a fresh plate of selective medium (i.e. SC-leu) such that it was visible for use in a tetrad-dissecting microscope. Zygotes were identified (via their distinctive three-lobed

morphology) and plated in the matrix of the plate. Following zygote picking, the plate was incubated at 30°C until colonies formed from the original zygote. These were then transferred to sporulation media in order to begin the sporulation process.

2.12 Sporulation and Tetrad Dissection

Colonies were picked from the zygote plates and used to inoculate sporulation media (1% potassium acetate, amino acids at 25% normal concentration) and incubated at 23°C for 2-3 days until asci were observed. 1 ml of the culture was centrifuged (13,000 rpm, 1 min), washed in dH_2O and resuspended in 50 µl zymolyase solution (0.5 mg/ml in 1 M sorbitol) and incubated for 8-10 min at 30°C. Following incubation, 800 µl of sterile dH_2O was slowly added and the mixture allowed to rest on ice for 5 min. The supernatant was then slowly removed until the original volume was reached (~50-100µl). The tip of a p1000 pipet tip was cut off creating a larger bore tip (thus reducing the stress on the fragile spores) which was used to pipet the culture into a drop on a selective medium plate. The plate was then tilted allowing the drop to run down the plate forming a streak suitable for tetrad dissection. Tetrads were then dissected as per the Singer MSM ascus dissection protocol (Singer Instruments, Sussex, England).

2.13 Synchronizing Yeast Cultures

Synthetic α-factor, one of the *S. cerevisiae* mating pheromones (New England Peptide), was used to synchronize cultures in G1-phase. α-factor was added to each culture (~$5x10^6$ cells/ml) for 1.5-3 h. The actual amount of α-factor used in each experiment was determined by testing each strain, although typically 30 µg/ml was used for most strains. Cell morphology (i.e. few buds and the presence of shmoos), as determined by light

microscopy was used to evaluate the efficiency of the arrest before progressing with the experiment. After the arrest, cells were washed with dH_2O and released into either fresh medium lacking α-factor or the overnight growth medium (as it has a high concentration of Bar protein produced normally by the growing cells which would help degrade the α-factor) containing 50 μg/ml Pronase E (Sigma) which also helps to degrade any remaining α-factor. S-phase synchronization was accomplished through the use of hydroxyurea. Cells were initially diluted to ~$5x10^6$ cells/ml with the addition of 0.2 M HU (Sigma). Cultures were then incubated for 1-2 h (or longer as in the case of the Dbf4 depletion experiments) to arrest the cells. After the arrest, cells were washed with dH_2O and released into fresh medium lacking HU.

2.14 FACS Analysis

1 ml samples were centrifuged (13,000 rpm, 30 sec) and resuspended in 1 ml of 70% ethanol and stored at 4°C until processing. The fixed cells were treated with 500 ul RNase A (200 μg/ml in 50 mM Tris-HCl, pH8) for 2-4 hr at 37°C. This was followed by incubation in 500 μl proteinase K (2 mg/ml in 50 mM Tris-HCl, pH7.5) for 30-60 min at 50°C. Finally, the cells were centrifuged (13,000 rpm, 4 min) and resuspended in 50 μl FACS buffer (200 mM Tris-HCl, pH 7.5; 200 mM NaCl; 78 mM $MgCl_2$) before being transferred to 500 μl Sytox solution (50mM Tris-HCl, pH7.5, 1:5000 dilution Sytox [Molecular Probes; 5mM Sytox in DMSO]) to stain the DNA. Cells were stored at 4°C in the dark until they were analyzed. The analysis was performed with a BD FACSVantage SE cell sorting system in the Molecular Core Facility in the Department of Biology at the University of Waterloo.

Chapter 3: Dbf4 and Cdc7 promote DNA replication through interactions with distinct MCM subunits

Figure 3.3B contributed by Martina Spranger
Figure 3.3C contributed by Nicole Bardehle
Figure 3.8 contributed by Hagen Richter

3.1 Introduction

The minichromosome maintenance (MCM) complex is composed of six distinct subunits (Mcm2-7) that function together as an essential helicase required for DNA replication. The heterohexamer is assembled in the cytoplasm and is then co-imported into the nucleus with Cdt1 (Tanaka and Diffley, 2002). Mcm2-7 is targeted to origins of DNA replication through an interaction between Cdt1 and the Orc6 subunit of the origin recognition complex (ORC) (Semple *et al*., 2006; Chen *et al*., 2007), while the stable loading of two MCM heterohexamers with individual origins is brought about by the sequential hydrolysis of Cdc6- and ORC-bound ATP (Randell *et al*., 2006, Evrin *et al*., 2009, Remus *et al*., 2009). Several MCM subunits then undergo priming phosphorylation by multiple kinases, including Mec1 (Randell *et al*., 2010). In late G1-phase, levels of Dbf4 rise, activating the Dbf4-dependent kinase Cdc7 (DDK), which then phosphorylates primed MCM subunits, thereby stimulating DNA replication.

Several lines of evidence indicate that DDK activates Mcm2-7 by bringing about a conformational change to the complex. The essential function of DDK can be bypassed by the *mcm5-bob1* allele, even though it appears Mcm5 is not itself phosphorylated by DDK (Weinreich and Stillman, 1999; Randell *et al*., 2010). Structural analysis has suggested that this Mcm5 mutant may impart a conformational change to the MCM ring rendering it competent for DNA replication (Hardy *et al*., 1997; Hoang *et al*., 2007). Cell viability can also be rescued in cells lacking DDK activity through phosphomimetic mutations of DDK target sites in an amino terminal region of Mcm4 (the N-terminal Ser/Thr-rich domain or NSD), or by the removal of this domain altogether (Sheu and

Stillman, 2010). This indicates that the NSD plays an inhibitory role in the process of replication initiation, and that the role of DDK is to relieve this inhibition (Sheu and Stillman, 2010). Although the consequences of a DDK-dependant change in Mcm2-7 conformation have not been fully characterized, there is evidence to suggest it may stimulate association with two proteins required for recruiting DNA polymerases to origins, namely Sld3 and Cdc45 (Sheu and Stillman, 2006; Heller *et al*., 2011).

Deregulation of Mcm2-7 function has been implicated as a cause of genomic instability and mammalian cancer phenotypes. Altered levels of MCM subunits have been associated with numerous human cancer types (reviewed in Semple and Duncker, 2004; Gonzalez *et al*., 2005), and mice that are hypomorphic for MCM activity have demonstrated chromosomal abnormalities and a dramatic increase in cancer susceptibility (Shima *et al*., 2007; Chuang *et al*., 2010). Interestingly, although DDK phosphorylation of budding yeast Mcm2 is not required for normal growth, mutation of the two DDK target sites (S164, S170) to alanine rendered cells sensitive to both the DNA damaging agent methyl methanesulfonate (MMS) and caffeine, which inhibits the S-phase checkpoint kinases Tel1 and Mec1 (Stead *et al*., 2011). This suggests a potential role for DDK phosphorylation of Mcm2 in the checkpoint response.

Despite the precise mapping of amino acid residues phosphorylated by DDK (Bruck and Kaplan, 2009; Randell *et al*., 2010; Stead *et al*., 2011), the way in which this kinase complex is targeted to Mcm2-7 is still not well understood. It has been shown previously that two conserved regions of Dbf4 mediate interactions with the MCM complex (motifs C and M; Varrin *et al*., 2005; Jones *et al*., 2010). Mutation of these Dbf4 domains compromises cell growth, DNA replication, and MCM phosphorylation (Varrin

et al., 2005; Francis *et al*., 2009; Harkins *et al*., 2009; Jones *et al*., 2010). Similarly, Sheu and Stillman (2006) have identified a region of Mcm4 that binds to Dbf4/Cdc7, and mutation of this domain reduces the level of Mcm4 phosphorylation by DDK.

This chapter provides evidence that Dbf4 and Cdc7 interact with distinct subsets of the MCM subunits, that deletion of the MCM-interacting region of either protein compromises DNA replication, and that impairment of both the Dbf4- and Cdc7-MCM interactions results in lethality. Strains overexpressing Mcm2 or Mcm4 are also shown to be sensitive to genotoxic agents, while overexpression of Mcm2 in a strain background compromised for the Cdc7-Mcm4 interaction results in a severe growth impairment as well as sensitivity to genotoxic stress.

3.2 Results

3.2.1 Dbf4 and Cdc7 association with subunits of Mcm2-7

In order to determine the way in which DDK associates with the Mcm2-7 complex, the extent to which Dbf4 and Cdc7 are able to interact with each of the MCM subunits was explored. In the case of Dbf4, two-hybrid analysis revealed a robust interaction with Mcm2, and a much weaker, but reproducible, association with Mcm6 (Figure 3.1A). To confirm these results, co-immunoprecipation assays were carried out using extracts from a series of budding yeast transformants overexpressing Myc-tagged Dbf4 and each of the HA-tagged MCM subunits in turn. The interactions observed with the two-hybrid analysis were corroborated as only Mcm2 and Mcm6 were pulled down with Dbf4 (Figure 3.1B). The extent of the Dbf4-Mcm6 interaction however, was comparable to that of Dbf4-Mcm2 by immunoprecipitation. Strikingly, and in contrast to the observations

for Dbf4, no interaction was observed between Cdc7 and either Mcm2 or Mcm6 (Figure 3.2A, B). Instead, both the two-hybrid and co-immunoprecipitation results showed that Cdc7 interacts with both Mcm4 and Mcm5.

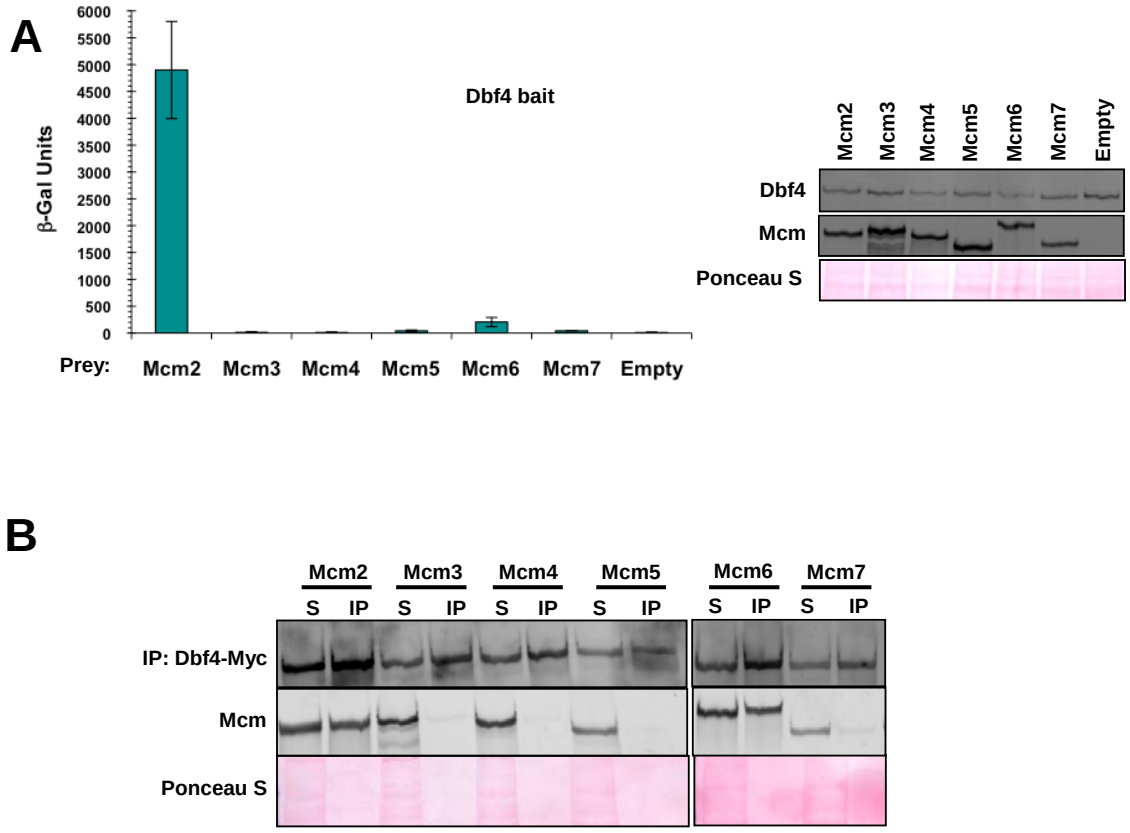

Figure 3.1: Dbf4 interacts with Mcm2 and Mcm6 by yeast-2-hybrid and co-immunoprecipitation. (A) Two-hybrid assays were carried out as described in Materials and Methods using bait construct pEG-Dbf4. pJG-Mcm2, -Mcm3, -Mcm4, -Mcm5, -Mcm6, -Mcm7, and pJG-4-6 (empty) were used as prey. To confirm that all baits and preys were properly expressed, culture aliquots were removed just prior to the measurement of β-galactosidase activity, and whole-cell extracts were prepared and subjected to immunoblot analysis. Bait proteins were detected with rabbit polyclonal anti-LexA antibody (Affinity Bioreagents), and prey proteins were detected with mouse monoclonal anti-HA antibody (Sigma). Ponceau S staining of the membrane was carried out to evaluate relative loading of input samples. (B) Co-immunoprecipitation (IP) experiments were carried out as described in Materials and Methods. Shown are immunoblots of IP and supernatant fractions (S) detected with either monoclonal anti-HA (for Mcm subunit detection) or anti-Myc antibodies (for Dbf4 detection). 20 μg of supernatant and one-fourth of the final bead suspension were loaded for the immunoblot

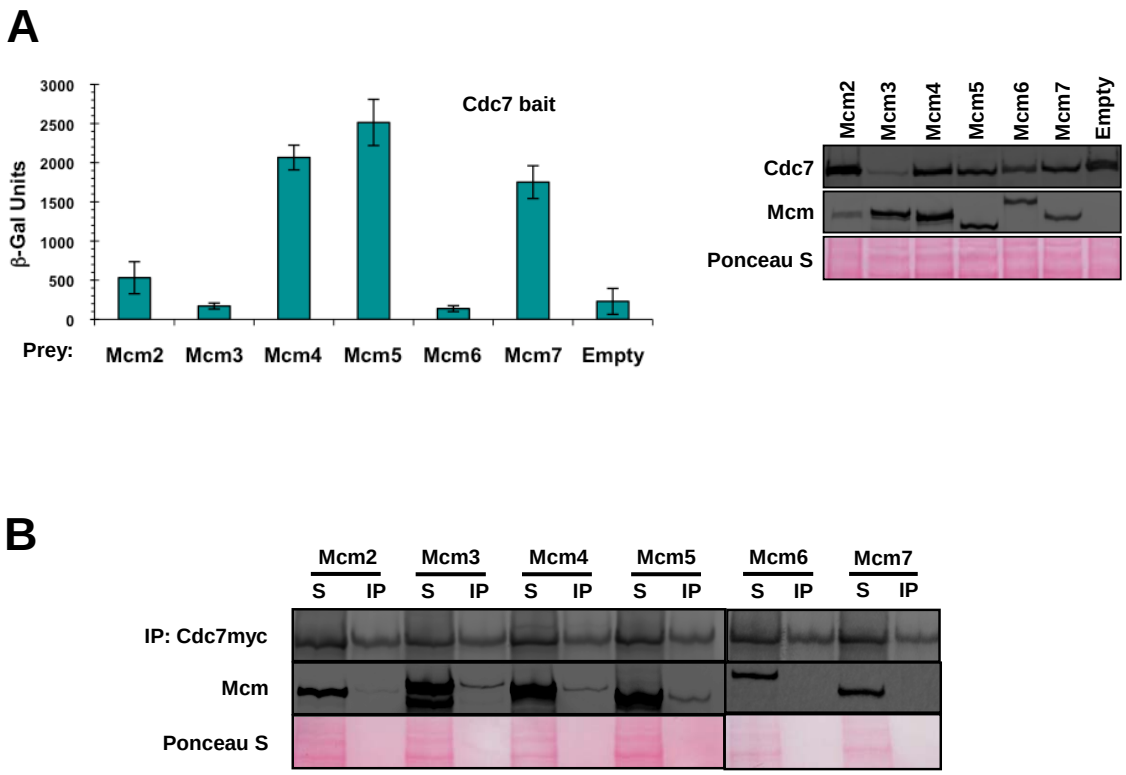

Figure 3.2: Cdc7 interacts with Mcm4 and Mcm5 but not with Mcm2 or Mcm6 by yeast-2-hybrid and co-immunoprecipitation. (A) Two-hybrid assays were carried out as described in Materials and Methods using bait construct pEG-Cdc7. pJG-Mcm2, -Mcm3, -Mcm4, -Mcm5, -Mcm6, -Mcm7, and pGJ4-6 (empty) were used as prey. To confirm that all baits and preys were properly expressed, culture aliquots were removed just prior to the measurement of β-galactosidase activity, and whole-cell extracts were prepared and subjected to immunoblot analysis. Bait proteins were detected with rabbit polyclonal anti-LexA antibody (Affinity BioReagents), and prey proteins were detected with mouse monoclonal anti-HA antibody (Sigma). Ponceau S staining of the membrane was carried out to evaluate relative loading of input samples. (B) Co-immunoprecipitation (IP) experiments were carried out as described in Materials and Methods. Shown are immunoblots of IP and supernatant (S) fractions detected with either monoclonal anti-HA (for Mcm subunit detection) or anti-Myc antibodies (Cdc7 detection). 50 μg of supernatant and one-fourth of the final bead suspension were loaded for the immunoblot.

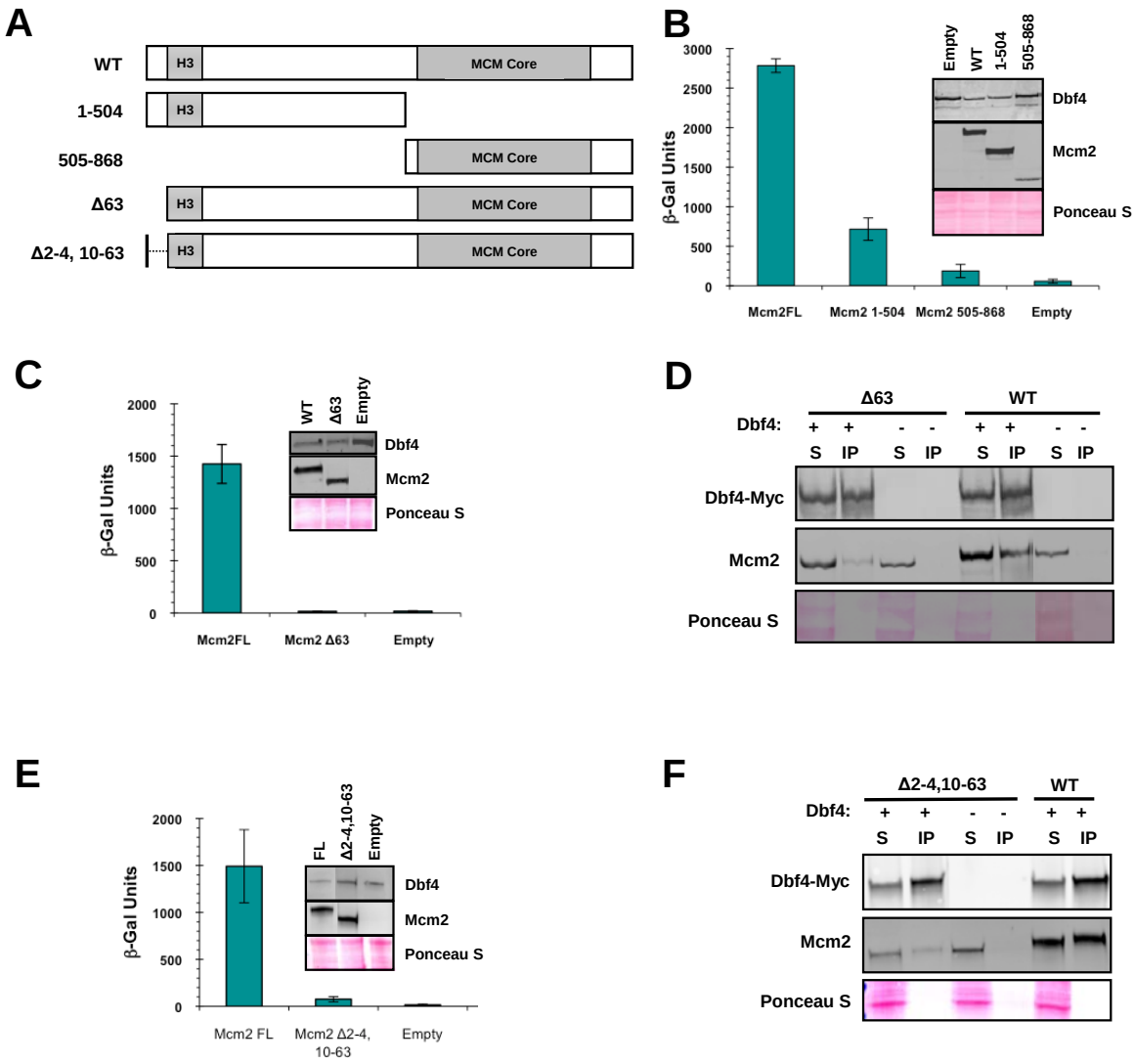

Figure 3.3: Mcm2 N-terminal deletion mutants have a reduced interaction with Dbf4 by yeast-2-hybrid and co-immunoprecipitation. (A) Schematics of full-length and truncated Mcm2 mutant constructs used in this study. (B, C, and E) Two-hybrid assays were carried out as described in Materials and Methods using bait construct pEG-Dbf4. pJG-Mcm2FL, -Mcm2 1-504, -Mcm2 505-868, -Mcm2Δ63, -Mcm2Δ 2-4,10-63, and pJG-4-6 (empty) were used as prey. Immunoblot analysis to verify bait and prey expression were carried out as described in the legend for Fig. 1. (D and F) Co-immunoprecipitation (IP) experiments were carried out as described in Materials and Methods. Shown are immunoblots of IP and supernatants (S) detected with either monoclonal anti-HA (for Mcm detection) and anti-Myc antibodies (for Dbf4 detection). 20 ug of input and one-fourth of the final bead suspension were loaded for the immunoblot.

Figure 3.4: Mcm2Δ2-4, 10-63 interacts with Mcm6 by yeast-2-hybrid. (A) Two-hybrid assays were carried out as described in Materials and Methods using bait construct pEG-Mcm2. pJG-Dbf4, -Mcm2, -Mcm3, -Mcm4, -Mcm5, Mcm6, -Mcm7, and pJG-4-6 (empty) were used as prey. Immunoblot analysis to verify bait and prey expression was carried out as described in the legend for Figgure 1. (B) Two-hybrid assays were carried out as described in Materials and Methods using prey constructs pJG-Mcm6 and pJG-4-6 (empty). pEG-Mcm2 and pEG-Mcm2Δ2-4,10-63 were used as bait. Immunoblot analysis to verify bait and prey expression was carried out as described in the legend for Figure 1.

A

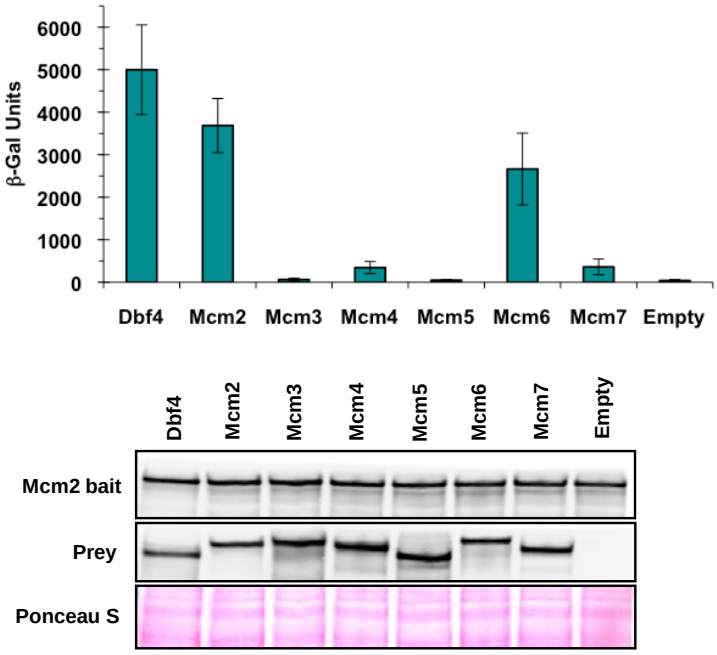
β-Gal Units
6000
5000
4000
3000
2000
1000
0
Dbf4
Mcm2
Mcm3
Mcm4
Mcm5
Mcm6
Mcm7
Empty
Mcm2 bait
Prey
Ponceau S

B

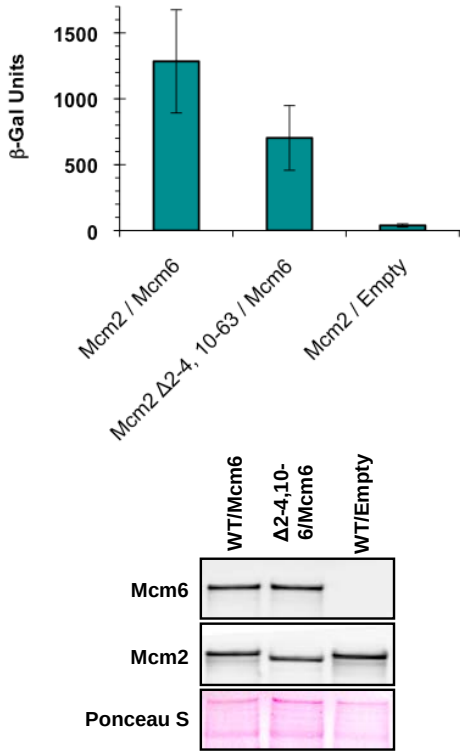
β-Gal Units
1500
1000
500
0
Mcm2 / Mcm6
Mcm2 Δ2-4, 10-63 / Mcm6
Mcm2 / Empty
WT/Mcm6
Δ2-4,10-6/Mcm6
WT/Empty
Mcm6
Mcm2
Ponceau S

Since Mcm2 was shown to be the major MCM subunit targeted by Dbf4, this interaction was examined in greater detail. A series of MCM2 truncation mutants were constructed (Figure 3.3A), and the ability of the corresponding proteins to interact with Dbf4 was assessed, as above. Neither the N-terminal (1-504) nor C-terminal (505-868) Mcm2 fragment was sufficient to mediate normal levels of binding to Dbf4 (Figure 3.3B). Because removal of the Mcm2 N-terminal region reduced the association with Dbf4 to a greater extent, this region of the protein was dissected further. Ultimately, it was determined that removal of the N-terminal 63 amino acids was sufficient for abrogation of the Mcm2-Dbf4 interaction (results not shown; Figure 3.3C, D). Mcm2-7 is targeted to the nucleus by two nuclear localization signals (NLS), one of which is located near the N-terminus of Mcm2 (amino acids 5-9, Liku et al., 2005). While the expression constructs used for the association assays described above included NLS sequences, in an effort to explore the effect of the native Mcm2 NLS on the Dbf4-Mcm2 interaction, this NLS sequence was restored to the Mcm2Δ63 construct, thus creating Mcm2Δ2-4,10-63 Figure 3.3A). As with the original N-terminal truncation, association with Dbf4 was disrupted with this mutant (Figure 3.3E, F). Of all the other MCM subunits, Mcm2 was shown to interact most strongly with Mcm6 (Mcm2's neighbor in the MCM ring complex), and this interaction was not significantly changed by the Δ2-4,10-63 mutation (Figure 3.4A, B).

Consistent with these findings, previous work from the Stillman lab has identified a region of Mcm4 (amino acids 175-333) which mediates association with Cdc7 and that is referred to as the DDK-docking domain (DDD; Sheu and Stillman, 2006). In light of this, the relative importance of the Dbf4-Mcm2 and Cdc7-Mcm4 interactions for cell

proliferation and DNA replication was explored, using the Mcm2Δ2-4,10-63 and Mcm4Δ175-333 mutants. Strains were established for which the single genomic copy of either *MCM2* or *MCM4* was deleted, and growth was supported by CEN (single copy per cell) plasmid-based expression of either wild-type or mutant Mcm2 or Mcm4 (plasmid shuffle strains, Figure 3.5). When Mcm2Δ2-4,10-63 and Mcm4Δ175-333 were used to support growth in *mcm2* and *mcm4* deletion strains, respectively, modest growth impairment was observed relative to wild-type controls (Figure 3.6A). Subsequently, DNA replication was assessed in these same strains. Log phase cultures were arrested in late G1 phase using the mating pheromone α-factor, followed by removal of the α-factor to allow for a synchronous release into the cell cycle. Both the Mcm2Δ2-4,10-63 and Mcm4Δ175-333 strains showed slight but reproducible defects in S-phase progression compared to their wild-type counterparts (compare FACS profiles at 40 min in Figure 3.6B, and at 35 min in Figure 3.6C).

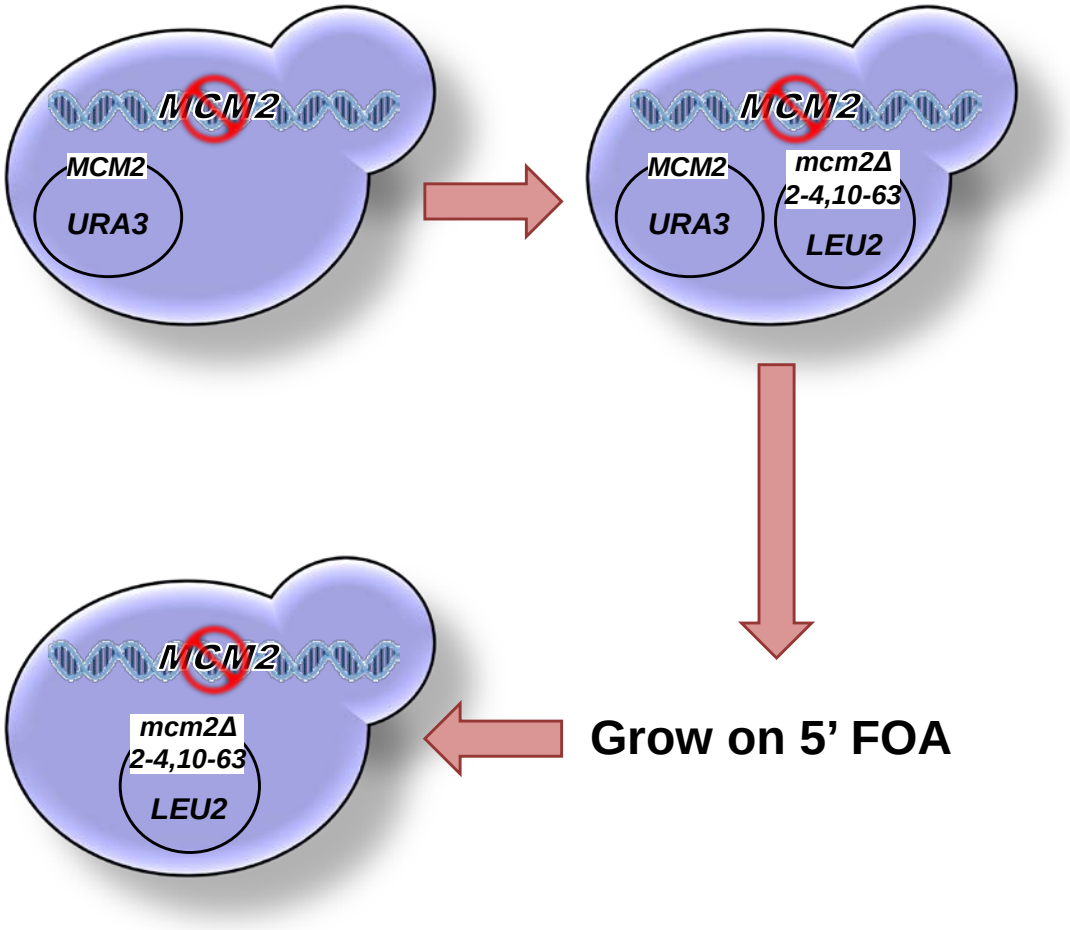

Figure 3.5: Schematic of the creation of plasmid shuffle strains. Mcm2 is used as the example. Strains for which the single genomic copy of either MCM2 or MCM4 was deleted was supported for growth with by a CEN (single copy per cell) plasmid containing a URA3-selectable marker expressing wild-type MCM2 or MCM4. This strains was then transformed with a second CEN plasmid containing a LEU2-selectable marker expressing either wild-type or mutant Mcm2 or Mcm4. Transformants were then grown on medium containing 5' fluoroorotic acid (FOA) which selects for cells that have lost the original URA3 plasmid. This results in a cell where the only source of Mcm2 or Mcm4 is from the CEN LEU2 plasmid.

The above results indicated that abrogation of either the Dbf4-Mcm2 or Cdc7-Mcm4 interaction had only minor consequences for DNA replication and cell cycle progression. This suggests that either one of these interactions is sufficient to target the DDK complex to Mcm2-7 and allow it to phosphorylate the critical MCM residues required to trigger DNA replication. To investigate whether the Dbf4-Mcm2 and Cdc7-Mcm4 interactions represent redundant targeting mechanisms, the Mcm2Δ2-4,10-63 and Mcm4Δ175-333 strains were crossed, sporulation was induced in the diploids, and the resultant tetrads were dissected. Of 55 spores analyzed, none were *mcm2Δ*, *mcm4Δ* supported by episomal Mcm2Δ2-4,10-63 and Mcm4Δ175-333. Conversely, in a control cross of the Mcm2 and Mcm4 wild-type plasmid shuffle strains, 10 of 36 spores analyzed were *mcm2Δ*, *mcm4Δ* supported by episomal Mcm2WT and Mcm4WT. These results suggest that the combination of Mcm2Δ2-4,10-63 and Mcm4Δ175-333 is synthetic lethal, consistent with a model whereby disruption of the redundant Mcm2-Dbf4 and Mcm4-Cdc7 interactions simultaneously, prevents targeting of the DDK complex to Mcm2-7.

Given the lethality of the Mcm2Δ2-4,10-63/Mcm4Δ175-333 combination, an induced disruption of the Mcm2-Dbf4 interaction in cells compromised for the Mcm4-Cdc7 association was investiagted. This was done by transforming the Mcm4Δ175-333 and Mcm4WT strains with either a doxycycline repressible Mcm2 expression vector, or an empty vector control. When doxycycline was present, all four transformants demonstrated comparable growth (Figure 3.7A). In the Mcm4WT strain, the absence of doxycycline and consequent overexpression of Mcm2 resulted in mild growth effects (Figure 3.7A, B), consistent the notion that surplus Mcm2 is able to partially titrate the DDK complex from the Mcm2-7 ring, through its interaction with Dbf4. Strikingly, when

Mcm2 was overexpressed in the Mcm4Δ175-333 strain, the growth defect was much more severe, supporting a model whereby simultaneous disruption of the Dbf4-Mcm2 and Cdc7-Mcm4 interactions compromises the ability of the DDK complex to associate with Mcm2-7.

3.2.2 Increased MCM subunit levels and the S-phase checkpoint

It was previously reported that Dbf4 motif C mutants that are compromised for their interaction with Mcm2 are hypersensitive to genotoxic stress (Jones et al., 2010). This is consistent with the idea that Dbf4/Cdc7 may help to stabilize and/or restart replication forks under checkpoint conditions by associating with Mcm2-7 and phosphorylating the helicase or another fork component. To investigate whether changes in the abundance of MCM subunits that impact Dbf4/Cdc7 targeting would have a similar effect, yeast strains were generated in which the genomic promoters controlling expression of individual MCM genes were replaced with a strong GAL1 promoter. This resulted in the ability to overexpress each of the MCM subunits individually. When these strains were exposed to the DNA alkylating agent methyl methanesulfonate (MMS) or the ribunuclease reductase inhibitor hydroxyurea (HU), both of which impede replication fork progression, those overexpressing Mcm2 and Mcm4 were highly sensitive, whereas those overexpressing other subunits were not (Figure 3.8). These results are consistent with the notion that excess Mcm2 and Mcm4 can compete with the Mcm2-7 ring for interaction with Dbf4 and Cdc7, respectively. This ‘loosening’ of the Dbf4/Cdc7 association with the MCM helicase, then, would have a more severe consequence under conditions of replication stress. Mcm4Δ175-333 cells overexpressing Mcm2 were subjected to the same genotoxic

compounds and it was observed that these cells were more sensitive than those overexpressing Mcm2 with wild-type Mcm4 present (Figure 3.9). This is consistent with the idea that the ability to respond to replication stress is correlated to the degree of impairment of the association between Dbf4/Cdc7 and the Mcm2-7 complex.

Figure 3.6: Mcm2Δ2-4,10-63 and Mcm4Δ175-333 impede growth and S-phase progression. Plasmid shuffle was performed as described in the Materials and Methods. CEN/ARS plasmid constructs YCplac111-Mcm2WT, -Mcm2Δ2-4, 10-63, and -empty were transformed into a mcm2::his3 background supported for growth by Mcm2WT on a URA+ CEN/ARS plasmid; YCplac111-Mcm4WT, -Mcm4Δ175-333, and -empty were transformed into a mcm4::KanMX background supported for growth by Mcm4WT on a URA+ CEN/ARS plasmid. Transformant colonies were plated on selective medium containing FOA to select for loss of the URA+ plasmids. (A) Plasmid shuffle strains containing the YCplac111 constructs were grown in selective medium and the cell concentration determined at the indicated timepoints. Error bars represent the standard deviation of three independent experiments. (B and C) Cultures of the plasmid shuffle stains were arrested in α-factor (30 µg/ml) for 2.5 hrs followed by release into pheromone-free medium containing 50 µg/ml of pronase E (Sigma) with samples taken at the indicated intervals for FACS analysis.

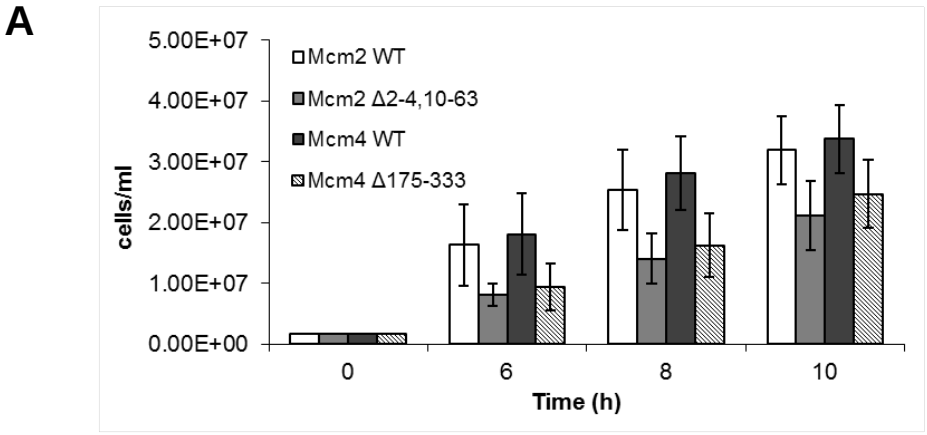
A
5.00E+07
4.00E+07
3.00E+07
2.00E+07
1.00E+07
0.00E+00
cells/ml
Mcm2 WT
Mcm2 Δ2-4,10-63
Mcm4 WT
Mcm4 Δ175-333
0
6
8
10
Time (h)

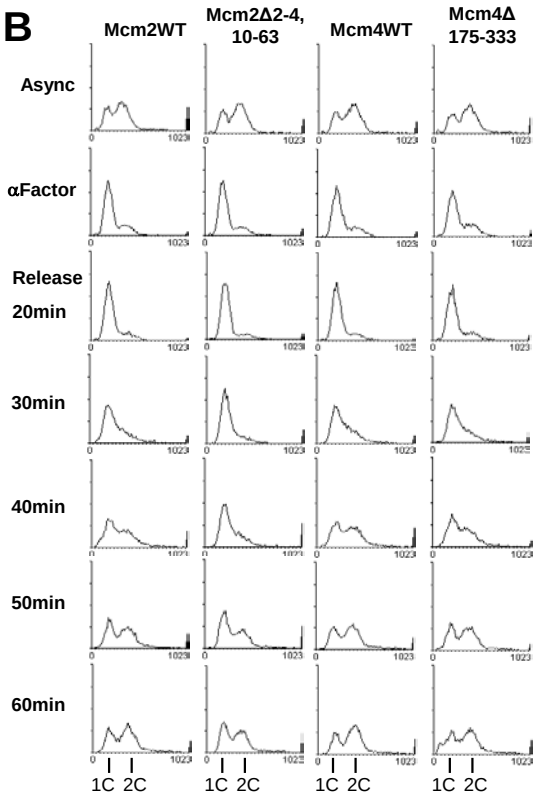
B
Mcm2WT
Mcm2Δ2-4, 10-63
Mcm4WT
Mcm4Δ 175-333
Async
αFactor
Release 20min
30min
40min
50min
60min
1C 2C

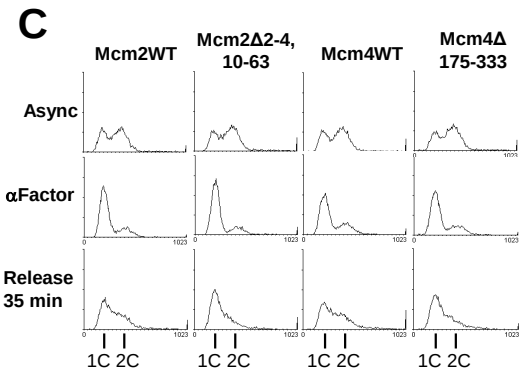
C
Mcm2WT
Mcm2Δ2-4, 10-63
Mcm4WT
Mcm4Δ 175-333
Async
αFactor
Release 35 min
1C 2C

Figure 3.7: Overexpression of Mcm2 in the presence of Mcm4Δ175-333 further inhibits growth. Mcm4WT and Mcm4Δ175-333 plasmid shuffle strains were transformed with either pCM190-Mcm2FL in which Mcm2 expression is under the control of a doxycycline (DOX)-repressible promoter, or pCM190 (empty) vector. (A) 10-fold serial dilutions of each transformant were spotted on selective medium with or without DOX, with a starting concentration of 1 x 107 cells/ml. Plates were incubated at 30ºC for 2 days. (B) The transformed plasmid shuffle strains were grown in selective medium without DOX and the cell concentration determined at the indicated timepoints. Error bars represent the standard deviation of three independent experiments.

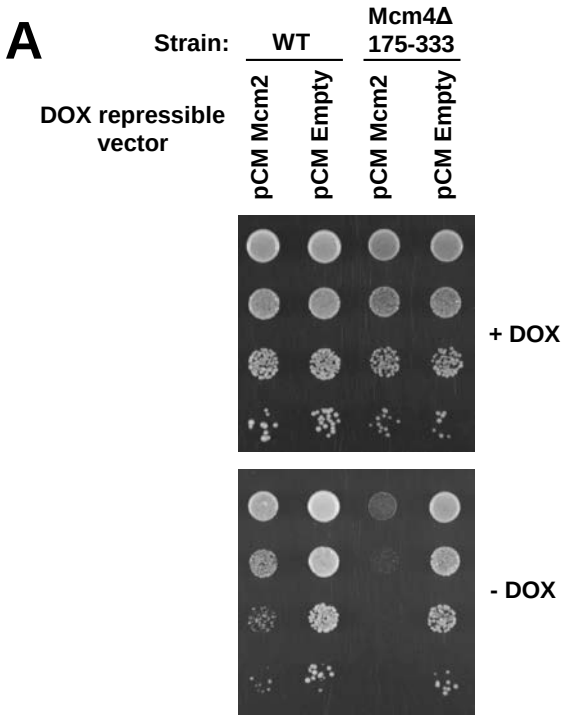
A
Strain:
WT
Mcm4Δ 175-333
DOX repressible vector
pCM Mcm2
pCM Empty
pCM Mcm2
pCM Empty
+ DOX
- DOX

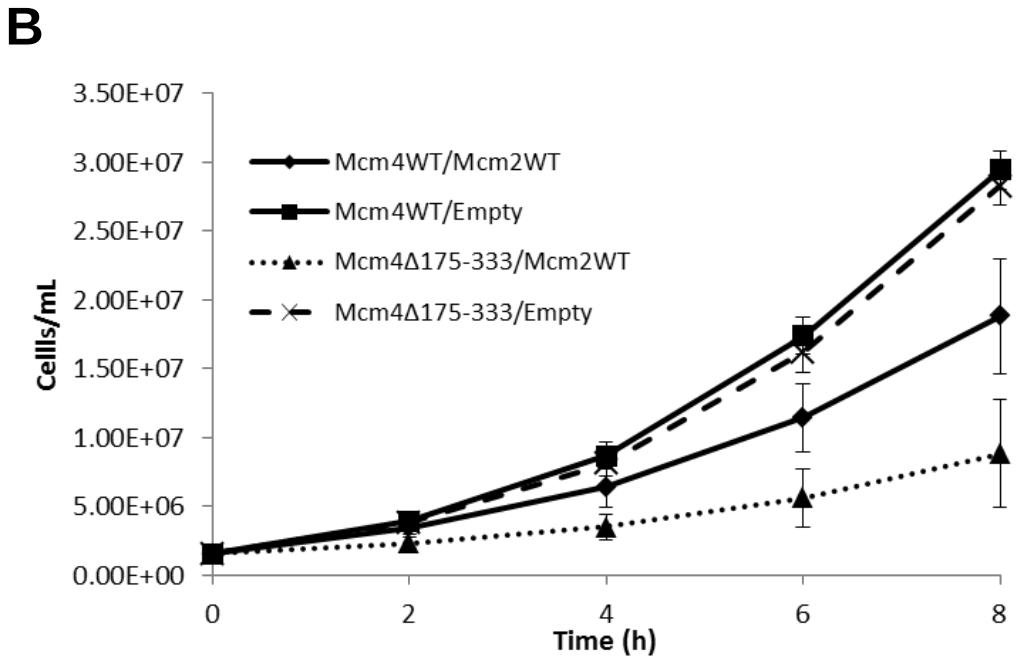
B
3.50E+07
3.00E+07
2.50E+07
2.00E+07
1.50E+07
1.00E+07
5.00E+06
0.00E+00
Cells/mL
Mcm4WT/Mcm2WT
Mcm4WT/Empty
Mcm4Δ175-333/Mcm2WT
Mcm4Δ175-333/Empty
0
2
4
6
8
Time (h)

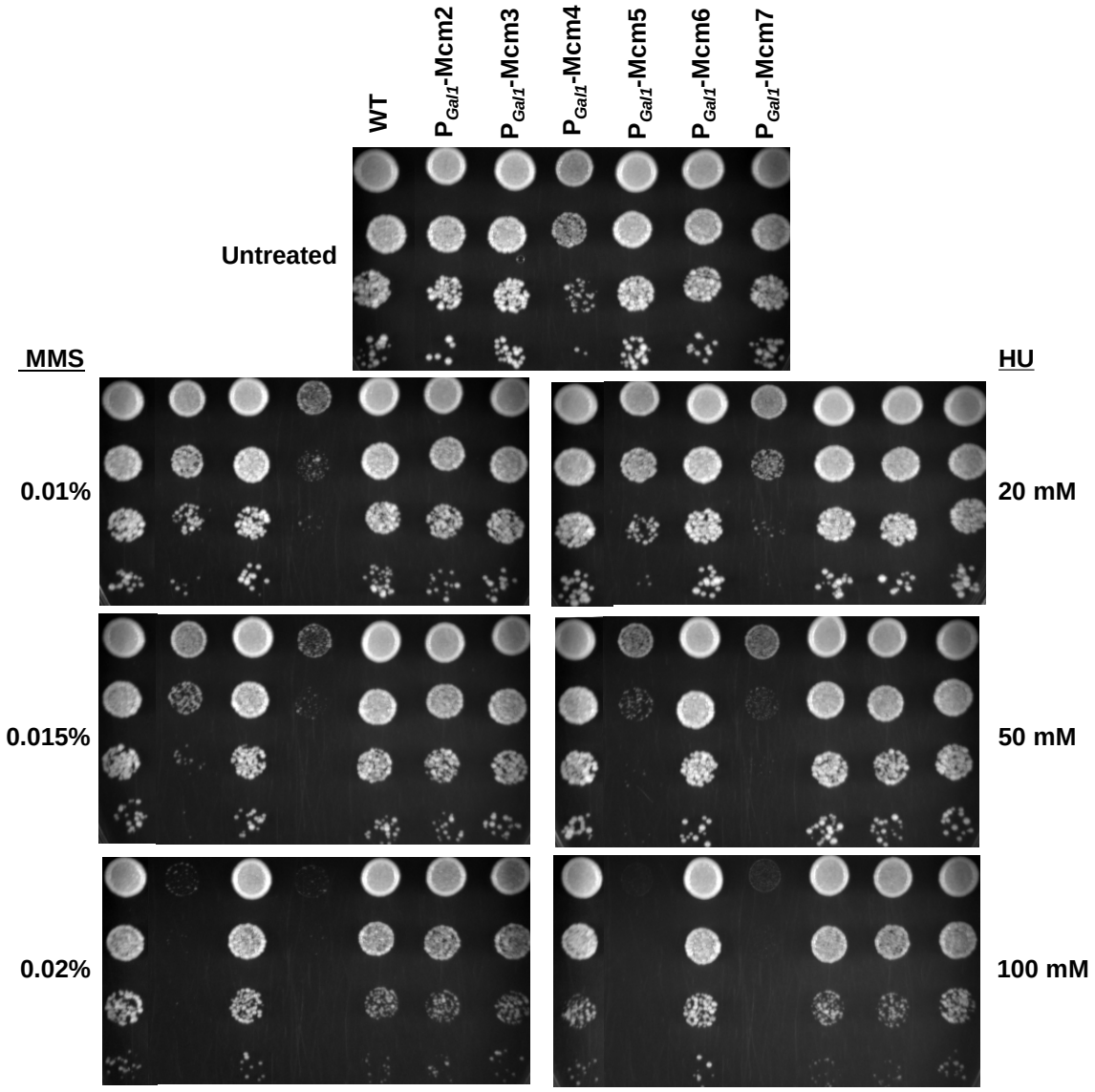

Figure 3.8: Overexpression of Mcm2 and Mcm4 impart sensitivity to genotoxic agents. The endogenous promoters for each of the Mcm2-7 subunits were individually replaced with a strong GAL1 promoter. A) 10-fold serial dilutions of each Mcm-subunit overexpression strain were plated on YPD containing the indicated concentrations of HU or MMS with a starting concentration of 1 x 10^7 cells/ml. Plates were grown at 30ºC for 3 days.

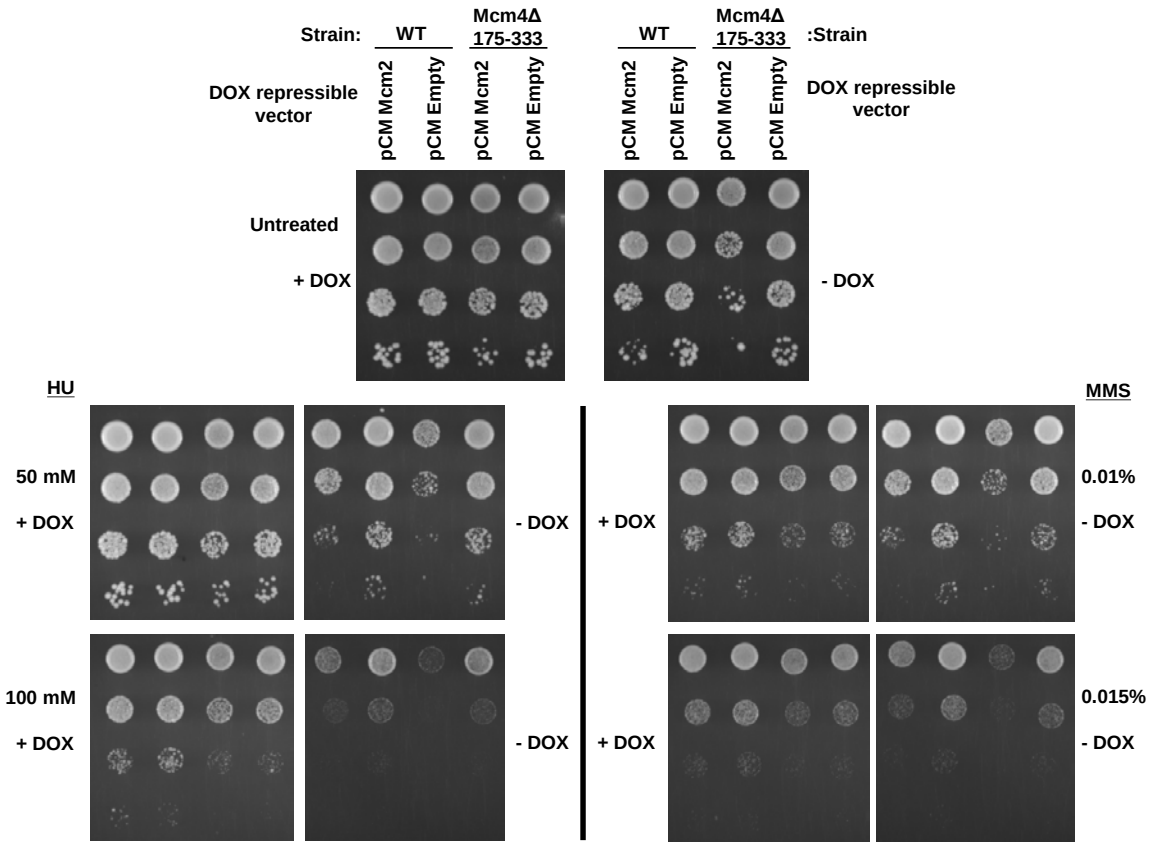

Figure 3.9: Strains overexpressing Mcm2 in the presence Mcm4Δ175-333 are sensitive to genotoxic agents. Mcm4WT and Mcm4Δ175-333 plasmid shuffle strains transformed with either pCM190-Mcm2FL or pCM190 (empty) were tested for sensitivity to genotoxic agents. 10-fold serial dilutions of each transformed strain were plated on selective medium containing the indicated concentrations of HU or MMS and with or without DOX with a starting concentration of 1 x 10^7 cells/ml. The plates were incubated at 30ºC for 4 days.

3.3 Discussion

3.3.1 The Dbf4-Mcm2 and Cdc7-Mcm4 interactions

Previous studies have shown that DDK acts locally throughout S-phase to bring about the sequential activation of early-, middle- and late-firing origins of DNA replication (reviewed in Pasero and Schwob, 2000). Although it had been well established that the critical physiological targets of DDK are Mcm2-7 subunits, little was known about the way in which this essential replicative kinase is targeted to the MCM complex.

The data presented in Figures 3.1 and 3.2 represent the first systematic examination of the way in which the two DDK complex subunits, Dbf4 and Cdc7, each contribute to the interaction with Mcm2-7. In the case of Dbf4, these results suggest that the major interaction is with Mcm2, while an association with Mcm6, which lies adjacent to Mcm2 in the MCM ring (Davey *et al*., 2003), was also observed. Strikingly, these two MCM subunits were not among those we found to associate with Cdc7. These observations are consistent with previous work indicating that Dbf4, but not Cdc7, binds tightly to Mcm2 (Bruck and Kaplan, 2009). Examination of various Mcm2 domains revealed that residues in both the N- and C-terminal halves of the protein participate in the Dbf4 interaction, though the N-terminus appeared to make the larger contribution. The identification of a region encompassing most of the N-terminal 63 amino acids as being required for interaction with Dbf4, represents a heretofore uncharacterized functional domain in the protein. Interestingly, a second Mcm2 region spanning amino acids 204-278, has also been reported to mediate interaction with Dbf4, although the effect of removing this region from full-length Dbf4 was not evaluated (Bruck and Kaplan, 2009). Along with the observations for Dbf4, the identification of Mcm4 and Mcm5 as interaction partners

for Cdc7 indicates that the two DDK complex components interact with mutually exclusive subsets of the MCM subunits. This suggests at least two mechanisms for DDK complex interaction with the MCM ring. In the first scenario, both Dbf4-MCM and Cdc7-MCM interactions are required for DDK targeting, ensuring that free Dbf4 or Cdc7 does not interfere with the association of the complex. A second possibility is that the interactions are largely redundant, but promote a more efficient DDK complex-MCM association, and minimize the consequences of mutations that might interfere with either subunit interaction alone. The results presented in this chapter clearly support the latter model (Figure 3.10). The identification of a short N-terminal Mcm2 region necessary for interaction with Dbf4, along with data from the Stillman lab identifying a region of Mcm4 that docks with Cdc7 (Sheu and Stillman, 2006), allowed the investigation of the relatively minor effects of disrupting the Dbf4-Mcm2 and Cdc7-Mcm4 interactions on their own, with the severe consequences of abrogating both targeting mechanisms. Although Mcm5 and Mcm6 were identified as additional binding partners for Cdc7 and Dbf4, respectively, the synthetic lethality observed when combining the Mcm2Δ2-4,10-63 and Mcm4Δ175-333 mutations, suggests that the combined effect of Cdc7-Mcm5 and Dbf4-Mcm6 interactions is not sufficient to target the DDK complex to Mcm2-7. Nevertheless, it would be of interest to evaluate the relative importance of these additional interactions for cell cycle progression in future studies.

Figure 3.10: Model for the interaction of Dbf4 and Cdc7 to subunits of the Mcm2-7 complex. (A) Dbf4 interacts with Mcm2 and Cdc7 interacts with Mcm4. DDK phosphorylation of Mcm4 leads to normal DNA replication. (B) and (C) The Dbf4-Mcm2 interaction or the Cdc7-Mcm4 interaction alone is sufficient for DDK complex association with Mcm2-7 and phosphorylation of Mcm4. D) Abrogation of both the Dbf4-Mcm2 and the Cdc7-Mcm4 interactions prevent DDK interaction with Mcm2-7.

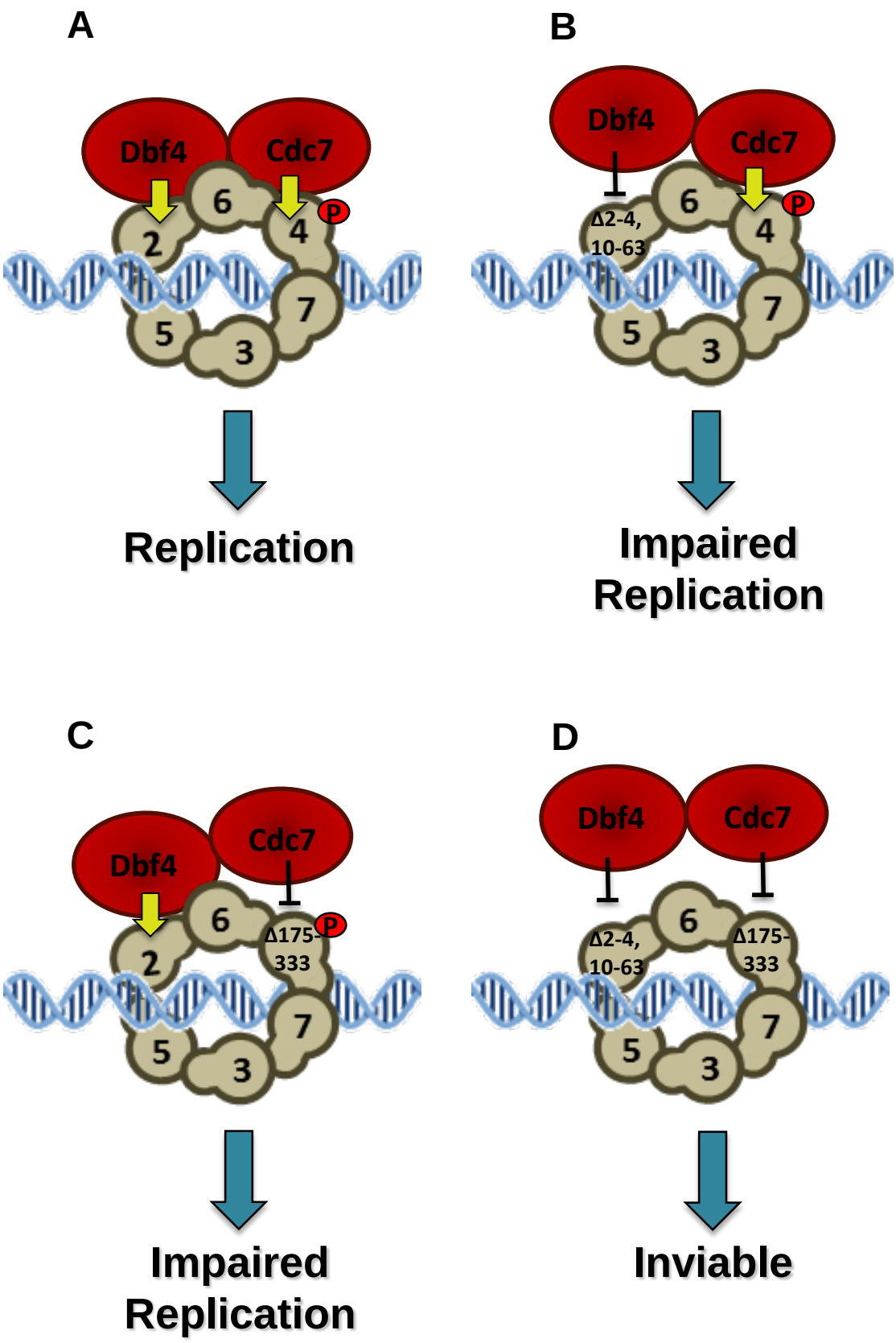
A
Dbf4
Cdc7
6
2
4
P
7
5
3
Replication
B
Dbf4
Cdc7
Δ2-4,
10-63
6
4
P
7
5
3
Impaired
Replication
C
Dbf4
Cdc7
6
Δ175-
333
P
2
7
5
3
Impaired
Replication
D
Dbf4
Cdc7
Δ2-4,
10-63
6
Δ175-
333
7
5
3
Inviable

3.3.2 MCM subunit overexpression and the S-phase checkpoint

The observation that genotoxic compounds exacerbated the growth impairment in cells overexpressing Mcm2 in the presence of Mcm4Δ175-333 is reminiscent of the effect imparted by Dbf4 C motif mutants which are compromised for interaction with Mcm2 (Jones *et al*., 2010). Furthermore, recent data from the Davey lab demonstrated similar sensitivity when the two Mcm2 DDK target sites (serines 164 and 170) were mutated to alanine (Stead *et al*., 2011), suggesting that efficiency of DDK complex targeting to the MCM ring may be particularly important during conditions of replication stress. An intriguing possibility is that DDK phosphorylation of one or more MCM subunits may help to stabilize and/or restart stalled or blocked replication forks. Another possible scenario is that interaction with the MCM ring serves to direct DDK to other targets at or near the forks. Candidates include Cdc45 and the polα-primase complex, both of which are DDK substrates (Weinreich and Stillman, 1999; Nougarede *et al*., 2000), as well as histone H3, since its phosphorylation by DDK has recently been shown to play a role in maintaining genomic integrity (Baker *et al*., 2010).

Intriguingly, a number of the phenomena described here for budding yeast mirror findings in higher eukaryotes. For example, roles for both Mcm2-7 and Dbf4/Cdc7 during replication stress have been identified in *Xenopus* (Woodward *et al*., 2006; Tsuji *et al*., 2008) and altered abundance of both MCM and DDK subunits have been implicated in human cancers (Bonte *et al*., 2008; Lau *et al*., 2010). The extent to which the Dbf4-Mcm2 and Cdc7-Mcm4 interactions are conserved, influence control of DNA replication and help preserve genome integrity in metazoan organisms is an important subject for future study.

Chapter 4: Dbf4 and Cdc7 at origins – an investigation of DDK action using chromatin immunoprecipitation

4.1 Introduction

In *Saccharomyces cerevisiae*, origins of DNA replication are ordered in a temporal fashion such that some origins fire earlier in S-phase than others, leading to their classification as either early-, mid-, or late-firing origins (Raghuraman *et al*., 2001). While the timing of each origin's firing is quite regimented, the way in which the cell regulates this timing is unknown (reviewed in Goldar *et al*., 2009). There is however, some evidence that points to the involvement of the checkpoint kinase Rad53 in this regulation. The Rad53 *mec2-1* mutation impairs Rad53 for its checkpoint activity and when origin timing was monitored in *rad53* mutants under both normal and checkpoint conditions, it was observed that origins that normally fire later in S-phase actually fire precociously (Santocanale and Diffley, 1998; Shirahige *et al*., 1998). This indicates that Rad53 may play a role in preserving the temporal order of origin firing. The action of the Dbf4-dependant kinase Cdc7 (DDK) is required at the onset of S-phase and it has been hypothesized that DDK acts as the final trigger to initiate replication at the level of origins (reviewed in Sclafani and Holzen, 2007). It remains unclear however, whether the active DDK associates with all origins at the beginning of S-phase (in which case DDK activity, while essential, would not be the final trigger for initiation) or if it associates in a sequential manner with early-, mid-, and late-firing origins to activate them (i.e. acting as the final trigger for initiation).

The levels of Cdc7 have been shown to be relatively constant throughout the cell cycle while the levels of Dbf4 fluctuate, thus allowing for the regulation of DDK activity (Pasero *et al*., 1999; Weinreich and Stillman, 1999). It has also been shown that a fraction of cellular Cdc7 is chromatin bound throughout the cell cycle; however it must be noted

that chromatin bound does not necessarily mean origin bound (Weinreich and Stillman, 1999). While the phosphorylation targets of DDK have been mapped, the way in which the kinase is targeted to origins remains unclear. While Chapter 3 of this thesis addresses the contributions made by various subunits of DDK and the MCM complex in their binding, the question remains as to whether the active complex is targeted to origins at the time of origin firing (i.e. Cdc7 is bound to non-origin chromatin regions until re-directed to origins by Dbf4 at the time of origin firing) or if Cdc7 binds origins throughout the cell cycle and is activated by Dbf4 upon its arrival and binding at origins thus triggering origin firing and DNA replication.

Chromatin immunoprecipitation (ChIP) is a tool that allows for the investigation of DNA sequences bound by a protein of interest and has a much higher resolution than other protein-chromatin assays (such as a chromatin fractionation assay, Tanaka, 2001). By designing PCR primers that amplify a specific region of DNA (i.e. origin DNA) the association pattern of a protein with that region can be determined. In this chapter ChIP is used in an attempt to discern the temporal association pattern of Dbf4 and Cdc7 with early and late origins and elucidate the most likely targeting model of DDK recruitment to origins of replication. Evidence is presented for the potential existence of a pool or reservoir of Dbf4 in the upstream origin flanking region which may redistribute to the origin at the time of firing. Attempts to optimize the ChIP protocol have also led to the development of a modified ChIP assay which has the potential to circumvent technical issues inherent in the ‘classic’ ChIP assay and initial results point to a possible model for the temporal association of Dbf4 with origins.

Figure 4.1: Schematic of the chromatin immunoprecipitation (ChIP) protocol. A detailed protocol is found in the Materials and Methods (Chapter 2). Briefly, proteins are crosslinked to DNA in live yeast cells using formaldehyde followed by cell lysis and sonication to shear the DNA into fragments that average 0.5-1.0 kb in length. The protein of interest is immunoprecipitated using antibody-coated beads while a sample of the whole cell extract (WCE) is reserved as the input (In) sample. The crosslink is reversed in both the IP and In samples and the DNA is isolated. This DNA then serves as the template for a PCR using both origin-specific primer pairs as well as non-specific (i.e. up- and down-stream) primer pairs as controls.

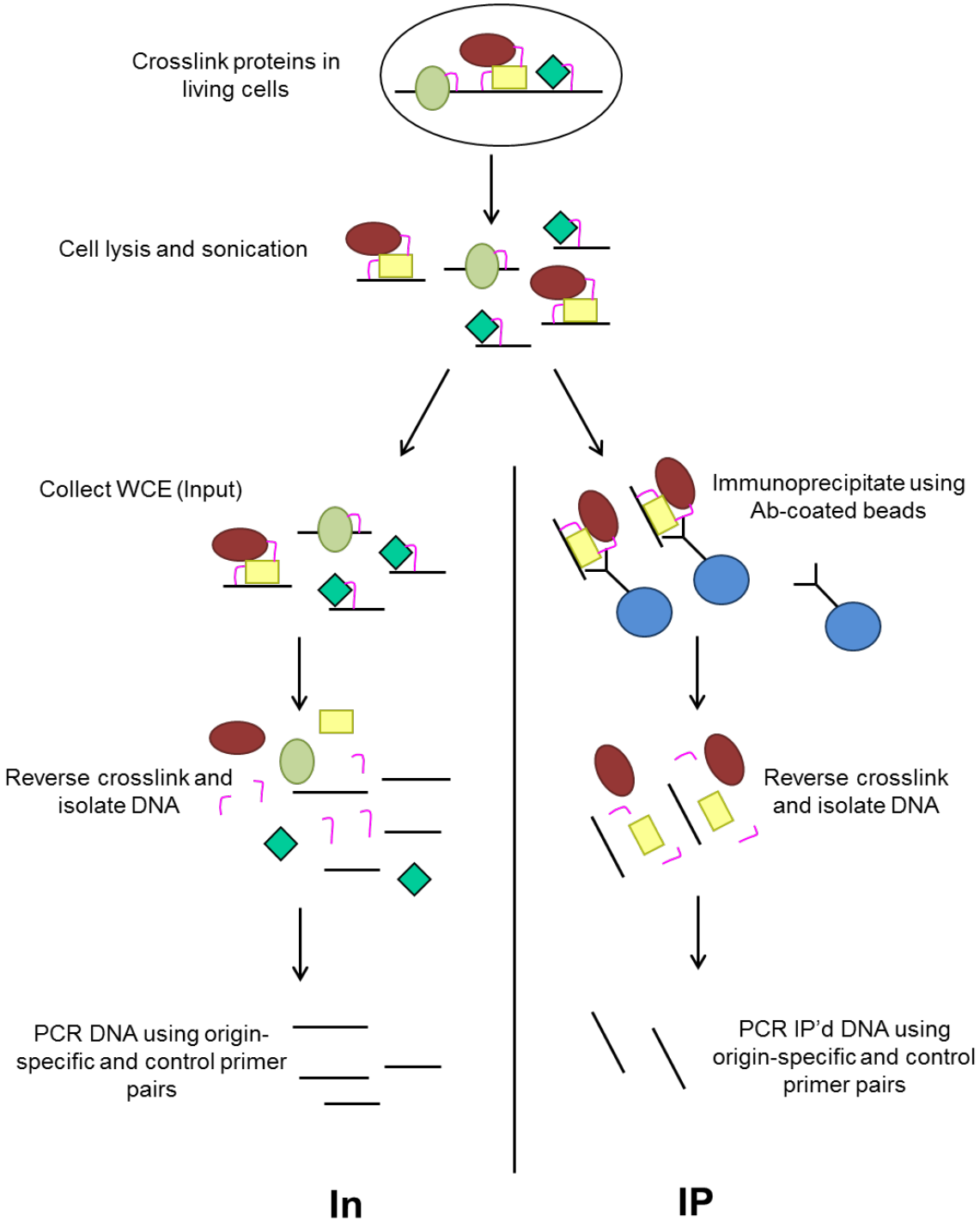
Crosslink proteins in living cells
Cell lysis and sonication
Collect WCE (Input)
Immunoprecipitate using Ab-coated beads
Reverse crosslink and isolate DNA
Reverse crosslink and isolate DNA
PCR DNA using origin-specific and control primer pairs
PCR IP'd DNA using origin-specific and control primer pairs
In
IP

4.2 Results

4.2.1 Classic ChIP of Dbf4 and Cdc7

The chromatin immunoprecipitation (ChIP) assay relies on the consistent binding of an antibody with its antigen (Figure 4.1). Because such a strong binding characterizes the Myc antibody/epitope interaction, epitope-tagged Dbf4 and Cdc7 yeast strains were used in order to facilitate these factors' immunoprecipitation. An Orc2-Myc strain previously generated in the lab was used as a positive control since Orc2 is origin bound throughout the cell cycle (Bell and Dutta, 2002). While a Dbf4-Myc strain was already available, a Cdc7-Myc tagged strain had to be created. This was accomplished through the PCR amplification of a tagging cassette and its subsequent transformation and integration into the yeast genome by homologous recombination as previously described (see Chapter 2; Longtine et al., 1998). Proper tagging was confirmed by western blot analysis with a band being visible when detected with anti-Myc antibody (Figure 4.2A). Western blot detection with an anti-Cdc7 antibody showed an upward shift in the Cdc7-Myc sample compared to an untagged control (Figure 4.2B) thus confirming proper tagging of Cdc7.

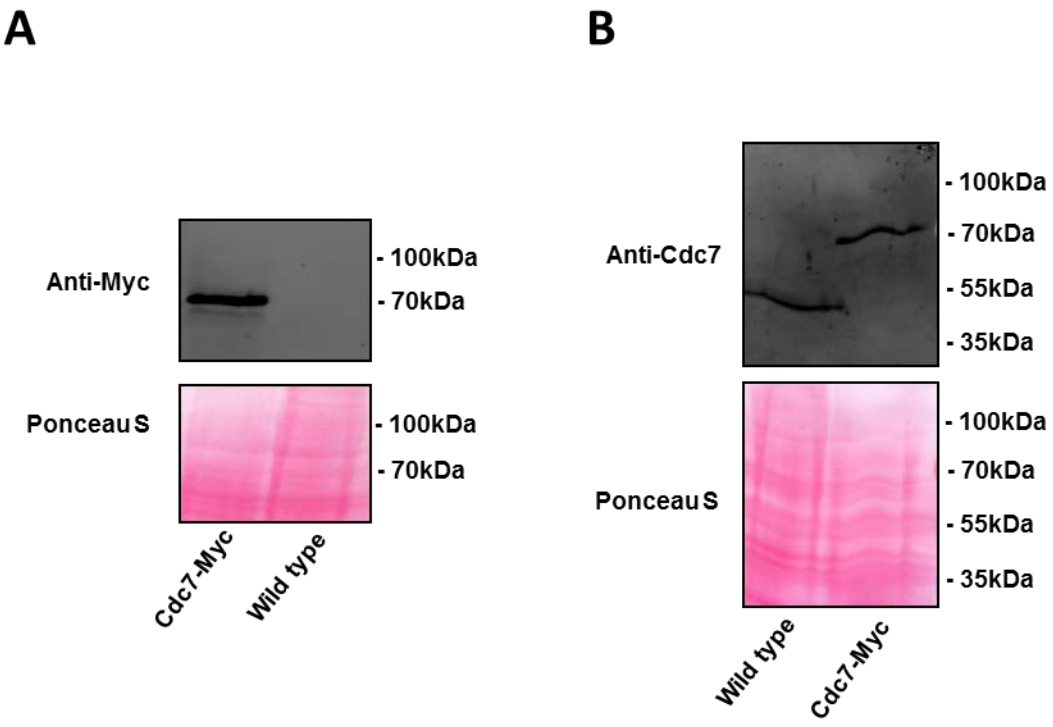

Figure 4.2: Western blot confirmation of Myc-tagged Cdc7. The coding sequence for the Myc13 epitope was added to the genomic copy of Cdc7 as described in Chapter 2. (A) 75µg WCE samples of Dbf4-Myc, Cdc7-Myc, and an un-tagged strain were run on a western blot which was detected with anti-Myc primary antibody. Both the Dbf4-Myc and Cdc7-Myc samples show a band at the predicted sizes for these protiens being tagged, while the negative control shows no band. (B) 75µg WCE samples of an un-tagged control and Cdc7-Myc strains were run on a western blot which was then detected with anti-Cdc7 primary antibody. An upward shift is evident in the Cdc7-Myc strain indicating that Cdc7 is indeed tagged with the Myc epitope. The Ponceau S staining shows equal loading of all samples

Figure 4.3: ChIP shows localization of Dbf4 and Cdc7 association to origin-flanking regions. (A) Schematic of ChIP PCR primer-pair design for all ARS regions investigated in this chapter. Input (In) and anti-Myc-immunoprecipitated (IP) samples are presented for the indicated protein tagged with Myc. There seems to be enrichment for the flanking regions for both Dbf4 and Cdc7 at early (B) and late (C) origins (as indicated by *). There seems to be enrichment of this association for both up- and downstream flanking regions as compared to the origin (top and bottom band versus the middle band in the IP lanes) in contrast to Orc2 (which is the positive control for this assay) where the origin band is clearly enriched. D) FACS profiles for each time-point for each of the isogenic strains. Cultures were arrested in late G1-phase with α-factor for 2 h and released into pheromone-free media at 16°C containing 50 μg/ml of Pronase E. Samples were collected at the indicated timpoints.

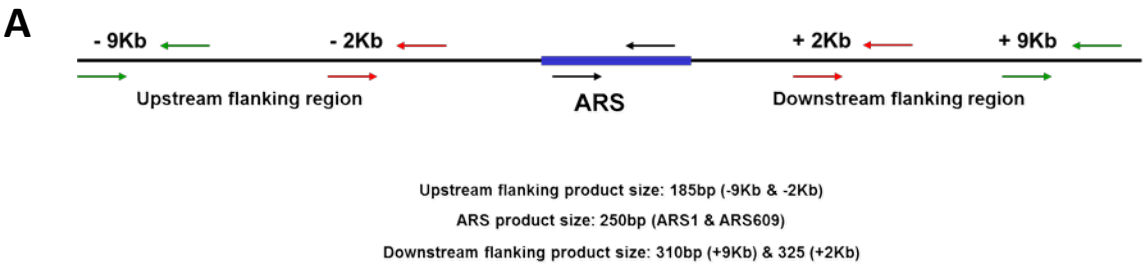
A
- 9Kb
- 2Kb
+ 2Kb
+ 9Kb
Upstream flanking region
ARS
Downstream flanking region
Upstream flanking product size: 185bp (-9Kb & -2Kb)
ARS product size: 250bp (ARS1 & ARS609)
Downstream flanking product size: 310bp (+9Kb) & 325 (+2Kb)

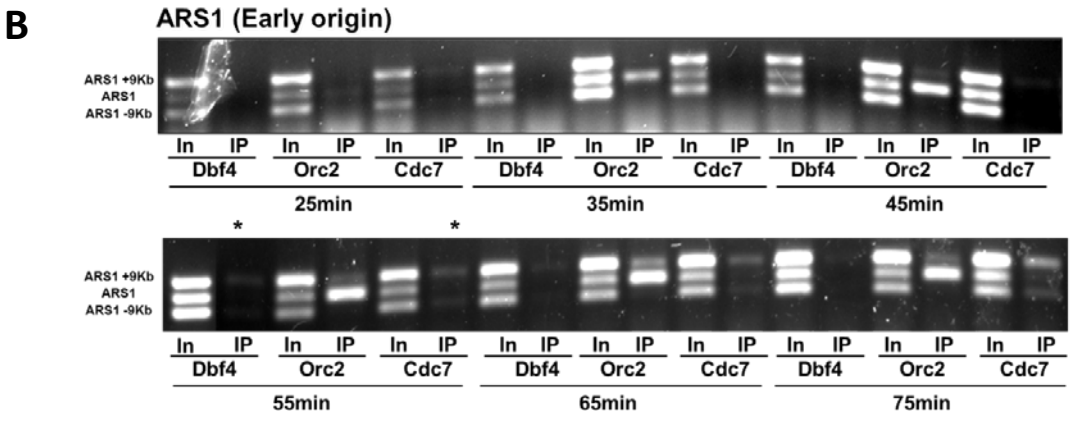
B
ARS1 (Early origin)
ARS1 +9Kb
ARS1
ARS1 -9Kb
In IP In IP In IP In IP In IP In IP In IP In IP In IP
Dbf4 Orc2 Cdc7 Dbf4 Orc2 Cdc7 Dbf4 Orc2 Cdc7
25min 35min 45min
55min 65min 75min

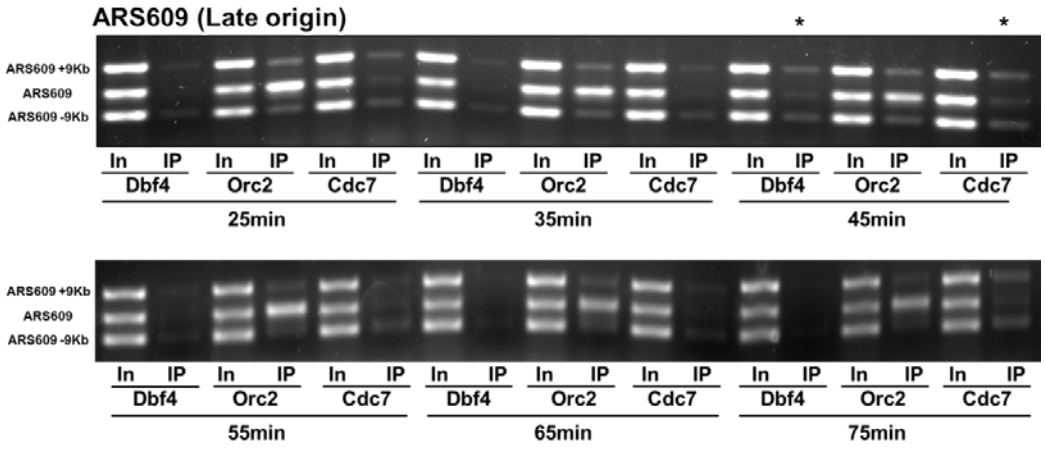
C
ARS609 (Late origin)
ARS609 +9Kb
ARS609
ARS609 -9Kb
In IP In IP In IP In IP In IP In IP In IP In IP In IP
Dbf4 Orc2 Cdc7 Dbf4 Orc2 Cdc7 Dbf4 Orc2 Cdc7
25min 35min 45min
55min 65min 75min

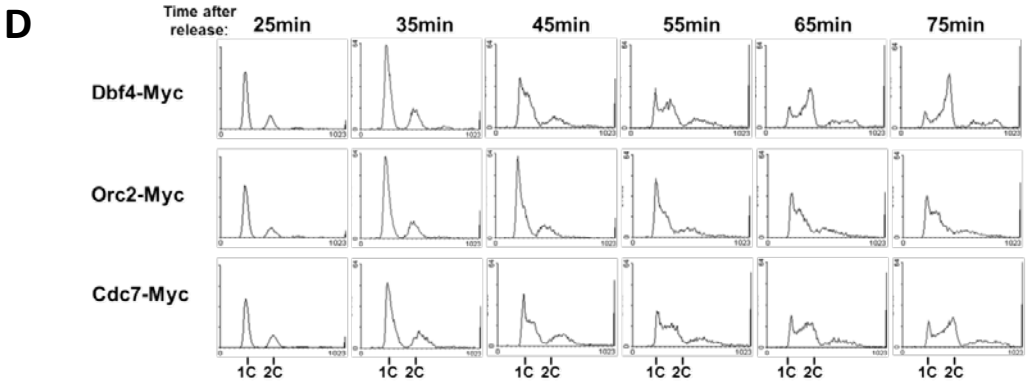
D
Time after release:
25min 35min 45min 55min 65min 75min
Dbf4-Myc
Orc2-Myc
Cdc7-Myc
1C 2C

In order to explore the association of Dbf4 and Cdc7 with origin DNA in S-phase, yeast cultures were synchronized in late G1-phase (with α-factor) and then released into pheromone-free media at 16°C in order to slow the progression of S-phase to allow samples to be collected at more timepoints. ChIP and FACS samples were taken following a 25 minute release and every 10 minutes thereafter for a total of 75 minutes as shown in Figure 4.3. Three primer sets were used to amplify the isolated ChIP DNA by triplex PCR; one set was designed to amplify a region of the origin itself, while the other two sets were controls for non-specific DNA contamination (Figure 4.3A). These control primers were designed to amplify regions of the genome 9 kbp up- and downstream of the origin of interest. Because the size of the ChIP-isolated DNA fragments is designed to be between 500 bp and 1 kb, this distance from the origin was an appropriate control. For each strain at each timepoint, PCR was performed using purified DNA as template from both the input ([In], which is essentially a whole cell extract) and the immunoprecipitated (IP) fractions (Figure 4.3B, C). Since the input fractions have all of the cellular DNA, three PCR bands are expected as both the origin and the flanking regions will be present to act as template for the reaction. Conversely the IP fraction should only be enriched for the DNA that was bound to the specific protein being purified (i.e. Orc2, Dbf4, or Cdc7), thus a single origin specific band would be expected to predominate if the protein interacts with the origin.

The origin association pattern of Dbf4, Cdc7, and Orc2 at both an early (ARS1) and a late (ARS609) origin were explored at 10 minute intervals through S-phase; FACS samples were taken to monitor the DNA content of the cells (Figure 4.3B, C, D). There seems to be little if any enrichment of the origin specific band for Dbf4 or Cdc7 as

opposed to Orc2 which shows a strong origin specific band, as expected. Surprisingly however, it looks as though the signal may be enriched for the flanking regions for the Dbf4 and Cdc7 IP samples at both the early and late origin (denoted by asterisk). Although subtle, this result was very reproducible over multiple experiments.

Because some enrichment was observed in the flanking regions, it was thought that Dbf4 and Cdc7 might be sequestered in these regions until redistributing to origins at the time of firing. It was also thought that perhaps this flanking pool of Dbf4 and Cdc7 might be located closer to the origin to facilitate this redistribution. Thus new flanking primers were designed that amplify regions 2 kb up- and downstream of the origin in order to assess the degree of Dbf4 and Cdc7 enrichment in these regions (Figure 4.3A). In the case of the early origin (ARS1) for Cdc7, there seems to be enrichment for the origin band at the 25 minute timepoint followed by a reduction in the origin:flanking band ratio as S-phase progresses. There is little change in the origin:flanking band ratios for Dbf4 at the early origin as S-phase progresses, as determined by FACS analysis (compare blue arrows in Figure 4.4A, B; C FACS profiles through S-phase). There does appear to be some redistribution of Dbf4 and Cdc7 signal from the flanking regions to the origin in the case of the late origin (Figure 4.4A and B; compare green arrows). Because these are admittedly subtle changes in signal (especially for Dbf4 where any changes were too subtle to observe by simple visual inspection), qPCR was used in an attempt to get a more quantitative analysis of the ChIP results. Orc2 and Dbf4 were immunoprecipitated in a new ChIP timecourse (Figure 4.5A). The collected samples were subjected to qPCR comparing the origin signal to that of the upstream flanking region for both Dbf4 and Orc2 for ARS1 (Figure 4.5B). The qPCR results corroborate those of the normal PCR in

that Orc2 shows strong enrichment for the origin as compared to the flanking region while there is a modest enrichment for the flanking signal as compared to the origin for Dbf4 and this enrichment lessens as S-phase progresses consistent with a model whereby Dbf4 is redistributed to origins at the time of firing.

Figure 4.4: ChIP PCR corresponding to regions +/- 2 kb from origins show enrichment for Dbf4 and Cdc7 association. Origin flanking regions were examined using primers +/- 2 kb from the origin (see Figure 4.3A). Input (In) and anti-Myc-immunoprecipitated (IP) samples are presented for the indicated protein tagged with myc. (A) At the early origin there seems to be enrichment for the origin band for Cdc7 (25 min) followed by a reduction in the origin:flanking band ratio as S-phase progresses (compare blue arrows). At the late origin there is some redistribution of from flanking regions to the origin (compare green arrows). (B) There is little change in the origin:flanking band ratios for Dbf4 in the case of the early origin (compare blue arrows). For the late origin, there is some redistribution from flanking regions to the origin (compare green arrows). C) FACS profiles for each time-point for each of the strains.

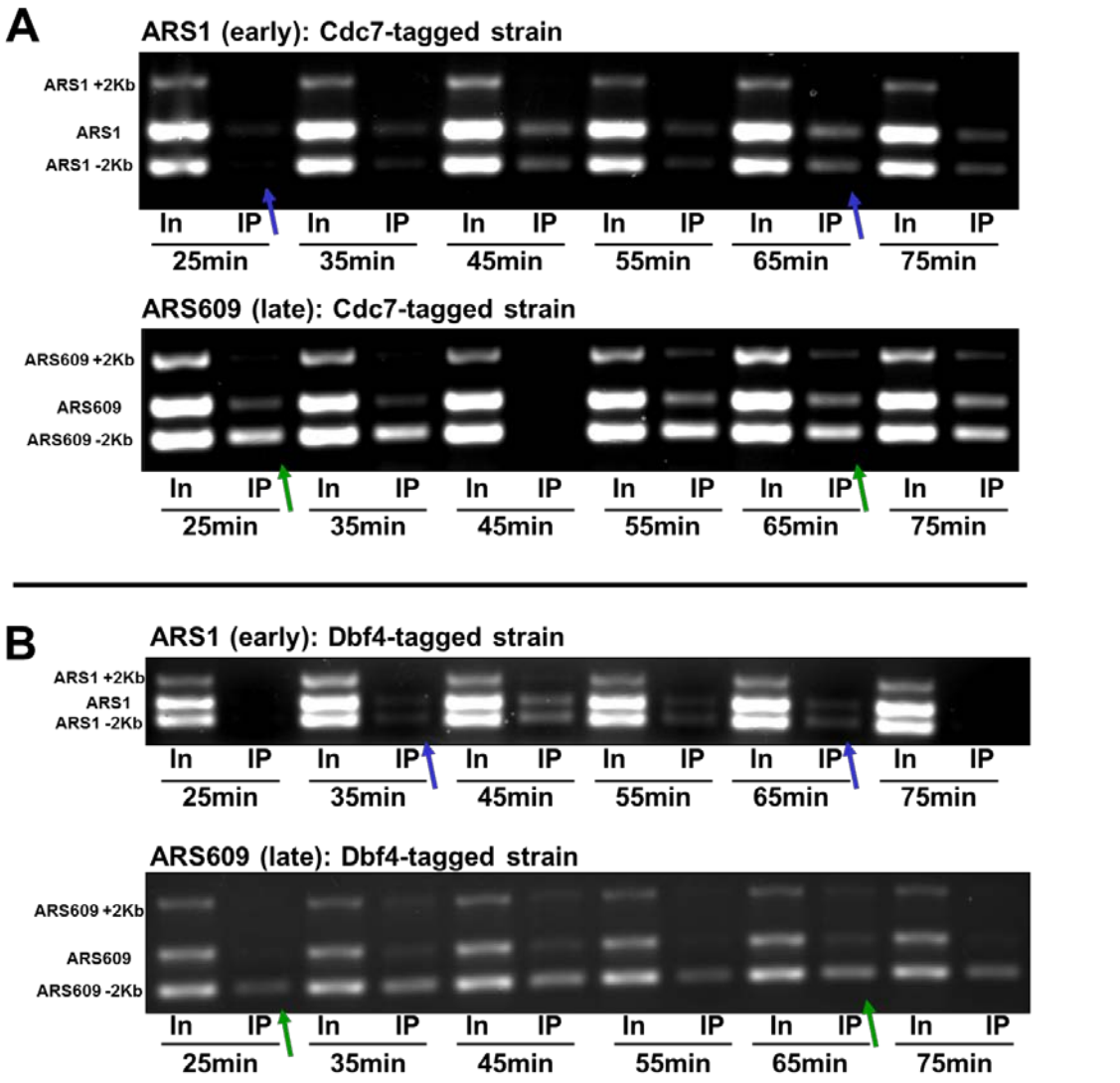
A
ARS1 (early): Cdc7-tagged strain
ARS1 +2Kb
ARS1
ARS1 -2Kb
In IP In IP In IP In IP In IP In IP
25min 35min 45min 55min 65min 75min
ARS609 (late): Cdc7-tagged strain
ARS609 +2Kb
ARS609
ARS609 -2Kb
In IP In IP In IP In IP In IP In IP
25min 35min 45min 55min 65min 75min
B
ARS1 (early): Dbf4-tagged strain
ARS1 +2Kb
ARS1
ARS1 -2Kb
In IP In IP In IP In IP In IP In IP
25min 35min 45min 55min 65min 75min
ARS609 (late): Dbf4-tagged strain
ARS609 +2Kb
ARS609
ARS609 -2Kb
In IP In IP In IP In IP In IP In IP
25min 35min 45min 55min 65min 75min

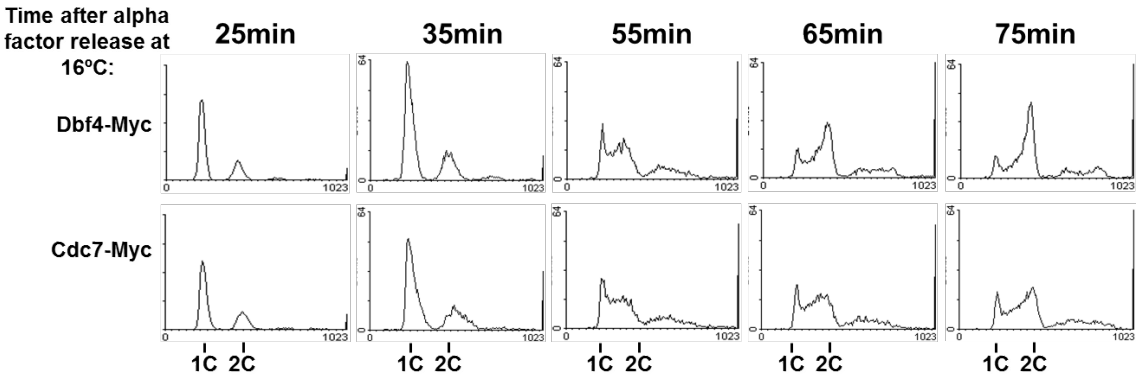
C
Time after alpha factor release at 16°C:
25min
35min
55min
65min
75min
Dbf4-Myc
Cdc7-Myc
1C 2C
1C 2C
1C 2C
1C 2C
1C 2C

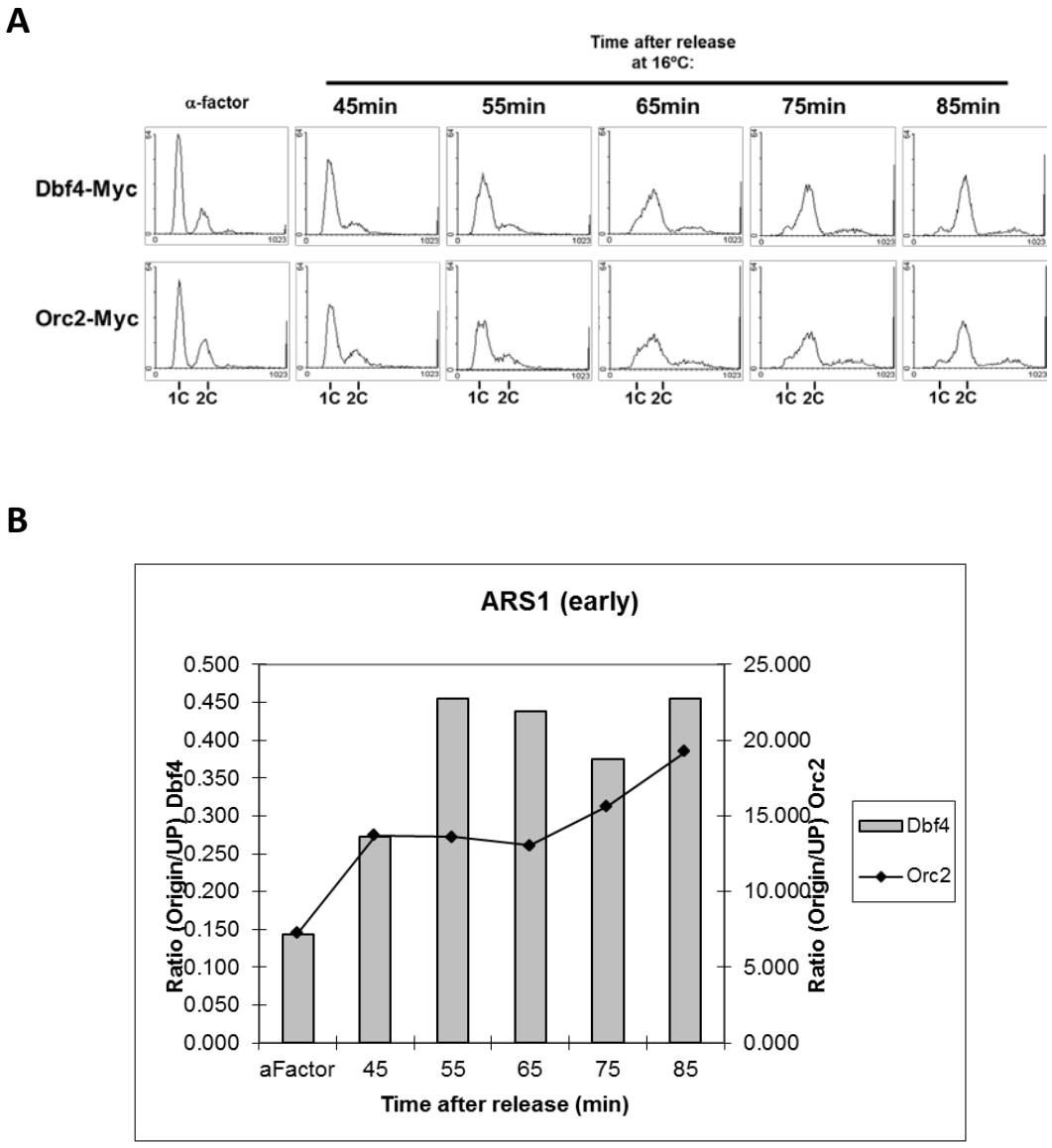

Figure 4.5: ChIP qPCR shows redistribution of Dbf4 from an origin flanking region to the origin. qPCR was used to monitor any redistribution of Dbf4 from flanking regions to the origin through S-phase. (A) FACS profiles for the isogenic Dbf4-Myc and Orc2-Myc strains. (B) Histogram showing the ratio of origin/upstream signal as determined by qPCR using the equation 2[Ct(In)-Ct(IP)]. There is some redistribution of Dbf4 from the origin flanking region to the origin (compare 45min and 55min timepoints). Orc2 shows strong enrichment for the origin as compared to the flanking region. Note the different scales for Dbf4 and Orc2.

4.2.2 Classic ChIP and the S-phase checkpoint

In order to further examine the importance of this potential enrichment of Dbf4 in upstream origin flanking regions, ChIP was performed on a *mec2-1* strain in which a point mutation in the checkpoint kinase Rad53 abrogates its checkpoint response to genotoxic agents and results in precocious firing of late origins even in an unperturbed S-phase. Cultures of *mec2-1* and a wild-type control were arrested in α-factor followed by a 45 minute release at which point ChIP and FACS samples were taken at 10 minute intervals (Figure 4.6). Normal PCR performed on the ChIP samples may show an increased origin:flanking ratio for Dbf4 signal with a late origin (ARS609) earlier in S-phase in the *mec2-1* strain than in the wild-type strain (Figure 4.6A). In the *mec2-1* strain, the increased origin:flanking ratio observed at 45 minutes is greatly reduced by 55 minutes and remains low for the rest of the assay (Figure 4.6A, blue arrows). In the wild-type strain, the origin:flanking ratio seems to increase at 55 minutes and remain elevated until the 85 minute timpoint (Figure 4.6A, green arrows). It should be noted that due to the low intensities of some of the PCR bands, it is difficult in some samples (*mec2-1* 55 minute IP, for example) to estimate the origin:flanking signal ratio.

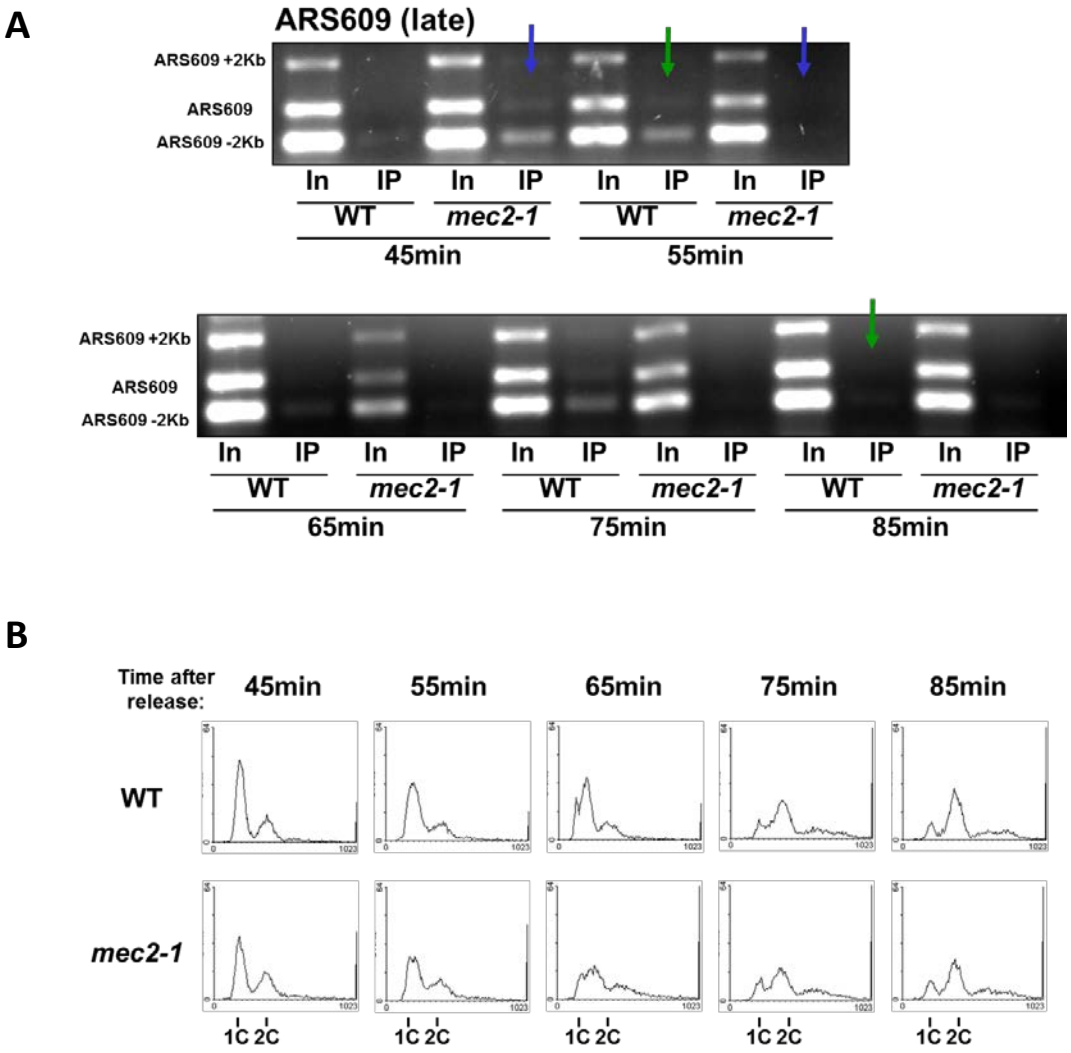

Figure 4.6: ChIP for Dbf4 in a Rad53 *mec2-1* strain may show an increase in the origin:flanking band ratio earlier in S-phase than for wild type. The importance of the flanking Dbf4 pool was examined using ChIP to assay a mec2-1 mutant to determine any differences in Dbf4-DNA association profiles as compared to wild type. Input (In) and anti-Myc-immunoprecipitated (IP) samples are presented for Myc-tagged Dbf4. (A) There seems to be an increase in the origin:flanking band ratio for Dbf4 earlier in S-phase in the *mec2-1* strain than in the wild type strain. For *mec2-1*, the increased origin:flanking ratio observed at 45 min seems to be greatly reduced by 55 min and remained low for the remainder of the assay (blue arrows), however band ratio were difficult to assess due to low signal intensities in these samples. In the wild type strain, the origin:flanking ratio increases at 55 min and remains elevated until 85 min (green arrows). (B) FACS profiles for each strain at each timepoint.

4.2.3 Modifying the ChIP protocol

It is possible that the modest changes in the association patterns of Dbf4 and Cdc7 with origin and flanking regions are due to technical drawbacks inherent in the ChIP protocol itself rather than an actual physiological phenomenon. Critical to the success of the ChIP assay is the strong binding of the antibody to its epitope, however the normal folding of the protein into its tertiary structure or the way in which the protein associates with other proteins in a complex may result in the tag being 'buried' or masked from the antibody. This interference between the antibody and the epitope could result in a compromised immunoprecipitation (and subsequent PCR amplification of the origin DNA) even though the protein is actually origin bound.

To circumvent this potential issue, a modified version of the ChIP protocol was created. The logic for the modification relies on the observation that Orc2 appears to be exclusively origin bound throughout the cell cycle and that it is efficiently immunoprecipitated (Bell and Dutta, 2002; this study). Thus in the modified ChIP, Orc2 is immunoprecipitated but rather than reversing the crosslink and isolating the DNA, the IP sample is run directly on a western blot. Because Orc2 is origin-bound, the IP will pull down origin specific sequences along with any proteins associated with them (i.e. Dbf4). Dbf4 can then be detected on the blot, thus revealing its presence at the pre-RC (Figure 4.7). Because of the lack of a reliable anti-Dbf4 antibody, Dbf4 was tagged with HA (in order to efficiently detect it on a western blot) in an Orc2-Myc strain (since Myc is the target of the immunoprecipitation). This HA tagging of Dbf4 was performed as described above for generating the Dbf4-Myc strain.

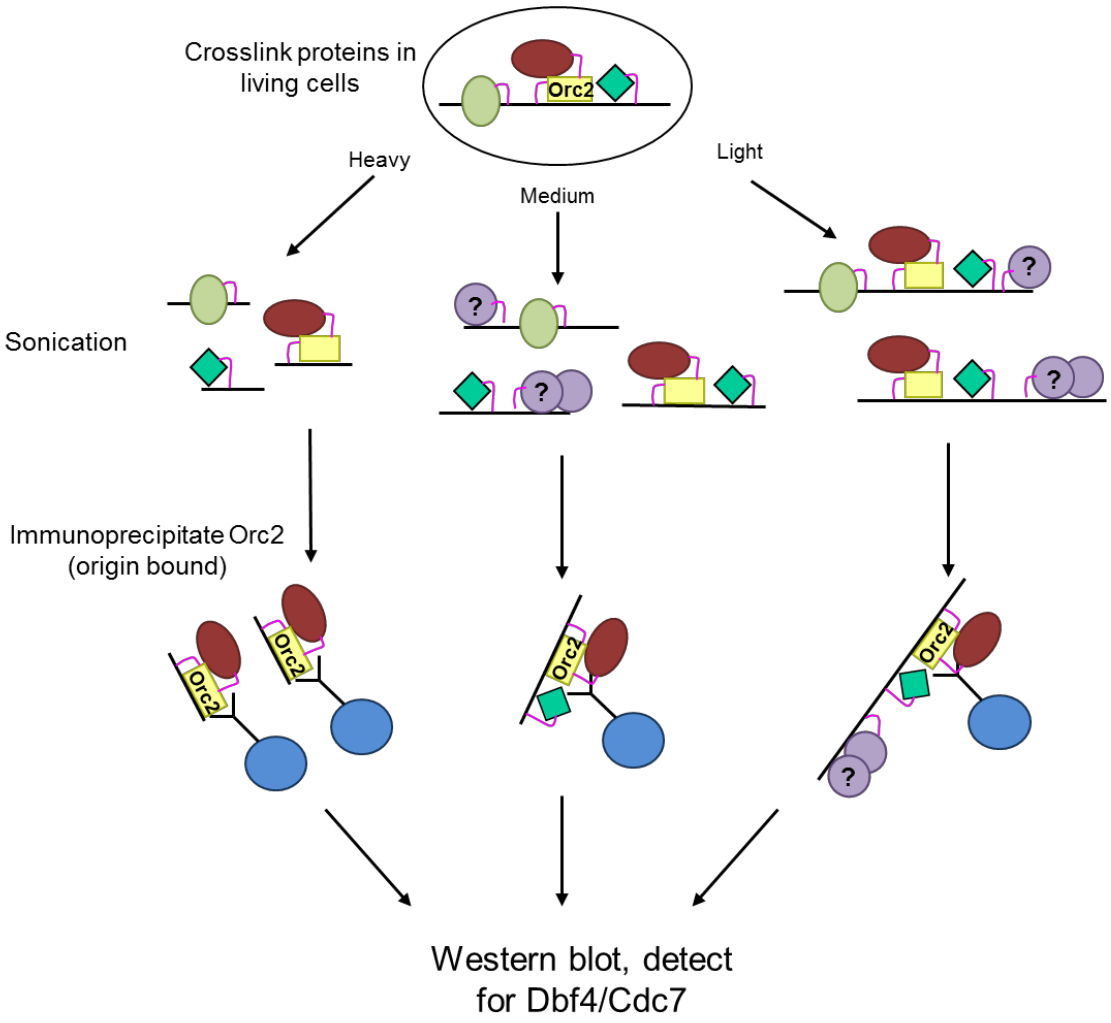

Figure 4.7: Schematic of the modified ChIP protocol. A detailed protocol is found in the Materials and Methods (Chapter 2). Briefly, proteins are crosslinked to DNA in live yeast cells using formaldehyde followed by cell lysis. The sonication regimen can be altered to generate origin-flanking regions of different lengths. Heavy sonication generates shorter flanking lengths while a lighter regimen produces longer flanking regions. Orc2 is immunoprecipitated using anti-Myc antibody-coated beads and the sample is run directly on a western blot. Importantly, the crosslink is not reversed in this protocol. Boiling the sample in conjunction with the sample buffer is sufficient to denature and separate the proteins for detection on a western blot. Potential novel protein-DNA associations in the origin flanking regions are indicated by ?.

As a proof of concept for this modified protocol, the newly created Orc2-Myc Dbf4-HA culture was synchronized in late G1-phase with α-factor and released into pheromone free media at 16°C. ChIP and FACS samples were collected at 10 minute intervals following an initial 45 minute release (Figure 4.8). Dbf4 was found to be present in the S-phase samples and interestingly, the signal seemed to be greater for the earlier S-phase timepoints and was reduced as S-phase progressed (compare 45 min to 75 min in Figure 4.8A). While this was an encouraging initial result, subsequent attempts to detect either Cdc7 or Orc2 (using both an anti-Myc antibody or an Orc2-specific antibody) were unsuccessful.

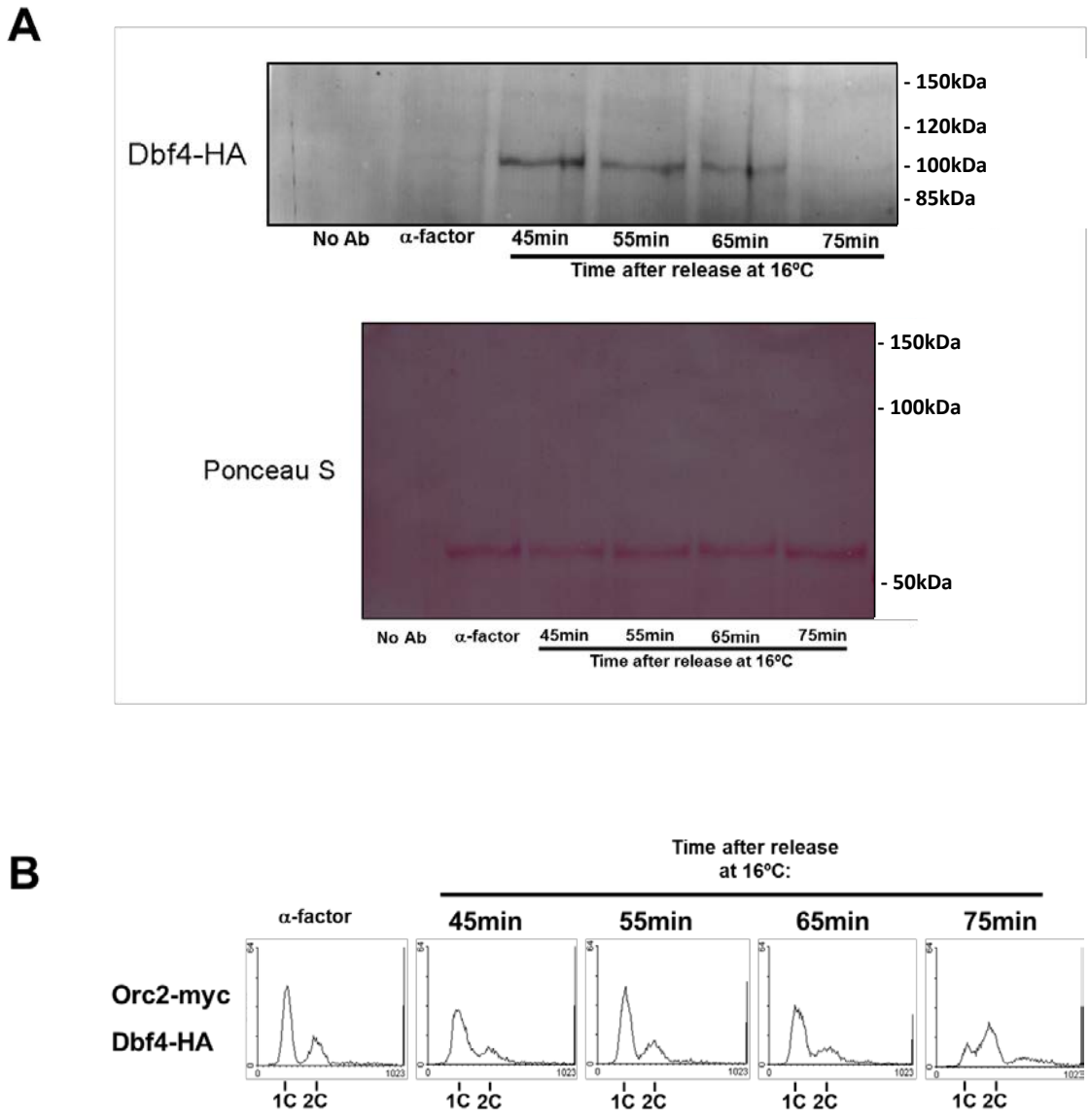

Figure 4.8: The modified ChIP protocol is a useful approach to studying protein association with origins of DNA replication. A modified ChIP assay was performed on an Orc2-Myc Dbf4-HA double tagged strain. The culture was arrested in late G1-phase then released into S-phase and ChIP samples were taken at the indicated timepoints. (A) Modified ChIP western blot detecting for HA-tagged Dbf4. (B) FACS profile for the Orc2-Myc and Dbf4-HA double tagged strain timecourse. The Dbf4-HA signal is absent in the α-factor arrested sample (as expected), appears in S-phase, and declines as S-phase progresses (compare 45min-75min). The Ponceau S shows equal loading of all samples.

4.3 Discussion

4.3.1 Dbf4 and Cdc7 origin association

The mechanism by which DDK is targeted to origins of DNA replication and the temporal organization of that association has been a topic of renewed interest in recent years. While the Mcm2/4/6 phosphorylation sites targeted by DDK have been mapped (Bruck and Kaplan, 2009; Randell *et al*., 2010; Stead *et al*., 2011), the question of how DDK is recruited to replication origins remains unresolved. The enrichment observed for the origin band for Cdc7 at the early timepoint for the early origin (Figure 4.4A) may reflect the presence of Cdc7 at the origin at the time of firing. The observation that there is little enrichment in general for the origin band in either Dbf4 or Cdc7 IP samples, while there was modest but reproducible enrichment for the upstream flanking region, was surprising (Figure 4.3, 4.4, and 4.5). Based on these results, the current hypothesis is that there is perhaps a transient Dbf4/Cdc7 origin association where DDK redistributes from flanking regions to the origins to trigger their firing. This idea is supported by experiments using a Rad53 *mec2-1* strain, a feature of which is the precocious firing of late origins (Santocanale and Diffley, 1998; Shirahige *et al*., 1998). Thus it was hypothesized that if the association of Dbf4 with a late origin was investigated in this strain background, that this redistribution effect would be observed earlier in S-phase as compared to the same origin in a wild-type strain background. Figure 4.6 may show this precocious redistribution effect, though estimating the origin:flanking band ratio is difficult in some samples due to low band intensities.

Following from the results generated using the classic ChIP protocol that there seems to be enrichment of Dbf4 and Cdc7 at the origin flanking regions, the idea of a

reservoir was proposed. This idea envisages 'pools' or reservoirs of Dbf4/Cdc7 that are localized to origin flanking regions. These factors are then redistributed from these reservoirs to origins themselves at the time of firing. While the data presented here supports this model, the observed changes in chromatin association are subtle and it would be important to optimize the ChIP protocol in order to observe with greater confidence a redistribution from the flanking regions to the origin by generating a stronger origin signal. Potential explanations for why this has proven problematic are discussed below.

4.3.2 The Modified ChIP Protocol

Because of the interest in DDK action and the potential power of the ChIP assay, it is an obvious tool for attempting to elucidate the origin binding patterns of Dbf4 and Cdc7, yet though attempts have been made, no other group has had success in doing so. While a number of reasons are possible for this lack of success, ranging from technical issues to experimental design flaws, two reasons come to the fore, either of which would explain researchers' inability to ChIP Dbf4 and Cdc7. The first is a technical issue whereby the antibody is unable to access the epitope to generate an efficient IP (either because the epitope is 'buried' in the three-dimensional structure of the folded protein, or because the epitope is being 'masked' by the other DDK subunit or other components of the pre-RC complex. To circumvent this problem, a modified ChIP protocol was designed which exploits the strong association of Orc2 with origins and relies on the proven ability to immunoprecipitate Orc2-Myc using an anti-Myc antibody (Figure 4.7). Initial experiments support the utility of this approach as Dbf4 can be detected in the Orc2-Myc

ChIP samples (Figure 4.8A). In fact, this result may even point to the temporal association pattern of Dbf4 with origins. As expected, there is no Dbf4 band in the α-factor arrested sample, since Dbf4 is actively degraded in an APC-dependant manner in G1-phase (Pasero *et al.*, 1999; Weinreich and Stillman, 1999). The strongest Dbf4 signal is observed at the first timepoint following the release into S-phase (Figure 4.8A, 45 min) and this signal is reduced in S-phase, finally disappearing as cells move into G2-phase. This data is consistent with a model whereby Dbf4 binds all origins at the beginning of S-phase since the overall level of Dbf4 signal goes down. This reduction in signal may correspond to the firing of more and more origins leading to the dissociation of Dbf4 from origins as S-phase progresses. This is in contrast to the other proposed model in which Dbf4 associates with origins sequentially as S-phase progresses; if this were the case, then one might expect the levels of detected Dbf4 signal to remain relatively constant throughout the S-phase timecourse as Dbf4 progressively associates, activates, and then dissociates from one origin followed by another.

While this modified ChIP protocol seems to allow for the previously unattainable detection of Dbf4, this protocol can no longer discriminate between specific origins, since Orc2 is bound to all origins throughout the cell cycle and is not limited to early, middle, or late origins. Though this decrease in sensitivity is less than ideal, the ability to detect Dbf4 means that the modified ChIP can contribute to the understanding of Dbf4 action at origins. While some optimization is no doubt required in order to perfect this protocol, the potential exists for valuable data to be garnered from this ChIP modification.

The modified ChIP protocol creates the possibility of a further variation whereby the length of the sonication regimen can be adjusted in order to generate DNA fragments

of varying sizes (Figure 4.7). This would allow for a more precise investigation of any proteins bound to the origin flanking region, and should the presence of a Dbf4 or Cdc7 reservoir be confirmed, the location of this reservoir could be accurately mapped by a stepwise shortening of the sonication time, resulting in longer and longer flanking regions.

A second explanation for the lack of success for Dbf4 and Cd7 ChIP is the way in which DDK itself may normally act at the origin. It is possible that the association of DDK with the origin is very transient in nature; DDK may only be present at any given origin for as long as it takes to phosphorylate the Mcm4 target. This timeframe may be too short to capture using ChIP, as it takes time (sometimes many minutes to upwards of a few hours) to crosslink the proteins to the DNA. Thus ChIP may simply 'miss' the rapid association/dissociation of DDK with the origins. This scenario is more difficult to address by technical modifications to the ChIP protocol. Because of the inherent instability of the Dbf4 protein itself, it may also be that Dbf4 degradation plays a role in the lack of ChIP success. One potential Dbf4 modification might be to generate a stable non-APC-degradable version of Dbf4, as previously described (Ferreira *et al*., 2000). This modified Dbf4 lacks the so-called 'destruction box' which is the region of Dbf4 that is targeted by the APC leading to its degradation. Dbf4 that lacks this box is not degraded and the protein is much more stable than the wild-type version. ChIP performed on strains containing this stabilized Dbf4 (Dbf4sb) might have more success since Dbf4 degradation would be less of an issue and the threshold for ChIP sensitivity might be reached. Of course the advantage that the Dbf4sb may offer for ChIP is also a potentially major drawback for the cell since the normal regulation of the initiation of DNA

replication requires the cycling of Dbf4 levels. The constant presence of Dbf4sb may lead to unpleasant consequences for the cell such as precocious origin firing and the potential for origin firing outside of S-phase. The interpretation of any ChIP results obtained would also be difficult in that the constant presence of Dbf4sb may lead to interactions that do not occur normally and there would be no way to know whether an observed association pattern is physiologically relevant or simply a construct of the Dbf4sb modification.

Taken together the results presented in this chapter point to the possibility of a reservoir of DDK bound to origin flanking regions which redistribute to origins at the time of firing. This would support the model whereby DDK is targeted to origins as an active complex rather than Dbf4 activating previously origin-bound Cdc7. Because of the potential for the ChIP results being impacted by an impairment of the antibody-epitope interaction, a modified version of the ChIP protocol was designed which exploits the strong IP capacity of Orc2-Myc. While this modified protocol requires further optimization, data provided here provides evidence that this protocol should be explored further.

Chapter 5: Initial characterization of the S-phase checkpoint role of Dbf4

Figure 5.6 assisted by Jay Yang

5.1 Introduction

While the role of DDK in the initiation of DNA replication has been the focus of much scholarly study and the central theme of Chapters 3 and 4, its role in the S-phase checkpoint response must not be overlooked. The S-phase checkpoint acts to slow DNA replication to allow time for repair via two mechanisms: the inhibition of late (unfired) origins, and the stabilization of stalled replication forks (Zegerman and Diffley, 2010; Duch *et al*., 2011). Previous work (Weinreich and Stillman, 1999; Varrin *et al*., 2005) has pointed to a role for DDK in the checkpoint response, including the observation that Dbf4 is phosphorylated and removed from chromatin in a Rad53-dependant manner. A Dbf4 mutant lacking the N-motif has also been shown to be sensitive to genotoxic agents (presumably due to its lack of interaction with Rad53, Varrin *et al*., 2005). While the Rad53-mediated inactivation of Dbf4 has been linked to the preservation of unfired origins, the contribution made by these unfired origins to checkpoint recovery seems to be minimal (Tercero *et al*., 2003; Duncker and Brown, 2003; Zegerman and Diffley, 2010). Thus the stabilization and subsequent restart of stalled replication forks is thought to be the major mechanism by which DNA replication resumes during the recovery from a checkpoint arrest. The potential role of DDK in the stabilization/restart of stalled replication forks is not well understood, though recent evidence suggests that the C-motif of Dbf4 may play a role in recovery from genotoxic insults (Harkins *et al*., 2009; Jones *et al*., 2010). This chapter describes the initial attempts to optimize two molecular tools that will elucidate the S-phase checkpoint role of Dbf4: DNA combing and live cell fluorescent microscopy.

DNA combing is a powerful tool that allows for the monitoring of DNA synthesis. This is accomplished through the incorporation of nucleoside analogues into the replicating DNA of live cells. *S. cerevisiae* is unable to incorporate exogenously added nucleosides into its replicating DNA since it lacks the necessary nucleotide kinases responsible for converting deoxynucleosides into usable monophosphate deoxynucleotides (Lengronne *et al*., 2001). However, ectopic expression of Herpes Simplex Virus thymidine kinase (HSV-TK) in yeast cells allows them to incorporate these analogues; thus the yeast background used for the DNA combing described here is a TK+ strain in which a TK+ cassette (seven tandem copies of the HSV-TK gene) is constitutively expressed (Lengronne *et al.*, 2001). Following the isolation, physical stretching, and binding of the DNA fibers onto salinized coverslips, fluorescent antibodies are then hybridized to these incorporated analogues or unlabeled DNA. Through fluorescence microscopy it is possible to image the actual DNA fibers and determine the amount of analogue incorporation, thus allowing for the monitoring of DNA synthesis (Michalet *et al*., 1997; Herrick *et al*., 2000).

Live-cell fluorescence microscopy is an attractive tool that would complement the biochemical assays for Dbf4, Cdc7, and Mcm2 described above and in Chapters 3 and 4. The major advantage of this technique is to be able to make direct observations of these factors without extra manipulation (such as crosslinking in the ChIP protocol). Using live cells also allows for the monitoring of replication factor localization in a single cell at multiple points throughout the cell cycle. Previous work using fixed cells and immunofluorescence showed that in yeast cells, DNA replication occurs at discrete subnuclear foci and that Dbf4 localizes in a similar punctate pattern (Pasero *et al*., 1997;

1999). Moreover this Dbf4 staining pattern overlapped with that of Orc1 indicating the close association between Dbf4 and origins of replication (since ORC is exclusively bound to origin DNA, Pasero *et al*., 1999). While elegant in its experimental design, this study did rely on fixed cells and it is possible that the fixing process itself contributed to the observed staining pattern of Dbf4 and ORC. Because Orc6 has also been shown to localize to subnuclear foci using live-cell microscopy (Semple *et al*., 2006), it was reasonable to use these previous live-imaging results as a guide for the optimization of the live-cell imaging protocol. Initial imaging seems to show a punctate subnuclear signal pattern for Mcm2 during S-phase, consistent with Mcm2-7 localization to centers of DNA replication.

5.2 Results

5.2.1 Dbf4/Cdc7 Chromatin Association in a Perturbed S-Phase

Of the three well-conserved motifs in Dbf4, the N-motif has been the one shown to mediate the Dbf4-Rad53 interaction (Varrin *et al*., 2005). Removal of this motif (Dbf4ΔN) abrogates the Dbf4-Rad53 interaction and confers hypersensitivity to genotoxic stress (Varrin *et al*., 2005). Because previous work has indicated that Dbf4 is phosphorylated and displaced from chromatin in a Rad53-dependent manner during the S-phase checkpoint (reviewed in Duncker and Brown, 2002), it was hypothesized that Dbf4ΔN would remain chromatin-bound under checkpoint conditions. To investigate the importance of the Dbf4-Rad53 interaction for the removal of Dbf4 from chromatin during an HU-induced checkpoint, a Dbf4ΔN strain, a Rad53 *mec2-1* strain (deficient for

checkpoint function), and a wild-type strain were assayed. Cultures were synchronized in late G1-phase with α-factor and then released into pheromone-free media with or without HU. Following the incubation, a chromatin fractionation assay was performed on each of the cultures and FACS samples were collected (Figure 5.1A). The fractionation assay samples were analyzed by western blot and detected with the indicated antibodies (Figure 5.1B). For all samples, Orc2 was found predominantly in the pellet samples as expected, since ORC is almost exclusively origin bound. In the Rad53 *mec2-1* cells, Dbf4 was found to associate to a greater extent with the insoluble nuclear fraction when exposed to HU as compared to the wild-type cells (Figure 5.1B, P lanes). There does not seem to be any dissociation of Dbf4 under HU conditions in the Dbf4ΔN cells even though the Rad53 in these cells is wild-type (Figure 5.1B, P lanes). These results are consistent with the idea that in wild-type cells, Dbf4 dissociates from DNA during the S-phase checkpoint, and that this dissociation is Rad53-dependent. Similar to the observations for Dbf4, Cdc7 appears to remain chromatin bound under HU conditions in both the Dbf4ΔN and Rad53 *mec2-1* cells (Figure 5.1, P lanes).

5.2.2 DNA Combing

Because the major role of DDK in the S-phase checkpoint response does not seem to be the inhibition of late origin firing (see above), the best alternative is a role in replication fork stabilization and/or restart during recover from the checkpoint. DNA combing can be used to assess both this potential role for DDK, along with importance of the Rad53-Dbf4 interaction in the checkpoint response using the Dbf4ΔN mutant.

In order to be able to control the timing of Dbf4 and Cdc7 expression, construction of TK+ GAL-Dbf4 and GAL-Cdc7 strains was necessary. This was accomplished by PCR amplification of a cassette containing the *GAL1* promoter and sequence for the HA epitope, followed by the subsequent transformation and integration of this cassette into the yeast genome by homologous recombination (see Chapter 2; Longtine *et al*., 1998). This resulted in Dbf4 or Cdc7 being under the control of the *GAL1* promoter in the TK+ background thus allowing control of Dbf4 and Cdc7 expression through the composition of the growth medium (i.e. including or excluding galactose). Confirmation of proper cassette integration and the ability to deplete Dbf4 or Cdc7 was accomplished by initially growing cultures asynchronously in galactose medium (GAL expression on) followed by a switch to medium containing glucose (YPD, GAL expression off). Whole cell extract samples were collected at one hour intervals and run on a western blot to monitor depletion of the protein (Figure 5.2). Detection with an anti-HA antibody shows that there is depletion of Dbf4 below detectable levels by one hour of incubation in YPD while it requires four hours of incubation for Cdc7 depletion (Figure 5.2A, B).

Figure 5.1: A Dbf4 N-motif mutant remains chromatin bound upon HU treatment. Cultures of Dbf4ΔN, Rad53 mec2-1, and wild-type cells were synchronized in α-factor and released into pheromone-free media with or without HU. Following 1 hour of incubation, FACS samples were collected (A) and chromatin fraction assays performed on all samples as described in the Materials and Methods (Chapter 2). (B) Fractionation samples were assayed by western blot and detected with anti-Orc2, anti-Myc (since Dbf4 was Myc-tagged in each strain), and anti-Cdc7 primary antibodies. Whole cell extract (W), soluble (S), and insoluble (P) fractions are presented for each sample. Orc2 is found predominantly in the insoluble fraction for each sample

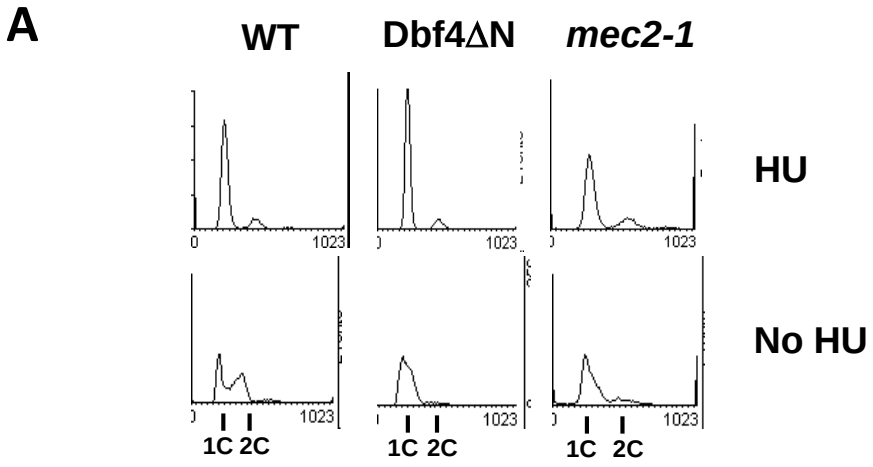
A
WT
Dbf4ΔN
mec2-1
HU
No HU
0
1023
1C 2C

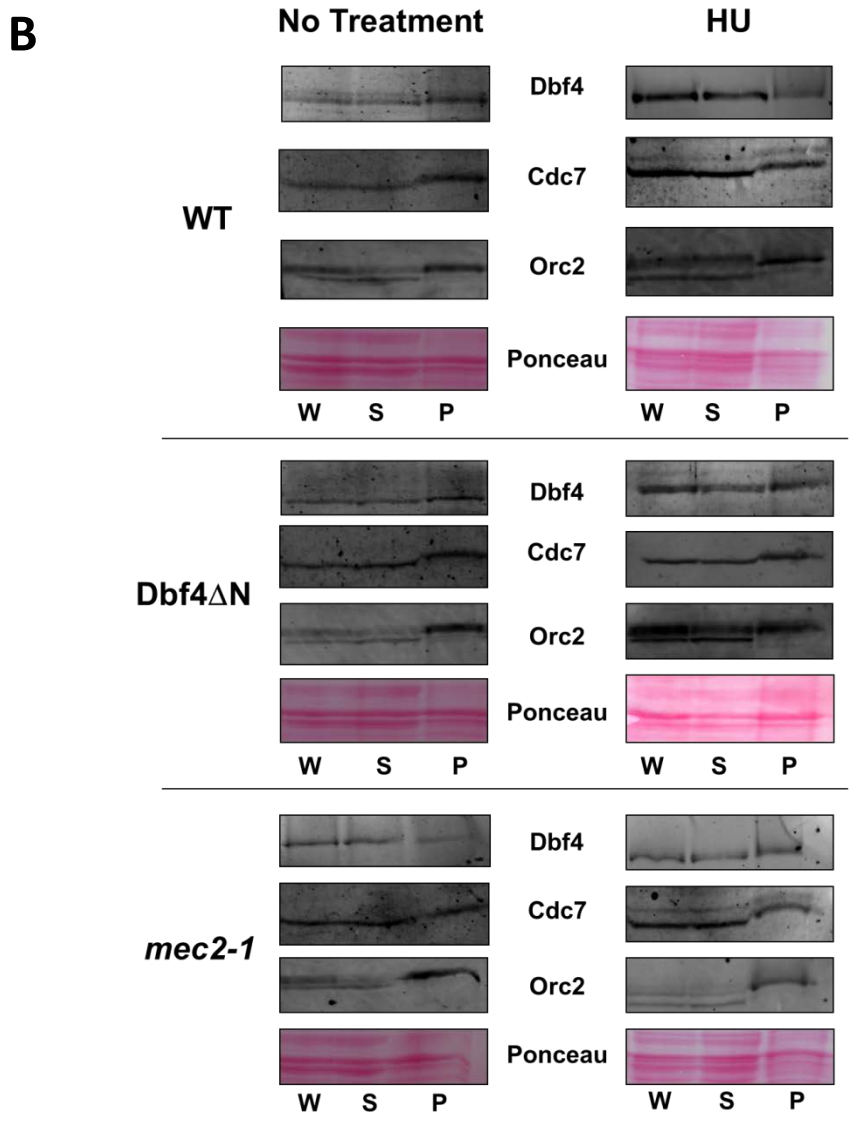
B
No Treatment
HU
WT
Dbf4ΔN
mec2-1
Dbf4
Cdc7
Orc2
Ponceau
W S P

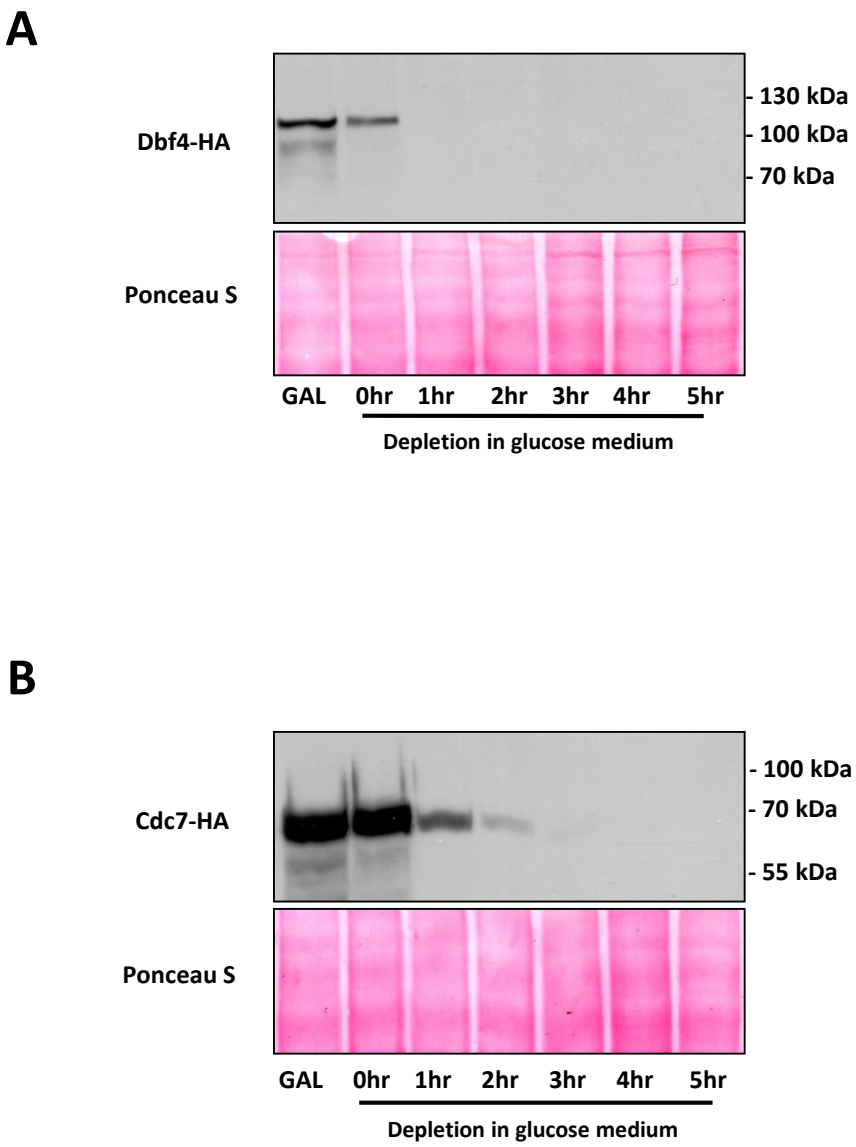

Figure 5.2: Dbf4 and Cdc7 are efficiently depleted in glucose medium. The endogenous promoters for Dbf4 and Cdc7 were replaced by a GAL1 promoter in the TK+ strain background as described in the Materials and Methods (Chapter 2). GAL-Dbf4 TK+ and GAL-Cdc7 TK+ strains were initially grown asynchronously in galactose medium and whole cell extract (WCE) samples were collected. The remaining cultures were then washed and resuspended in glucose medium to deplete the proteins. WCE samples were prepared at the indicated times and all samples were assayed by western blot and detected with anti-HA primary antibody. (A) Dbf4-HA signal is absent by the 1 hour timepoint. (B) Cdc7-HA signal is absent by the 4 hour timepoint. The Ponceau S staining in both (A) and (B) show equal loading of all samles.

DNA combing experiments involving the Dbf4ΔN mutant also require use of a TK+ strain, thus incorporation of this mutation in the TK+ background was also necessary. This strain was generated using the same integration cassette/homologous recombination principle described above, except that rather than simply tagging an endogenous gene, the entire Dbf4 gene was replaced with the Dbf4ΔN mutant version. This necessitated the creation of a novel integration cassette which comprised the entire Dbf4ΔN sequence along with 500 bp of the upstream un-translated region (Figure 5.3). The goal was for recombination to take place in this 5' UTR and in the region downstream of the stop codon, thus creating a Dbf4ΔN-HA-tagged endogenous mutant strain in the TK+ background (DY-261). Following cloning, transformation, and recombination, proper integration was confirmed by PCR and by sequencing.

Because of the potential role of DDK in the S-phase checkpoint response, a DNA combing experiment was designed in order to investigate the requirement of Dbf4 for the stabilization and/or restart of stalled replication forks (Figure 5.4A). In this design, Dbf4 is depleted from cells in an HU-induced S-phase block (i.e. after early origins had fired) followed by release of the cells into HU free medium, while still preventing Dbf4 expression. For comparison, wild-type cells (with normal Dbf4 levels) undergo the same treatment regimen. The extent of both replication origin firing and fork progression is monitored via the incorporation of two different base analogues: CldU marks DNA synthesized before and during the HU block, while IdU marks any DNA synthesized following the lifting of the checkpoint (Figure 5.4B).

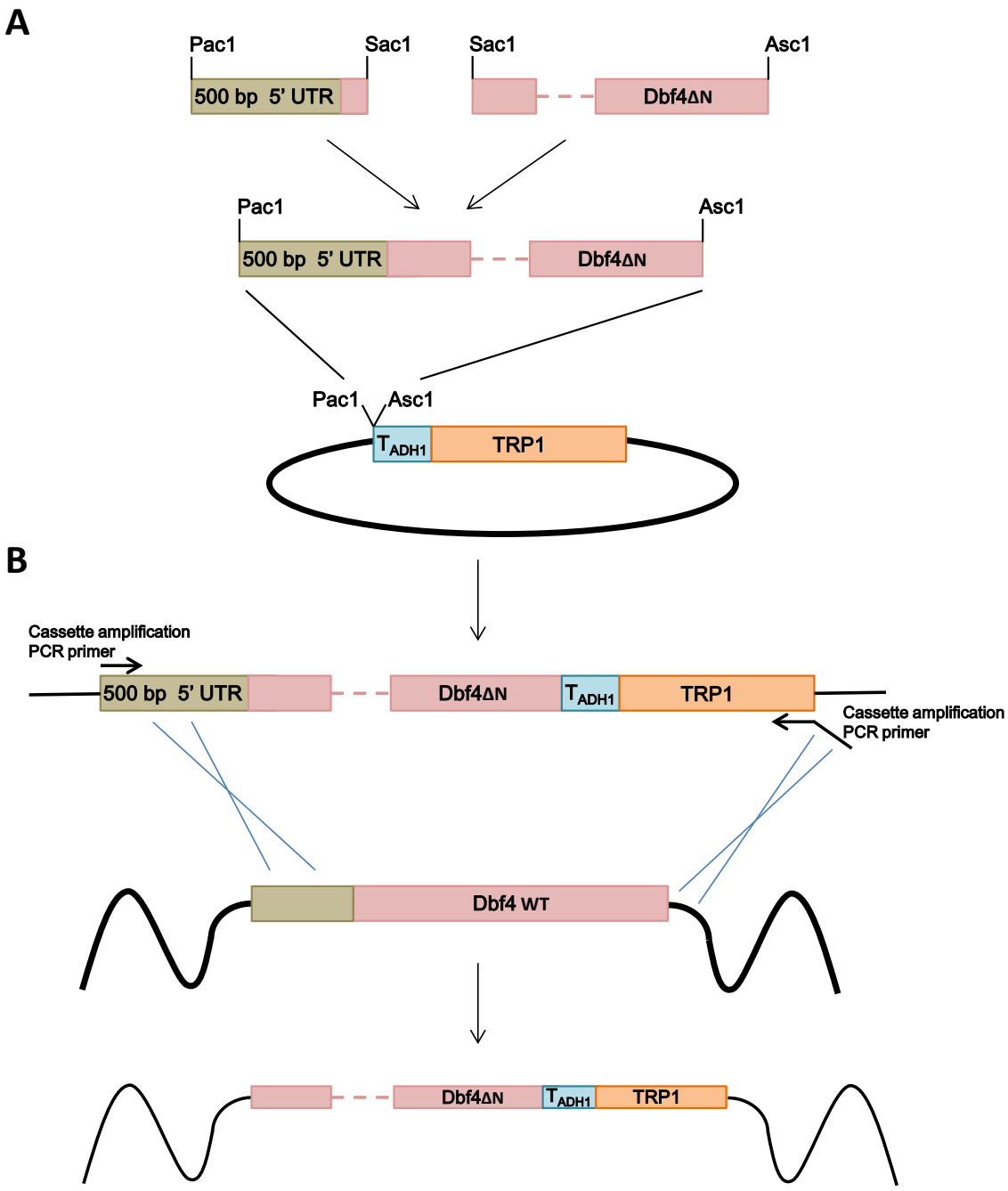

Figure 5.3: Schematic of the Dbf4ΔN TK+ strain creation strategy. (A) PCR was used to amplify Dbf4 fragments from DY-78 genomic DNA template. These fragments were cloned into the pFA6a-TRP1 vector using the PacI and AscI restriction sites in a single ligation reaction to create the integrating cassette vector. (B) This newly created vector was used as PCR template to amplify the integration cassette. This cassette was transformed into TK+ yeast cells followed by plating on SC-trp medium to select for cells that had undergone homologous recombination and had integrated the cassette, including the TRP1 marker.

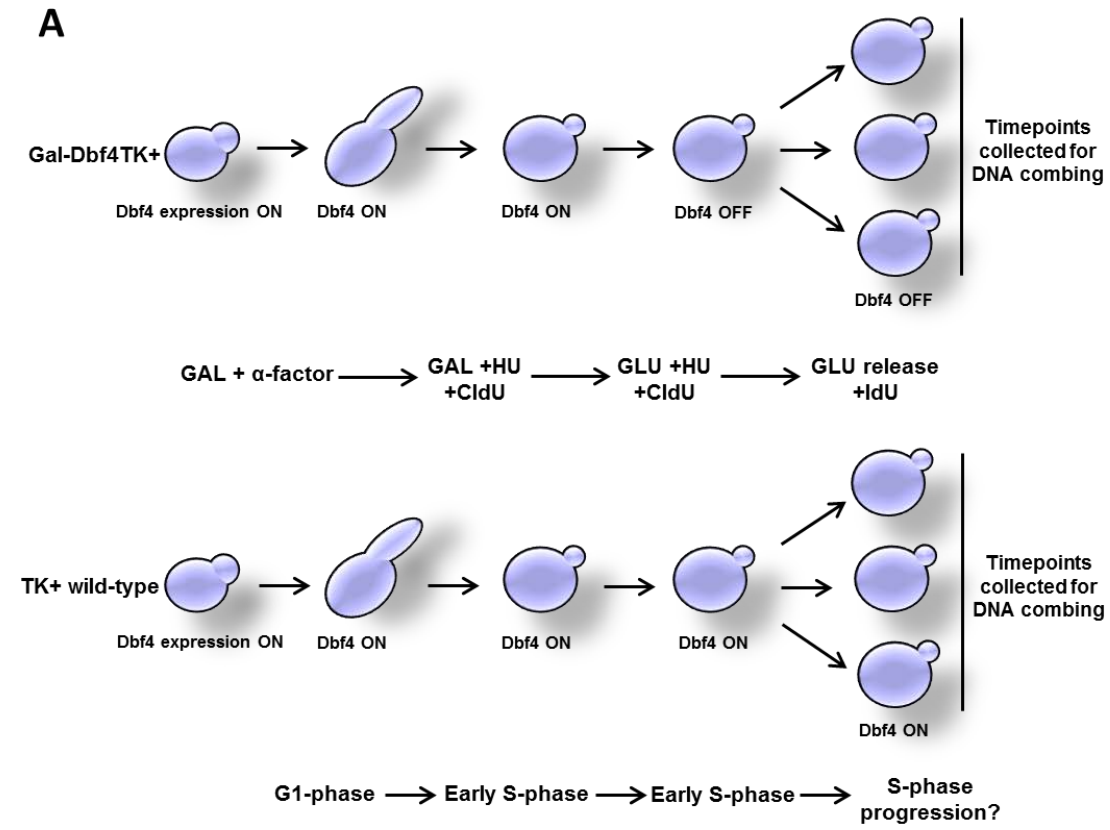

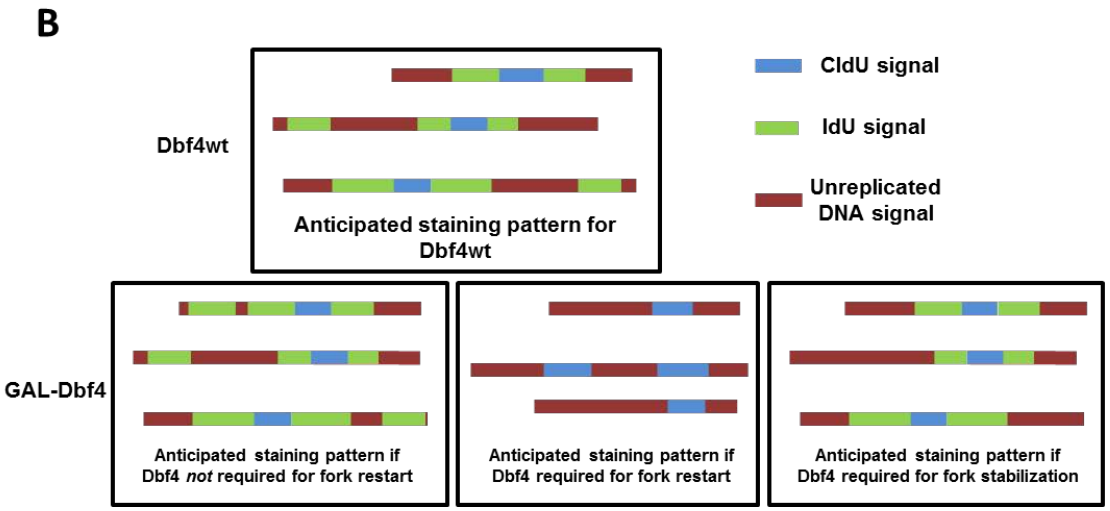

Figure 5.4: Experimental design of a DNA combing assay. (A) Schematic of the experimental design for the investigation of the requirement of Dbf4 for replication fork stabilization/restart during the recovery from the S-phase checkpoint by DNA combing. (B) Schematic of expected nucleotide analogue staining pattern in wild-type and Gal-Dbf4 strains following the arrest/release regimen described above.

In order to optimize the arrest/release regimen and plug creation for the combing protocol, the GAL-Dbf4TK+ strain along with an isogenic TK+ wild-type control were synchronized for 3.5 hours in galactose medium with α-factor followed by release from the block into galactose medium containing HU, for 1 hour. This should allow early origins to fire since Dbf4 expression is on. Because exogenous base analogues are not efficiently taken up by yeast cells, CldU was added for the final 30 minutes of the α-factor arrest (to allow the cell time to accumulate the analogue), and throughout the HU block in order to monitor DNA replication resulting from the firing of early origins. Following this initial arrest in HU, the cultures were transferred to glucose medium (repressing Dbf4 expression) containing HU and CldU for 3 hours. IdU was added for the final 30 minutes of the depletion (to allow accumulation of the analogue) before the cultures were released into glucose medium lacking HU but containing IdU. The IdU was added in order to monitor any DNA replication that occurred following the depletion of Dbf4. Cells were harvested at the indicated timepoints for plug creation and FACS samples were collected at the critical junctures to confirm proper arrest/release (Figure 5.5). As shown by the FACS profiles, S-phase is delayed in the Dbf4-depleted cells as compared to wild-type (compare 30 minute GLU release timpoints).

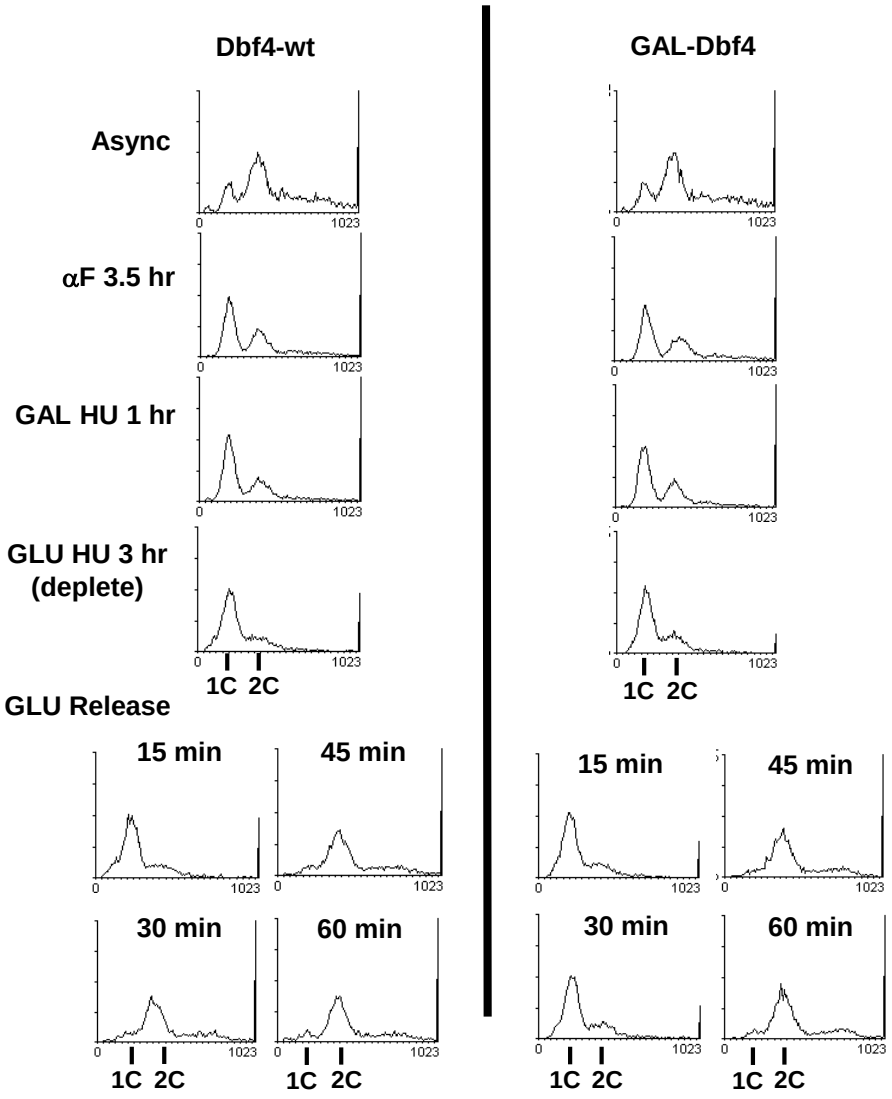

Figure 5.5: S-phase is delayed in Dbf4-depleted cells as compared to wild-type during recovery from HU treatment. Wild-type TK+ (Dbf4-wt) and GAL-Dbf4 TK+ (GAL-Dbf4) cultures were initially grown in galactose/raffinose medium (Gal/Raf) containing α-factor to synchronize the cells. 400µg/ml of CldU was added to each culture for the final 30 minutes of the α-factor incubation. The cultures were released into pheromone-free Gal/Raf medium containing 50µg/ml Pronase E, 0.2M HU, and 400µg/ml of CldU. Cultures were then switched into glucose (Glu) medium containing 0.2M HU, and 400µg/ml of CldU in order to deplete Dbf4 in the Gal-Dbf4 strain. 400 µg/ml of IdU was added to each culture for the final 30 minutes of the depletion incubation. Following depletion, the cultures were released into Glu medium lacking HU but containing 400µg/ml of IdU. DNA combing plugs were prepared for each of the timepoints during the Glu release with final concentration of 2 x 108 cells/plug. FACS profiles are shown for the arrest/release regimen. S-phase is delayed for the Gal-Dbf4 strain compared to wild-type, compare 30min timepoint in the Glu release

Initial experiments using the standard 2 x 10^8 cells/plug produced short and fragmented DNA fibers unsuitable for combing interpretation (Figure 5.6A). The initial imaging of combing samples used anti-CldU and anti-IdU antibodies to image the DNA fibers. Imaging of CldU/IdU was dispensed with in subsequent optimization samples in favour of bulk DNA imaging using an anti-Dbf4 antibody. The optimization of the DNA fiber length and density revealed that a concentration of 2 x 10^{10} cells/plug generated tract lengths of sufficient size and density (Figure 5.6B). Such a high cell concentration necessitated a much larger culture volume in order to maintain cells in logarithmic growth and prevent culture saturation, however this scale-up generated problems in both the proper arrest of cells and their synchronous release, which have yet to be resolved.

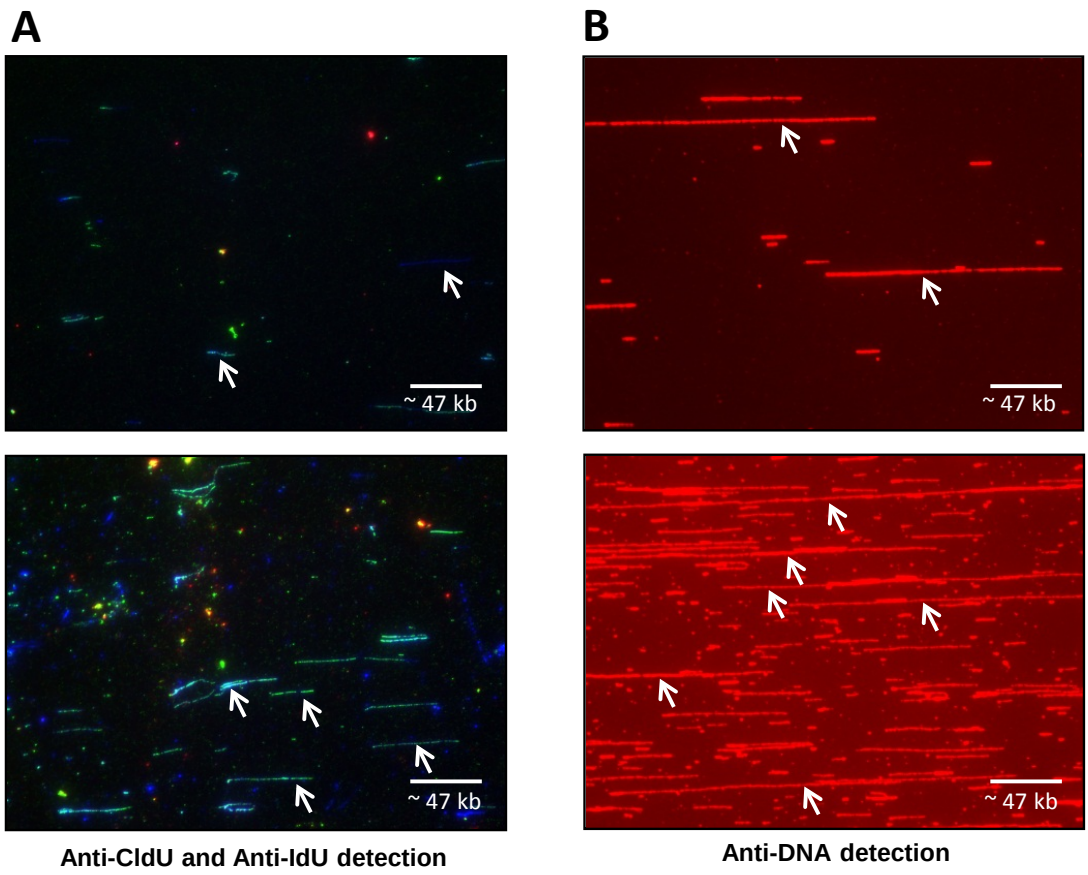

Figure 5.6: Initial DNA combing generated a small number of fragmented DNA fibres, while DNA fibres from subsequent optimization protocols were more numerous and of adequate length. Representative images of DNA fibres isolated from DNA combing experiments are presented. (A) The few DNA fibres isolated from the arrest/release regimen presented in Figure 5.5 were short and fragmented (arrows). DNA fibres were imaged using anti-CldU and anti-IdU antibodies. (B) Subsequent optimization of the number of cells/plug led to the isolation of DNA fibres of sufficient length and number at a concentration of 2 x 1010 cells/plug (arrows). DNA fibres were imaged using an anti-DNA antibody. CldU and IdU were not included in the optimization protocol.

5.2.3 Localization of Replication Factors by Fluorescence Microscopy

Live-cell fluorescence microscopy is an attractive tool for exploring the spatial and temporal localization of Dbf4 and Cdc7 as well as a role for DDK in the S-phase checkpoint. Any change in the localization pattern of Dbf4 and/or Cdc7 upon treatment with genotoxic agents could be tracked, offering the potential to visualize – in real time – any transition from a punctate to a more diffuse staining pattern as Dbf4 and Cdc7 are removed from chromatin. Thus, strains with fluorescently-epitope tagged versions of Dbf4 and/or Cdc7 were required. Individually tagged Dbf4 and Cdc7 strains were already available in the lab, however in order to perform co-localization studies exploring both Dbf4 and Cdc7 in the same cell, a double-tagged strain was required. The ability to visualize both factors simultaneously would show whether they co-localize – which suggests an active kinase – throughout S-phase or if there is a sequential co-localization of a subset of the populations. To this end, Dbf4 was tagged with eYFP (enhanced yellow fluorescent protein) in the same background in which Cdc7 had been previously tagged with eCFP (enhanced cyan fluorescent protein). This was accomplished using the same tagging-cassette amplification, transformation, and homolgous recombination into the yeast genome as described above (see also Chapter 2 and Longtine *et al*., 1998). Proper integration was confirmed by PCR of genomic DNA and western blot analysis was performed to confirm expression (Figure 5.7).

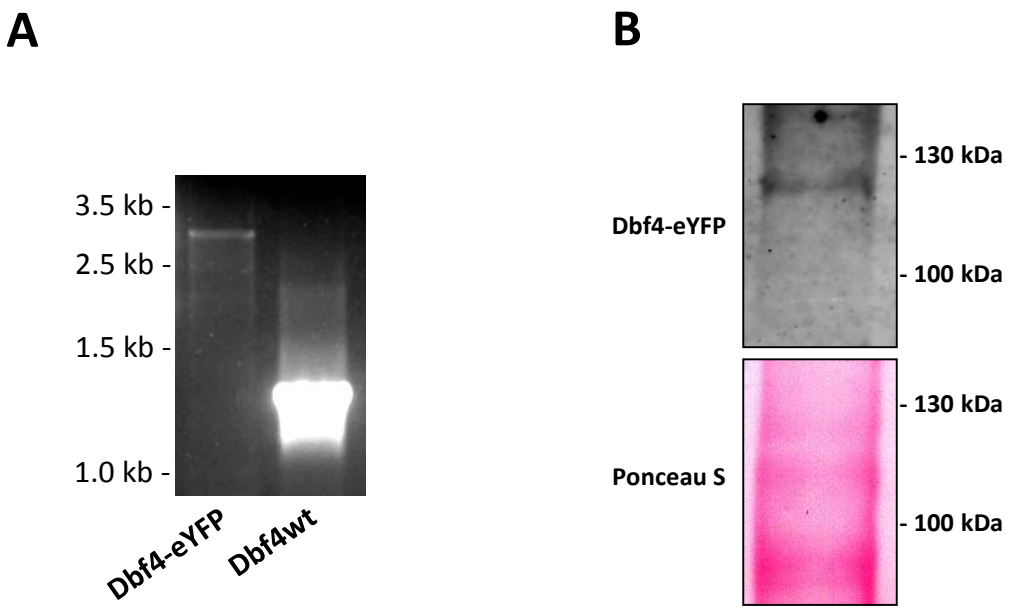

Figure 5.7: Confirmation of eYFP-tagged Dbf4 in a Cdc7-eCFP strain background. The coding sequence for the eYFP fluorescent epitope was added to the genomic copy of Dbf4 as described in the Materials and Methods (Chapter 2). (A) PCR was performed on genomic DNA to confirm proper genomic integration of the eYFP cassette. An internal Dbf4 forward primer was used in conjunction with a reverse Dbf4-flanking primer for the PCR reaction. A correctly integrated tag gives a PCR product of ~3.3kb which is observed in the Dbf4-eYFP lane. The 3.5 minute extension time used for this PCR may have been less than ideal for efficient elongation, and likely accounts for the difference in signal intensity. (B) A whole cell extract was prepared from a culture of the double-tagged strain (Dbf4-eYFP and Cdc7-eCFP) and run on a western blot which was detected with anti-Dbf4 antibody to show stable expression of the fusion.

Nup49 is a high abundance nuclear pore protein that serves as a marker for the nuclear envelope. Since a Nup49-eYFP tagged strain (DY-45) was already available, and had been successfully imaged in the lab previously (Semple *et al*., 2006), it was initially used in order to optimize the microscope settings to detect eYFP signal. Images of live cells were collected over a two hour period at 5 minute intervals (Figure 5.8A). Nup49 is clearly visible and the sequence of images even captures the division of the nucleus during mitosis (Figure 5.8A, arrows). While there is a strong eYFP signal even after repeated rounds of imaging, some photobleaching is observed at later timepoints (Figure 5.8A, compare 85-115min to earlier timepoints).

Because replication factors are located in the nucleus during S-phase, it was prudent to ask whether images of replication factors in the nuclear compartment could be generated. Since there is a relatively high cellular concentration of the MCM subunits compared to many other replication factors (Lei *et al*., 1996) and given that an eYFP-tagged Mcm2 strain (DY-137) was available in the lab, it was decided that attempts at sub-nuclear fluorescence imaging would begin there. Imaging of Mcm2-eYFP in live cells revealed a punctate signal in G1 and S-phase. This signal disappears during G2 and M-phase, before being restored during the subsequent G1-phase (Figure 5.8B). The cell cycle stage was determined by bud morphology (see Chapter 1, Figure 1.1)

Initial attempts to visualize Dbf4 and Cdc7 by taking individual images (as for Nup49 and Mcm2) produced a low signal:noise ratio, making it difficult to distinguish Dbf4 or Cdc7 signal from background noise even with noise filtering and de-speckling adjustments made using ImageJ software (Figure 5.9A). Because previous work with fixed cells had shown sub-nuclear foci staining for Dbf4 but was not attempted for Cdc7

(Pasero et al., 1999), generation live-cell images for Dbf4 was the focus of further optimization experiments. In order to increase the signal to noise ratio, 10 images were taken in succession for Dbf4-eYFP and the data summed (Figure 5.9B). The images generated through this summing process may show a sub-nuclear punctate pattern in S-phase cells (Figure 5.9B, arrows). It remains difficult however, to assess whether these are true foci or simply enhanced background noise. Timecourse images that follow a single cell through S-phase were not achievable following capture of the data required to generate a single summed image due to the severe bleaching of the fluorescent signal.

Figure 5.8: Fluorescence microscopy suggests punctate subnuclear staining for Mcm2-eYFP in S-phase. Cultures of eYFP-tagged strains were prepared and imaged as described in the Materials and Methods (Chapter 2). (A) To optimize the microscope settings for eYFP detection, single live-cell images of the nuclear pore protein Nup49-eYFP were collected at 5 minute intervals for 2 hours. The nuclear boundry is clearly visible and the sequence of images even captures nuclear division during mitosis (arrows). Some bleaching of the fluorescent signal is observed as the timecourse progresses (compare 85-115 min to earlier timepoints). (B) Single live-cell images for Mcm2-eYFP were collected throughout the cell cycle and selected images representing the different phases of the cell cycle (as assessed by bud morphology) are presented. Imaging revealed a punctate subnuclear signal for Mcm2-eYFP in G1 and S-phase. This signal is absent during G2 and M-phase, but is restored in the subsequent G1-phase. Arrows in the dark-field fluorescence panels provide a reference for eYFP signal in the indicated cell throughout the cell cycle.

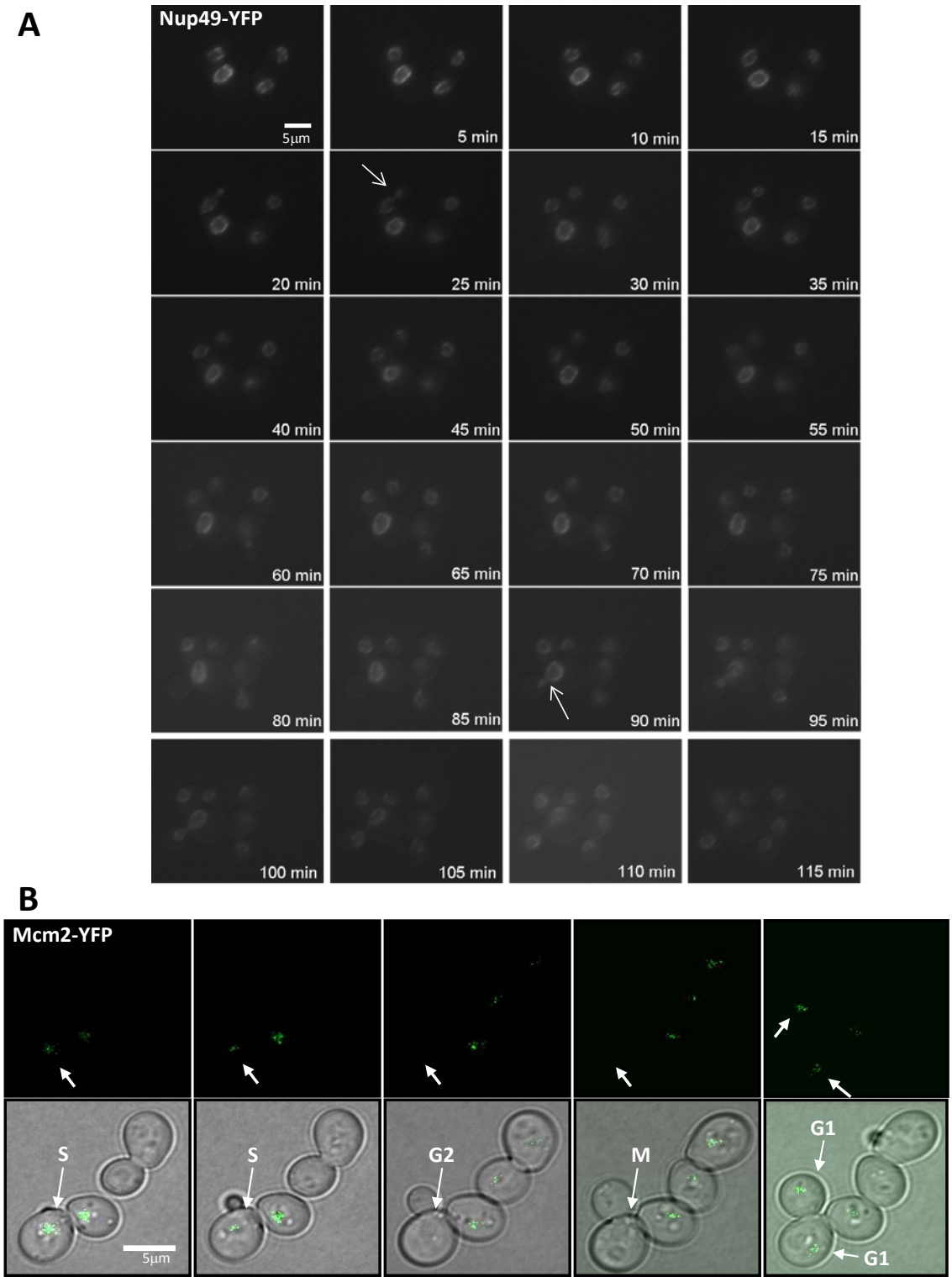
A
Nup49-YFP
5μm
5 min
10 min
15 min
20 min
25 min
30 min
35 min
40 min
45 min
50 min
55 min
60 min
65 min
70 min
75 min
80 min
85 min
90 min
95 min
100 min
105 min
110 min
115 min
B
Mcm2-YFP
S
S
G2
M
G1
G1
5μm

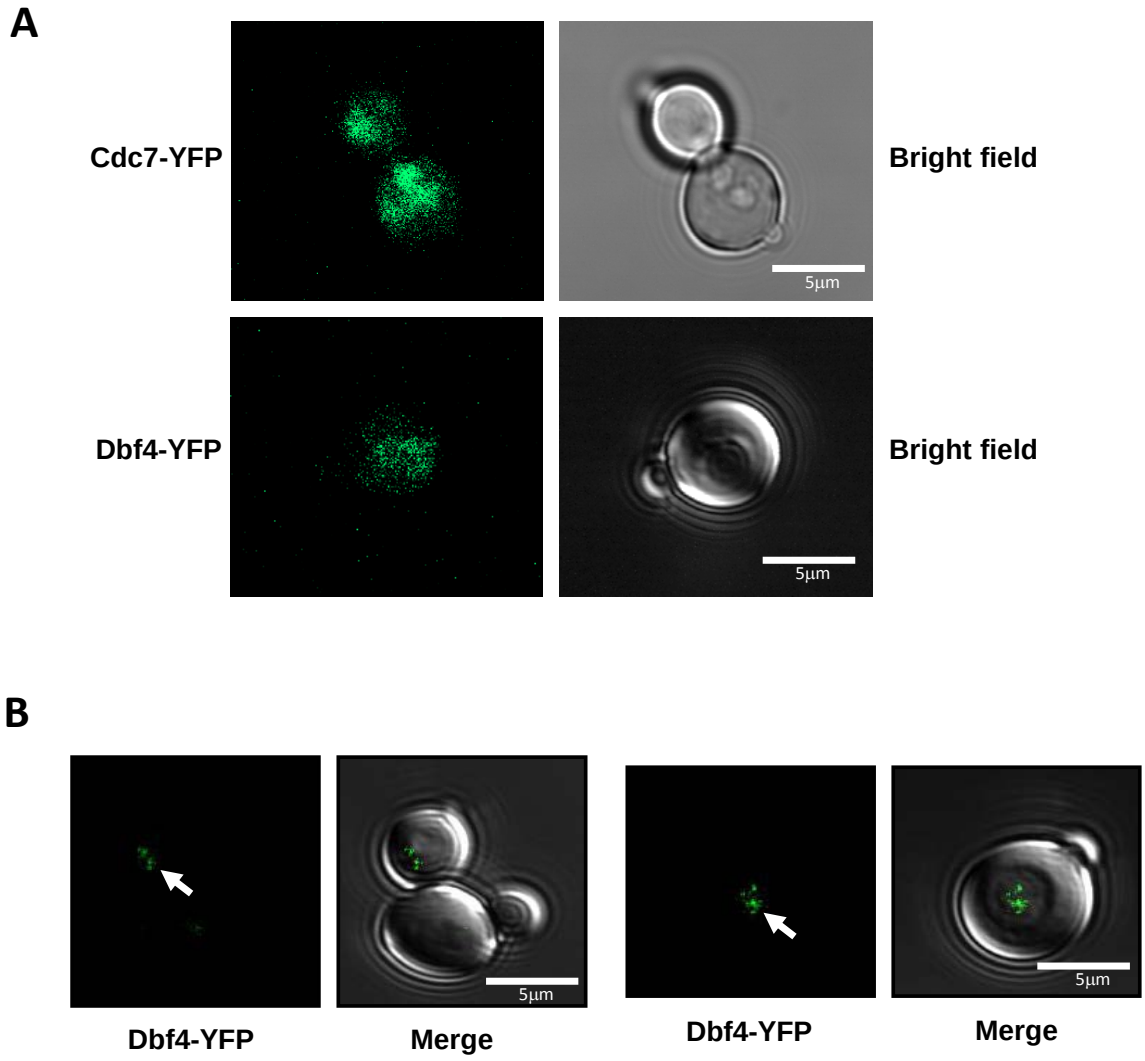

Figure 5.9: Initial optimization of Dbf4-eYFP and Cdc7-eYFP. Cultures of eYFP-tagged strains were prepared and imaged as described in the Materials and Methods (Chapter 2). (A) Single live-cell images were collected for both Dbf4-eYFP and Cdc7-eYFP. The background was reduced and the image de-speckled using ImageJ 1.38x software to produce the representative images shown. (B) A Dbf4-eYFP image with a stronger signal and reduced background was generated by collecting 10 images in succession. These images were then summed using ImageJ 1.38x software, de-speckled, and background adjusted; representative summed images are presented and may show a punctate subnuclear signal pattern in S-phase cells as determined by bud morphology.

5.3 Discussion

5.3.1 Dbf4/Cdc7 Chromatin Association

During S-phase checkpoint conditions Dbf4 has been shown to be phosphorylated and displaced from chromatin in a Rad53-dependent manner (Santocanale and Diffley, 1998; Pasero *et al*., 1999). Previous work from our lab has shown that Dbf4 interacts with Rad53 via the N-motif in Dbf4, and that deletion of this motif abrogates the interaction with Rad53 and confers hypersensitivity to genotoxic stress (Varrin *et al*., 2005). It was therefore interesting to ask whether the displacement of Dbf4 from chromatin under checkpoint conditions requires the Dbf4-Rad53 interaction mediated by the N-motif. To this end a strain lacking the N-motif (Dbf4ΔN) along with a checkpoint-deficient Rad53 strain (*mec2-1,* Weinert *et al*., 1994), and a wild-type strain were treated with HU and assayed by a chromatin fractionation assay (Figure 5.1B). The observation that Dbf4 was found to associate to a greater extent with the insoluble chromatin fraction in the *mec2-1* strain compared to the wild-type is consistent with published data (Pasero *et al*., 1999). Interestingly, there seems to be little if any dissociation of Dbf4ΔN from chromatin under HU conditions compared to wild-type. Both of these results are consistent with the model whereby in wild-type cells, Dbf4 dissociates from chromatin during the S-phase checkpoint and that this dissociation requires interaction with Rad53 via the N-motif of Dbf4; this finding may also help explain the Dbf4ΔN mutant's sensitivity to genotoxic agents (Varrin *et al*., 2005).

The observation that levels of chromatin-bound Cdc7 seem to mirror those of Dbf4 is interesting since it supports a model whereby DDK chromatin association is Dbf4-dependent. While the removal of Dbf4 from chromatin during the checkpoint may be

sufficient to prevent kinase activity at the origin, it may also serve to actively stabilize the stalled replication fork. This stabilization might be accomplished through the retargeting of the displaced DDK to other fork-associated factors known to be DDK substrates including Cdc45 and the polα-primase complex (Nougarede *et al*., 2000; Weinreich and Stillman, 1999). DDK phosphorylation of one or both of these factors may prevent their dissociation from the stalled fork, and help to stabilize the replisome there. Because Dbf4 is displaced from chromatin by Rad53, it is also possible that a Rad53-Dbf4-(Cdc7?) complex may be responsible for the stabilization of Mcm2-7 known to be required to prevent fork collapse (see Chapter 1 section *1.4.3 The role of DDK and Mcm2-7 in the intra-S-phase checkpoint*). Because the chromatin fractionation assay cannot discriminate between origin and non-origin DNA, it is also possible that the Dbf4 is removed from non-origin regions (perhaps the putative reservoirs described in Chapter 4) as a method of Dbf4 sequestration in conjunction with its previously described stabilization (discussed in Pasero *et al*., 1999). This stabilized and sequestered Dbf4 would be prevented from performing its replication activity, but could quickly resume its function upon lifting of the checkpoint. Exploration of these ideas will need to wait until determination of the origin association pattern of Dbf4 and Cdc7 is possible through techniques such as ChIP.

5.3.2 DNA Combing

Although delayed, S-phase did in fact progress in the Dbf4 depleted cells (Figure 5.5). Because DDK activity is required for late origins to fire initially (reviewed in Sclafani and Holzen, 2007) and since DDK is likely inactive in the Dbf4-depleted cells, the recovery from the HU block and subsequent completion of S-phase is not likely the result

of late origin firing. The restart of stalled replication forks is another potential role for DDK in the recovery from a checkpoint. Again however, because S-phase progression was observed to be impaired but not abrogated in Dbf4-depleted cells, it is unlikely that DDK activity is required for fork restart; if this were the case, no forks would restart and S-phase would not complete. It may be that while DDK activity is not essential for fork restart, the efficiency of fork restart may be improved by DDK action. The remaining possible role for DDK in the checkpoint response is one in the stabilization of stalled forks to prevent their collapse and allow them to be restarted once the checkpoint is lifted. The data presented in Figure 5.5 is compatible with such a role in the checkpoint response since Dbf4 is still present during the initial HU arrest, and so DDK could perform its critical function in fork stabilization before being depleted following the subsequent medium switch to glucose. The HU block is not a true arrest in that replication continues but at a much slower pace (Alvino *et al*., 2007), thus it is possible that replication forks might be stalling and restarting multiple times for brief periods throughout the block (possibly due to a lack of dNTPs available for synthesis). Should these cells also lack Dbf4 (as is the case in the depleted cells), and by extension the stabilizing effect of DDK, there would be a greater chance of catastrophic fork collapse thus resulting in DNA damage that would need to be repaired before replication could be completed. This could account for the delay but not halt in S-phase progression observed in Figure 5.5. There also remains the possibility that the depletion of Dbf4, while quite efficient as judged by western blot (Figure 5.2A), may not be complete. This residual Dbf4 might be below the detection threshold of a western blot but may be sufficient to perform an active and essential role in the restart of stalled forks.

With the experimental design presented in this chapter, should Dbf4 be required to restart stalled replication forks, then IdU tracks immediately adjacent to CldU tracks would be expected in the wild-type but not the Dbf4-depleted samples; should it not be required, these adjacent tracts would be present in both strains. The requirement of Dbf4 for late origin firing would be evidenced by isolated IdU tracts present only in the wild-type cells and not the Dbf4-depleted cells (Figure 5.4B).

The initial protocol that called for 2×10^8 cells/plug was based on protocols found in the literature (Versini *et al*., 2003) and provided by collaborators on this project who had successfully combed yeast DNA in the past (J. Yang, pers. comm.). Thus the high concentration of cells per DNA combing plug (2×10^{10}) I found to be required to generate a sufficient quantity of DNA tracts of adequate length was surprising. Because of the increased volumes required to ensure that growing cultures were in log phase, and the subsequent issues this produced in the proper arrest/release regimen, it would be useful to explore the downstream plug processing protocol to ascertain whether there is efficient cell lysis and DNA isolation. Inefficeint cell lysis and/or DNA isolation in the round of experiments described above would explain why a lower cell concentration was sufficient previously but not for the experiments described here. Should this be optimized, then there would be no need for scaling up the size of the culture volumes and the arrest/release issues could be circumvented.

5.3.3 Fluorescence Microscopy

Initial work with the Nup49-eYFP strain allowed imaging of an eYFP signal in the case of this high-abundance protein (Figure 5.8A). Subsequent investigation of Mcm2-eYFP

localization showed an apparent subnuclear punctate pattern of staining present only during G1 and S-phases. This is somewhat consistent with MCM localization described in the literature, namely that Mcm2-7 is imported into the nucleus and loaded onto DNA at origins in G1-phase. In late G1 however, unbound Mcm2-7 is exported from the nucleus until it is excluded (discussed in Liku *et al*., 2005). Thus the Mcm2-eYFP signal captured for S-phase cells in Figure 5.8B might represent only the loaded fraction of the Mcm2-7. It is thought that DNA synthesis occurs in a handful of discrete 'replication factories' (observed as subnuclear foci by fluorescence microscopy, Pasero *et al*., 1999; Kitamura *et al*., 2006), and the foci observed in Figure 5.8B is consistent with this model. Further co-localization studied might be considered to confirm that these foci are indeed located in the nucleus (using a fluorescent epitope-tagged Nup49, for example).

While a double-tagged strain (Dbf4-eYFP, Cdc7-eCFP) was created for this study, the fact that eYFP, in general, generates a more robust fluorescent signal (Shaner *et al*., 2005) meant that the optimization of image collection was focused on eYFP. The newly created double-tagged strain was used for Dbf4-eYFP imaging while Cdc7 imaging was performed using the previously generated single-tagged Cdc7-eYFP strain. Because its abundance is much lower than that of Nup49 and Mcm2 a single image for Dbf4 that could distinguish true signal from background noise was not achievable. Thus, a different procedure for collecting fluorescent images was required. It was necessary to take 10 images in succession and sum the data together in order to generate an image with a lower background. This process produce potentially interesting images (representative images presented in Figure 5.9B), since subnuclear foci similar to those described in the literature (Pasero *et al*., 1999; Semple *et al*., 2006) were generated. It must be noted that

it took approximately 20 seconds to capture all of this data. In that time it is quite likely that the cell would experience slight movement due to Brownian motion; this coupled with the low likelihood that replication factors would remain stationary inside the nucleus for that length of time, leads to the possibility that the summed Dbf4-eYFP signal is simply background noise. Another major draw back to this 10-image-summing process is the photobleaching of the fluorescent signal that occurs, making the imaging of the same cell over multiple timpoints through S-phase unachievable.

Fluorescence imaging has been optimized to the extent possible with the available equipment. Further imaging will require a higher resolution microscope and imaging capability. There are also new generations of fluorescent proteins available which might be better suited to these studies; in fact some argue that eYFP is obsolete and should be replaced with newer variants such as mCitrine, Venus, or YPet (Shaner *et al.*, 2005). Once this equipment is available in-house or a suitable collaboration is secured and the possibilities of newer fluorescent proteins explored, it would be of interest to continue this project. Co-localization studies of Dbf4 and Cdc7 could help to elucidate the model of DDK targeting: continually co-localized signals organized in subnuclear foci would support a model whereby the active complex is targeted to origins, whereas intermittent co-localization might indicate Dbf4 activation of Cdc7 already present at origins. Similarly, the effect of S-phase perturbation (by HU, for example) on Dbf4 and Cdc7 localization could be explored and these investigations could be further examined by using the Dbf4ΔN mutant (once a suitable epitope-tagged strain is generated).

The results presented in this chapter represent important first steps in the development and optimization of powerful tools that will allow future studies to investigate the mechanism of DDK action in both normal and perturbed S-phase.

Chapter 6: General conclusions and future directions

6.1 Why study DNA replication?

There is much similarity between the DNA replication factors and cell division mechanisms of *S. cerevisiae* and other eukaryotic organisms including humans, and so yeast is a valuable tool for exploring these processes. DNA replication is a highly coordinated series of protein-DNA interactions that culminates in the synthesis of a cell's genome in S-phase. This process is regulated by numerous proteins and complexes some of which associate with chromatin to promote replication initiation, the pre-RC, for example, while other factors and processes (such as CDK phosphorylation of ORC) work to prevent initiation from occurring more than once per cell cycle. Cellular checkpoints provide a mechanism for ensuring that the entire genome is replicated exactly once during S-phase and that any genetic damage is repaired before the cell divides. Disturbances in the balance of replication or checkpoint factors can contribute to disease, including cancer, in higher eurkaryotes (see section 6.6 Relevance to Cancer, below), and so it is important to understand how the factors involved in DNA replication function and are regulated in a normal cell.

6.2 DDK interactions with the MCM complex

In *S. cerevisiae* there are more than 300 confirmed origins of DNA replication distributed throughout the genome to ensure that the entire genetic complement is replicated in a reasonable timeframe. DNA replication is initiated from these origins following the formation of the pre-replicative complex in G1-phase. The ultimate goal of the pre-RC is to load the MCM complex which, upon activation by DDK, forms an integral part of the

replicative helicase. In the four decades since the initial discovery of DDK, much has been learned about its regulation by Dbf4, its physiological targets (subunits of Mcm2-7, Sheu and Stillman, 2010; Randell *et al*., 2010), and its involvement in the S-phase checkpoint response (Weinreich and Stillman, 1999; Varrin *et al*., 2005). It remained unclear however, how DDK is targeted to origins at the time of firing and exploration of this question was a major focus of this project. Systematic examination of the interactions between the DDK subunits and the MCM subunits revealed that Dbf4 and Cdc7 interact with mutually exclusive subunits of the Mcm2-7 complex. Disruption of the interaction between either Mcm2 and Dbf4 or Mcm4 and Cdc7 only imparted a modest growth impairment suggesting that either interaction is sufficient for the targeting of DDK to the MCM complex. It also seems that the cell requires at least one of these interactions to target DDK since a double mutant could not be isolated and disrupting the Dbf4-Mcm2 interaction in the Mcm4Δ175-333 background imparted a severe growth impairment. Taken together, these data suggest a model whereby DDK is targeted to the MCM complex via an interaction between both the extreme N-terminal region of Mcm2 and Dbf4 and the DDD of Mcm4 and Cdc7. These interactions may work together to ensure efficient DDK targeting, though either one on its own is sufficient for cell viability.

Because the Mcm2Δ2-4,10-63 mutation affects the region flanking one of the nuclear localization signals required for the proper targeting of the MCM complex to the nucleus (Liku *et al.*, 2005), it would be worth testing the efficiency of the nuclear localization of the MCM complex in this mutant. This could be accomplished by creating a Mcm2Δ2-4,10-63-GFP construct and comparing nuclear localization to Mcm2wt-GFP by fluorescence microscopy. It would be interesting to further characterize Mcm2 and

Mcm4 to identify the residue(s) responsible for the interactions with DDK, as mutation of the smallest region necessary to abrogate the interaction would increase confidence that other interactions involving Mcm2 and Mcm4 are not affected. It would also be important to link the reduction in DDK targeting reported here to origin firing. 2D agarose gel analysis could be used to compare the efficiency/timing of origin firing in wild-type and Mcm2Δ2-4,10-63 and Mcm4Δ175-333 strains.

6.3 Chromatin immunoprecipitation of Dbf4 and Cdc7

Two models exist for DDK action; the first envisages DDK being targeted to origins as an active complex, whereas the other proposes that Dbf4 activates Cdc7 already present at origins. Previous work looking at Dbf4- and Cdc7-DNA interactions has relied on assays that do not discriminate origin from non-origin sequence (Weinreich and Stillman, 1999; Pasero *et al.*, 1999) and so a goal of this project was to explore these interactions using chromatin immunoprecipitation. The lack of origin-specific enrichment observed for Dbf4 or Cdc7, but the seeming enrichment in flanking regions led to the idea that DDK is localized in origin-flanking pools or reservoirs and is actively excluded from the origin until redistributing there at the time of firing. While this may be evidence supporting the model of active DDK being targeted to origins, interpretation of the origin:flanking band ratios is difficult due to the lack of origin signal in many samples. A possible avenue of approach to link this redistribution of DDK to origins at the time of firing would be to perform 2D agarose gel analysis in conjunction with ChIP. Thus it might be possible to show origin firing at the same time that there is redistribution of Dbf4 and/or Cdc7 to the origin. Because of the potential technical issues with ChIP

described in Chapter 4, a modified version of the protocol was designed that has the potential to contribute valuable information not only about DDK origin association, but also any association with origin flanking regions. The preliminary success of the modified ChIP (Chapter 4, Figure 4.8) in detecting a signal for Dbf4 should be followed up with optimizations for the detection of Cdc7 and Orc2 in order to finally elucidate the model of DDK origin targeting. The modified ChIP also offers the potential to investigate protein association with stretches of origin flanking sequence of differing lengths. Future studies using this technique could evaluate the validity of the Dbf4 reservoir hypothesis outlined in Chapter 4 by systematically exploring flanking regions at increasing distances from an origin. It may be that this Dbf4 reservoir exists in discrete inter-origin regions, or that its distribution is fairly even across non-origin sequences. Researchers have been attempting to ChIP Dbf4 for a number of years with little success and it may be that newer technologies such as ChIP-on-chip or ChIP-Seq will be required to finally visualize Dbf4 at origins of DNA replication. Next generation *in vitro* systems that allow for the re-capitulation of the assembly and activation of the pre-RC may also be of value in elucidating the model of DDK action (Heller *et al.*, 2011). It must be pointed out however, that while *in vitro* systems can provide important insights, these synthetic constructs may not always reflect the situation *in vivo* and so the *in vitro* data should always be considered in conjunction with observations made *in vivo*.

6.4 Dbf4 and DNA combing

In recent years links have been established between DDK and the S-phase checkpoint (Varrin *et al.*, 2005; Tsuji *et al.*, 2008; Zegerman and Diffley, 2010). It had been well

documented that Dbf4 is inactivated and removed from chromatin by a Rad53-dependant phosphorylation event during the S-phase checkpoint (Weinreich and Stillman, 1999; Zegerman and Diffley, 2010), and that the Dbf4 N-motif is required for interaction with Rad53 (Varrin *et al*., 2005). The final piece of evidence showing the requirement of the N-motif-mediated Dbf4-Rad53 interaction for proper checkpoint removal of Dbf4 from chromatin was provided in this study (Chapter 5, Figure 5.1). This Dbf4ΔN mutant, then, has the potential to be a powerful tool in the exploration of the role of DDK in the S-phase checkpoint. An important experiment that should be completed following the optimization of the DNA combing protocol is to use the Dbf4ΔN mutant to evaluate how impairing the normal removal of Dbf4 from chromatin during the checkpoint affects fork stabilization/recovery and late origin firing (similar to the experiment outlined in Chapter 5). The consequences of an impaired Dbf4-Rad53 interaction could also be assayed using the Dbf4ΔN strain in conjunction with microarray analysis of dense-isotope substitution experiments which were initially used to show that HU treatment causes an extreme slowdown but not block of S-phase (Alvino *et al*., 2007). It would be interesting to see whether Dbf4ΔN could rescue this HU-induced S-phase slowdown, and what effect that might have on replication fork stability. Through the creation of the various Dbf4 TK+ strains described in Chapter 5, and the initial optimization of the combing protocol itself, the groundwork has been laid for future studies to explore the consequences of Dbf4 activity in the checkpoint response.

6.5 Replication factors and fluorescence microscopy

Mcm2 seems to localize in a punctate pattern by live-cell fluorescence microscopy. This is consistent with previous work showing that DNA replication occurs in discrete 'replication factories' visible as subnuclear foci in fixed yeast cells (Pasero *et al*., 1999; Kitamura *et al*., 2006). Initial live-cell fluorescent microscopy imaging of Dbf4 may show a similar punctate pattern and again, is similar to the pattern observed in fixed cells (Pasero *et al*., 1999). In both cases it would be of value to confirm these signals are in fact localized to the nucleus; this could be accomplished imaging Mcm2 and Dbf4 in Nup49-fluorescently tagged strains. Because of the difficulty of imaging these replication factors, it would be prudent to explore new-generation fluorophores and imaging technology in order to have the greatest chance at generating interesting images. Once imaging of Dbf4, Cdc7, and Mcm2 can be reliably accomplished, it would be interesting to perform co-localization studies with Dbf4 and Cdc7 as well as with Dbf4 or Cdc7 and Mcm2. These studies would show when Dbf4 and Cdc7 are present together both spatially and temporally (indicative of their interaction), and how this interaction compares to localization with Mcm2. The origin localization of these factors throughout S-phase could also be explored by imaging them in strains where a specific origin has also been fluorescently tagged. This is accomplished by the integration of a cassette of tandem *lac* repressor binding sites into the genome adjacent to an origin of interest. Expression of a fluorescently tagged-*lac* repressor fusion in these cells would allow for the origin to be imaged (Heun *et al*., 2001). All of these studies would help elucidate the model of DDK action and because they would be performed in live cells, this microscopy would provide convincing support for the biochemical assays described above.

6.6 Relevance to cancer

With an estimated 178,000 new cases of cancer being diagnosed, and nearly 75,000 deaths from cancer predicted occur in Canada in 2011 (Canadian Cancer Society, 2011), research into the mechanisms of this disease and potential avenues of treatment are currently areas of great interest. Because DNA replication is required for cell division it logical to think that deregulation of factors involved in this process may play a role in the cancer phenotype. Indeed, studies involving replication initiation factors such as Mcm2, Mcm5, and Cdc6 indicate that these factors are up-regulated to different degrees in bladder, colon, cervix, and lung cancers (Going *et al*., 2002; Korkolopoulou *et al*., 2005; Murphy *et al*., 2005), meaning that they could be used as indicators of cancer pathology. Cdc7 has also been implicated in human cancers; Cdc7 mRNA levels were shown to be elevated in seven of eight cancer cell lines tested as compared to normal tissue (Hess *et al*., 1998). A more recent study investigated the levels of both Cdc7 and Dbf4 protein in the NCI-60 human cell lines (a panel of 59 human cancer tumour cell lines that represent the most common forms of cancer) compared to normal cell lines (Bonte *et al*., 2008). Low or undetectable levels of Cdc7 protein were observed in the normal cell lines, whereas about 50% of the tumour cell lines showed high levels of Cdc7 and Dbf4. Furthermore, the increase in Cdc7 levels in these cell lines was correlated to actual primary tumour tissue, in that Cdc7 protein could be detected in 25/37 of these primary tumours but not in matched normal tissue. Interestingly, 15 of 20 breast carcinomas showed increased Cdc7 expression, a characteristic, the authors say, which may be a common feature of breast cancer (Bonte *et al*., 2008). Cdc7 is also being investigated as a therapeutic drug target and there have been some very encouraging findings that show the

reduction of Cdc7 levels by siRNA leads to apoptosis in cancer cell lines but not in normal dermal fibroblast cells (Montagnoli *et al*., 2004). Thus Cdc7 has the potential to be a potent drug target in cancer therapy and indeed there are a number of clinical trials testing the efficacy of different Cdc7 inhibitors (Menichincheri *et al*., 2009; Swords *et al*., 2010). While cancer was not the main focus of the work presented in this thesis, the data presented here provides valuable insight into the normal process of the initiation of DNA replication and can serve as a benchmark for comparison with the disease state.

References

Alcasabas, A. A., Osborn, A. J., Bachant, J., Hu, F., Werler, P. J. H., Bousset, K., Furuya, K., Diffley, J. F. X., Carr, A. M. and Elledge, S. J. (2001). Mrc1 transduces signals of DNA replication stress to activate Rad53. Nat. Cell Biol. *11*, 958-965.

Alvino, G. M., Collingwood, D., Murphy, J. M., Delrow, J., Brewer, B. J. and Raghuraman, M. (2007). Replication in hydroxyurea: it's a matter of time. Mol. Cell. Biol. *18*, 6396.

Amberg, D.C., Burke, D.J., and Strathern, J.N. (2005). Methods in yeast genetics. Cold Spring Harbor Laboratory Press, Cold Spring Harbor, NY.

Aparicio, O. M., Stout, A. M. and Bell, S. P. (1999). Differential assembly of Cdc45p and DNA polymerases at early and late origins of DNA replication. Proceedings of the National Academy of Sciences *16*, 9130.

Aparicio, O. M., Weinstein, D. M. and Bell, S. P. (1997). Components and dynamics of DNA replication complexes in S. cerevisiae: redistribution of MCM proteins and Cdc45p during S phase. Cell *1*, 59-69.

Araki, H. (2010). Regulatory mechanism of the initiation step of DNA replication by CDK in budding yeast. Biochimica et Biophysica Acta (BBA)-Proteins & Proteomics *3*, 520-523.

Ausubel, F., Brent, R., Kingston, R.E., Moore, D.D., Seidman, J.G., Smith, J.A., and Struhl, K. (1995). Short protocols in molecular biology, 3rd edition. Wiley Press, New York, NY.

Bailis, J. M., Luche, D. D., Hunter, T. and Forsburg, S. L. (2008). Minichromosome maintenance proteins interact with checkpoint and recombination proteins to promote s-phase genome stability. Mol. Cell. Biol. *5*, 1724.

Baker, S. P., Phillips, J., Anderson, S., Qiu, Q., Shabanowitz, J., Smith, M. M. and Yates, J. R. (2010). Histone H3 Thr 45 phosphorylation is a replication-associated post-translational modification in S. cerevisiae. Nat. Cell Biol. *3*, 294.

Bardwell, L. (2004). A walk-through of the yeast mating pheromone response pathway. Peptides *9*, 1465-1476.

Bell, S. P. and Dutta, A. (2002). DNA replication in eukaryotic cells. Annu. Rev. Biochem., 333.

Bochman, M. L., Bell, S. P. and Schwacha, A. (2008). Subunit organization of Mcm2-7 and the unequal role of active sites in ATP hydrolysis and viability. Mol. Cell. Biol. *19*, 5865.

Bochman, M. L. and Schwacha, A. (2009). The Mcm complex: unwinding the mechanism of a replicative helicase. Microbiology and Molecular Biology Reviews *4*, 652.

Bochman, M. L. and Schwacha, A. (2007). Differences in the Single-stranded DNA Binding Activities of MCM2-7 and MCM467. J. Biol. Chem. *46*, 33795.

Bonte, D., Lindvall, C., Liu, H., Dykema, K., Furge, K. and Weinreich, M. (2008). Cdc7-Dbf4 kinase overexpression in multiple cancers and tumor cell lines is correlated with p53 inactivation. Neoplasia (New York, NY) *9*, 920.

Bousset, K. and Diffley, J. F. X. (1998). The Cdc7 protein kinase is required for origin firing during S phase. Genes Dev. *4*, 480.

Branzei, D. and Foiani, M. (2009). The checkpoint response to replication stress. DNA repair *9*, 1038-1046.

Branzei, D. and Foiani, M. (2006). The Rad53 signal transduction pathway: Replication fork stabilization, DNA repair, and adaptation. Exp. Cell Res. *14*, 2654-2659.

Branzei, D. and Foiani, M. (2005). The DNA damage response during DNA replication. Curr. Opin. Cell Biol. *6*, 568-575.

Brewer, B. J. and Fangman, W. L. (1987). The localization of replication origins on ARS plasmids in S. cerevisiae. Cell *3*, 463-471.

Bruck, I. and Kaplan, D. (2009). Dbf4-Cdc7 phosphorylation of Mcm2 is required for cell growth. J. Biol. Chem. *42*, 28823.

Canadian Cancer Society/National Cancer Institute of Canada. Canadian Cancer Statisitics, 2011. (2011). Toronto.

Cavalieri, D., McGovern, P. E., Hartl, D. L., Mortimer, R. and Polsinelli, M. (2003). Evidence for S. cerevisiae fermentation in ancient wine. J. Mol. Evol., 226-232.

Chan, S. W. L. and Blackburn, E. H. (2003). Telomerase and ATM/Tel1p protect telomeres from nonhomologous end joining. Mol. Cell *5*, 1379-1387.

Chen, S., De Vries, M. A. and Bell, S. P. (2007). Orc6 is required for dynamic recruitment of Cdt1 during repeated Mcm2–7 loading. Genes Dev. *22*, 2897.

Cheng, L., Collyer, T. and Hardy, C. F. J. (1999). Cell cycle regulation of DNA replication initiator factor Dbf4p. Mol. Cell. Biol. *6*, 4270.

Chong, J. P. J., Thömmes, P. and Blow, J. J. (1996). The role of MCM/P1 proteins in the licensing of DNA replication. Trends Biochem. Sci. *3*, 102-106.

Chuang, C. H., Wallace, M. D., Abratte, C., Southard, T. and Schimenti, J. C. (2010). Incremental Genetic Perturbations to MCM2-7 Expression and Subcellular Distribution Reveal Exquisite Sensitivity of Mice to DNA Replication Stress. PLoS genetics *9*, e1001110.

Cobb, J. A., Bjergbaek, L., Shimada, K., Frei, C. and Gasser, S. M. (2003). DNA polymerase stabilization at stalled replication forks requires Mec1 and the RecQ helicase Sgs1. EMBO J. *16*, 4325-4336.

Cobb, J. A., Schleker, T., Rojas, V., Bjergbaek, L., Tercero, J. A. and Gasser, S. M. (2005). Replisome instability, fork collapse, and gross chromosomal rearrangements arise synergistically from Mec1 kinase and RecQ helicase mutations. Genes Dev. *24*, 3055.

Corbett, M., Xiong, Y., Boyne, J. R., Wright, D. J., Munro, E. and Price, C. (2006). IQGAP and mitotic exit network (MEN) proteins are required for cytokinesis and re-polarization of the actin cytoskeleton in the budding yeast, Saccharomyces cerevisiae. Eur. J. Cell Biol. *11*, 1201-1215.

Costanzo, V., Shechter, D., Lupardus, P. J., Cimprich, K. A., Gottesman, M. and Gautier, J. (2003). An ATR-and Cdc7-dependent DNA damage checkpoint that inhibits initiation of DNA replication. Mol. Cell *1*, 203-213.

Culotti, J. and Hartwell, L. (1971). Genetic control of the cell division cycle in yeast* 1:: III. Seven genes controlling nuclear division. Exp. Cell Res. *2*, 389-401.

Davey, M. J., Indiani, C. and O'Donnell, M. (2003). Reconstitution of the Mcm2-7p heterohexamer, subunit arrangement, and ATP site architecture. J. Biol. Chem. *7*, 4491.

Devault, A., Gueydon, E. and Schwob, E. (2008). Interplay between S-cyclin-dependent kinase and Dbf4-dependent kinase in controlling DNA replication through phosphorylation of yeast Mcm4 N-terminal domain. Mol. Biol. Cell *5*, 2267.

Dickinson, J.R. (1999). Life cycle and morphogenesis. The metabolism and molecular physiology of *Saccharomycese cerevisiae*. Taylor & Francis Ltd, Philadelphia.

Donaldson, A. D., Fangman, W. L. and Brewer, B. J. (1998). Cdc7 is required throughout the yeast S phasetoactivatereplication origins. Genes Dev. *4*, 491.

Duch, A., Palou, G., Jonsson, Z. O., Palou, R., Calvo, E., Wohlschlegel, J. and Quintana, D. G. (2011). A Dbf4 Mutant Contributes to Bypassing the Rad53-mediated Block of Origins of Replication in Response to Genotoxic Stress. J. Biol. Chem. *4*, 2486.

Duncker, B. P. and Brown, G. W. (2003). Cdc7 kinases (DDKs) and checkpoint responses: lessons from two yeasts. Mutation Research/Fundamental and Molecular Mechanisms of Mutagenesis *1-2*, 21-27.

Evrin, C., Clarke, P., Zech, J., Lurz, R., Sun, J., Uhle, S., Li, H., Stillman, B. and Speck, C. (2009). A double-hexameric MCM2-7 complex is loaded onto origin DNA during licensing of eukaryotic DNA replication. Proceedings of the National Academy of Sciences *48*, 20240.

Fletcher, R. J., Bishop, B. E., Leon, R. P., Sclafani, R. A., Ogata, C. M. and Chen, X. S. (2003). The structure and function of MCM from archaeal M. thermoautotrophicum. Nature Structural & Molecular Biology *3*, 160-167.

Forsburg, S. L. (2008). The MCM helicase: linking checkpoints to the replication fork. Biochem. Soc. Trans. *Pt 1*, 114-119.

Francis, L. I., Randell, J. C. W., Takara, T. J., Uchima, L. and Bell, S. P. (2009). Incorporation into the prereplicative complex activates the Mcm2–7 helicase for Cdc7–Dbf4 phosphorylation. Genes Dev. *5*, 643.

Garcia, V., Furuya, K. and Carr, A. M. (2005). Identification and functional analysis of TopBP1 and its homologs. DNA repair *11*, 1227-1239.

Garg, P. and Burgers, P. M. J. (2005). DNA polymerases that propagate the eukaryotic DNA replication fork. Crit. Rev. Biochem. Mol. Biol. *2*, 115-128.

Godinho Ferreira, M., Santocanale, C., Drury, L. S. and Diffley, J. F. X. (2000). Dbf4p, an essential S phase-promoting factor, is targeted for degradation by the anaphase-promoting complex. Mol. Cell. Biol. *1*, 242.

Goffeau, A., Barrell, B., Bussey, H., Davis, R., Dujon, B., Feldmann, H., Galibert, F., Hoheisel, J., Jacq, C. and Johnston, M. (1996). Life with 6000 genes. Science *5287*, 546.

Going, J., Keith, W., Neilson, L., Stoeber, K., Stuart, R. and Williams, G. (2002). Aberrant expression of minichromosome maintenance proteins 2 and 5, and Ki-67 in dysplastic squamous oesophageal epithelium and Barrett's mucosa. Gut *3*, 373.

Goldar, A., Marsolier-Kergoat, M. C. and Hyrien, O. (2009). Universal temporal profile of replication origin activation in eukaryotes. PLoS One *6*, e5899.

Gonzalez, M. A., Tachibana, K. K., Chin, S. F., Callagy, G., Madine, M. A., Vowler, S. L., Pinder, S. E., Laskey, R. A. and Coleman, N. (2004). Geminin predicts adverse clinical outcome in breast cancer by reflecting cell-cycle progression. J. Pathol. *2*, 121-130.

Green, B. M., Morreale, R. J., Ozaydin, B., DeRisi, J. L. and Li, J. J. (2006). Genome-wide mapping of DNA synthesis in Saccharomyces cerevisiae reveals that mechanisms preventing reinitiation of DNA replication are not redundant. Mol. Biol. Cell *5*, 2401.

Greider, C. W. and Blackburn, E. H. (1985). Identification of a specific telomere terminal transferase activity in Tetrahymena extracts. Cell *2*, 405-413.

Hardy, C. F. J., Dryga, O., Seematter, S., Pahl, P. and Sclafani, R. A. (1997). mcm5/cdc46-bob1 bypasses the requirement for the S phase activator Cdc7p. Proceedings of the National Academy of Sciences *7*, 3151.

Hardy, C. and Pautz, A. (1996). A novel role for Cdc5p in DNA replication. Mol. Cell. Biol. *12*, 6775.

Harkins, V., Gabrielse, C., Haste, L. and Weinreich, M. (2009). Budding yeast Dbf4 sequences required for Cdc7 kinase activation and identification of a functional relationship between the Dbf4 and Rev1 BRCT domains. Genetics *4*, 1269.

Harrison, J. C. and Haber, J. E. (2006). Surviving the breakup: the DNA damage checkpoint. Annu. Rev. Genet., 209.

Hartwell, L. H. (1976). Sequential function of gene products relative to DNA synthesis in the yeast cell cycle* 1. J. Mol. Biol. *4*, 803-817.

Hartwell, L. H. (1974). Saccharomyces cerevisiae cell cycle. Microbiology and Molecular Biology Reviews *2*, 164.

Hartwell, L. H., Culotti, J., Pringle, J. R. and Reid, B. J. (1972). Genetic control of the cell division cycle in yeast. Geophys.Res, 5503.

Heller, R. C., Kang, S., Lam, W. M., Chen, S., Chan, C. S. and Bell, S. P. (2011). Eukaryotic Origin-Dependent DNA Replication InáVitro Reveals Sequential Action of DDK and S-CDK Kinases. Cell *1*, 80-91.

Hennessy, K.M., Lee, A., Chen, E., and Botstein, D. (1991). A group of interacting yeast DNA replication genes. Genes and Dev. *5*, 958-969.

Herrick, J., Michalet, X., Conti, C., Schurra, C. and Bensimon, A. (2000). Quantifying single gene copy number by measuring fluorescent probe lengths on combed genomic DNA. Proceedings of the National Academy of Sciences *1*, 222.

Herskowitz, I. (1988). Life cycle of the budding yeast Saccharomyces cerevisiae. Microbiology and Molecular Biology Reviews *4*, 536.

Hess, G. F., Drong, R. F., Weiland, K. L., Slightom, J. L., Sclafani, R. A. and Hollingsworth, R. E. (1998). A human homolog of the yeast CDC7 gene is overexpressed in some tumors and transformed cell lines. Gene *1*, 133-140.

Heun, P., Laroche, T., Shimada, K., Furrer, P. and Gasser, S. M. (2001). Chromosome dynamics in the yeast interphase nucleus. Science *5549*, 2181.

Hoang, M. L., Leon, R. P., Pessoa-Brandao, L., Hunt, S., Raghuraman, M., Fangman, W. L., Brewer, B. J. and Sclafani, R. A. (2007). Structural changes in Mcm5 protein bypass Cdc7-Dbf4 function and reduce replication origin efficiency in Saccharomyces cerevisiae. Mol. Cell. Biol. *21*, 7594.

Ishimi, Y. (1997). A DNA helicase activity is associated with an MCM4, -6, and -7 protein complex. J. Biol. Chem. *272*, 24508.

Jares, P., Luciani, M. G. and Blow, J. J. (2004). A Xenopus Dbf4 homolog is required for Cdc7 chromatin binding and DNA replication. BMC molecular biology *1*, 5.

Johnston, L. H. and Thomas, A. P. (1982). A further two mutants defective in initiation of the S phase in the yeastSaccharomyces cerevisiae. Molecular and General Genetics MGG *3*, 445-448.

Johnston, L. H. and Thomas, A. P. (1982). The isolation of new DNA synthesis mutants in the yeastSaccharomyces cerevisiae. Molecular and General Genetics MGG *3*, 439-444.

Jones, D. R., Prasad, A. A., Chan, P. K. and Duncker, B. P. (2010). The Dbf4 motif C zinc finger promotes DNA replication and mediates resistance to genotoxic stress. Cell Cycle *10*, 2018-2026.

Kamimura, Y., Masumoto, H., Sugino, A. and Araki, H. (1998). Sld2, which interacts with Dpb11 in Saccharomyces cerevisiae, is required for chromosomal DNA replication. Mol. Cell. Biol. *10*, 6102.

Kamimura, Y., Tak, Y. S., Sugino, A. and Araki, H. (2001). Sld3, which interacts with Cdc45 (Sld4), functions for chromosomal DNA replication in Saccharomyces cerevisiae. EMBO J. *8*, 2097-2107.

Kanter, D. M., Bruck, I. and Kaplan, D. L. (2008). Mcm subunits can assemble into two different active unwinding complexes. J. Biol. Chem. *45*, 31172.

Kaplan, D. L., Davey, M. J. and O'Donnell, M. (2003). Mcm4, 6, 7 uses a “pump in ring” mechanism to unwind DNA by steric exclusion and actively translocate along a duplex. J. Biol. Chem. *49*, 49171.

Kelly, T. J. and Brown, G. W. (2000). Regulation of chromosome replication. Annu. Rev. Biochem. *1*, 829-880.

Kim, J., Kakusho, N., Yamada, M., Kanoh, Y., Takemoto, N. and Masai, H. (2007). Cdc7 kinase mediates Claspin phosphorylation in DNA replication checkpoint. Oncogene *24*, 3475-3482.

Kitamura, E., Blow, J. J. and Tanaka, T. U. (2006). Live-cell imaging reveals replication of individual replicons in eukaryotic replication factories. Cell *7*, 1297-1308.

Koc, A. and Merrill, G. F. (2007). Checkpoint deficient rad53-11 yeast cannot accumulate dNTPs in response to DNA damage. Biochem. Biophys. Res. Commun. *2*, 527-530.

Kockova-Kratochvilova, A. (1990). Yeasts and yeast-like organisms. VCH Publishers, New York, NY.

Koonin, E. V. (1993). A common set of conserved motifs in a vast variety of putative nucleic acid-dependent ATPases including MCM proteins involved in the initiation of eukaryotic DNA replication. Nucleic Acids Res. *11*, 2541.

Korkolopoulou, P., Givalos, N., Saetta, A., Goudopoulou, A., Gakiopoulou, H., Thymara, I., Thomas-Tsagli, E. and Patsouris, E. (2005). Minichromosome maintenance proteins 2 and 5 expression in muscle-invasive urothelial cancer: a multivariate survival study including proliferation markers and cell cycle regulators. Hum. Pathol. *8*, 899-907.

Labib, K. (2010). How do Cdc7 and cyclin-dependent kinases trigger the initiation of chromosome replication in eukaryotic cells?. Genes Dev. *12*, 1208.

Landis, G. and Tower, J. (1999). The Drosophila chiffon gene is required for chorion gene amplification, and is related to the yeast Dbf4 regulator of DNA replication and cell cycle. Development *19*, 4281.

Landry, C. R., Townsend, J. P., Hartl, D. L. and Cavalieri, D. (2006). Ecological and evolutionary genomics of Saccharomyces cerevisiae. Mol. Ecol. *3*, 575-591.

Lau, K., Chan, Q., Pang, J., Li, K., Yeung, W., Chung, N., Lui, P., Tam, Y., Li, H. and Zhou, L. (2010). Minichromosome maintenance proteins 2, 3 and 7 in medulloblastoma: overexpression and involvement in regulation of cell migration and invasion. Oncogene *40*, 5475-5489.

Lebedeva, L., Fedorova, S., Trunova, S. and Omelyanchuk, L. (2004). Mitosis: Regulation and organization of cell division. Russian Journal of Genetics *12*, 1313-1330.

Lei, M., Kawasaki, Y., Young, M. R., Kihara, M., Sugino, A. and Tye, B. K. (1997). Mcm2 is a target of regulation by Cdc7–Dbf4 during the initiation of DNA synthesis. Genes Dev. *24*, 3365.

Lengronne, A., Pasero, P., Bensimon, A. and Schwob, E. (2001). Monitoring S phase progression globally and locally using BrdU incorporation in TK yeast strains. Nucleic Acids Res. *7*, 1433.

Lengronne, A. and Schwob, E. (2002). The yeast CDK inhibitor Sic1 prevents genomic instability by promoting replication origin licensing in late G1. Mol. Cell *5*, 1067-1078.

Lew, D. J. and Burke, D. J. (2003). The spindle assembly and spindle position checkpoints. Annu. Rev. Genet. *1*, 251-282.

Li, P. C., Chretien, L., Côté, J., Kelly, T. J. and Forsburg, S. L. (2011). S. pombe replication protein Cdc18 (Cdc6) interacts with Swi6 (HP1) heterochromatin protein: Region specific effects and replication timing in the centromere. Cell Cycle *2*, 323.

Liang, C. and Stillman, B. (1997). Persistent initiation of DNA replication and chromatin-bound MCM proteins during the cell cycle in cdc6 mutants. Genes Dev. *24*, 3375.

Liku, M. E., Nguyen, V. Q., Rosales, A. W., Irie, K. and Li, J. J. (2005). CDK phosphorylation of a novel NLS-NES module distributed between two subunits of the Mcm2-7 complex prevents chromosomal rereplication. Mol. Biol. Cell *10*, 5026.

Longtine, M. S., McKenzie 3rd, A., Demarini, D. J., Shah, N. G., Wach, A., Brachat, A., Philippsen, P. and Pringle, J. R. (1998). Additional modules for versatile and economical PCR-based gene deletion and modification in Saccharomyces cerevisiae. Yeast (Chichester, England) *10*, 953.

Lopes, M., Cotta-Ramusino, C., Pellicioli, A., Liberi, G., Plevani, P., Muzi-Falconi, M., Newlon, C. S. and Foiani, M. (2001). The DNA replication checkpoint response stabilizes stalled replication forks. Nature *6846*, 557-561.

MacNeill, S. A. (2001). DNA replication: partners in the Okazaki two-step. Current Biology *20*, R842-R844.

Maine, G. T., Sinha, P. and Tye, B. K. (1984). Mutants of S. cerevisiae defective in the maintenance of minichromosomes. Genetics *3*, 365.

Majka, J. and Burgers, P. M. J. (2003). Yeast Rad17/Mec3/Ddc1: a sliding clamp for the DNA damage checkpoint. Proceedings of the National Academy of Sciences *5*, 2249.

Masai, H. and Arai, K. (2000). Dbf4 Motifs: Conserved Motifs in Activation Subunits for Cdc7 Kinases Essential for S-Phase* 1. Biochem. Biophys. Res. Commun. *1*, 228-232.

Menichincheri, M., Bargiotti, A., Berthelsen, J., Bertrand, J. A., Bossi, R., Ciavolella, A., Cirla, A., Cristiani, C., Croci, V. and D'Alessio, R. (2008). First Cdc7 Kinase Inhibitors: Pyrrolopyridinones as Potent and Orally Active Antitumor Agents. 2. Lead Discovery†. J. Med. Chem. *2*, 293-307.

Michalet, X., Ekong, R., Fougerousse, F., Rousseaux, S., Schurra, C., Hornigold, N., Slegtenhorst, M., Wolfe, J., Povey, S. and Beckmann, J. S. (1997). Dynamic molecular combing: stretching the whole human genome for high-resolution studies. Science *5331*, 1518.

Moir, D., Stewart, S.E., Osmond, B.C., and Botstein, D. (1982). Cold-sensitive cell-division-cycle mutants of yeast: isolation, properties, and pseudoreversion studies. Genetics *100*, 547-563.

Montagnoli, A., Tenca, P., Sola, F., Carpani, D., Brotherton, D., Albanese, C. and Santocanale, C. (2004). Cdc7 inhibition reveals a p53-dependent replication checkpoint that is defective in cancer cells. Cancer Res. *19*, 7110.

Mortimer, R. K. and Johnston, J. R. (1986). Genealogy of principal strains of the yeast genetic stock center. Genetics *1*, 35.

Muramatsu, S., Hirai, K., Tak, Y. S., Kamimura, Y. and Araki, H. (2010). CDK-dependent complex formation between replication proteins Dpb11, Sld2, Pol ε, and GINS in budding yeast. Genes Dev. *6*, 602.

Murphy, N., Ring, M., Heffron, C., King, B., Killalea, A., Hughes, C., Martin, C., McGuinness, E., Sheils, O. and O'Leary, J. (2005). p16INK4A, CDC6, and MCM5: predictive biomarkers in cervical preinvasive neoplasia and cervical cancer. J. Clin. Pathol. *5*, 525.

Nasmyth, K. (1996). Viewpoint: putting the cell cycle in order. Science *5293*, 1643.

Nguyen, V. Q. (2001). Cyclin-dependent kinases prevent DNA re-replication through multiple mechanisms. Nature *6841*, 1068-1073.

Nguyen, V. Q., Co, C. and Li, J. J. (2001). Cyclin-dependent kinases prevent DNA re-replication through multiple mechanisms. Nature, 1068-1073.

Nieduszynski, C. A., Knox, Y. and Donaldson, A. D. (2006). Genome-wide identification of replication origins in yeast by comparative genomics. Genes Dev. *14*, 1874.

Nougarede, R., Della Seta, F., Zarzov, P. and Schwob, E. (2000). Hierarchy of S-phase-promoting factors: yeast Dbf4-Cdc7 kinase requires prior S-phase cyclin-dependent kinase activation. Mol. Cell. Biol. *11*, 3795.

Nurse, P. (1997). Regulation of the eukaryotic cell cycle. Eur. J. Cancer *7*, 1002-1004.

Ostergaard, S., Olsson, L. and Nielsen, J. (2000). Metabolic engineering of Saccharomyces cerevisiae. Microbiology and Molecular Biology Reviews *1*, 34.

Pasero, P., Braguglia, D. and Gasser, S. M. (1997). ORC-dependent and origin-specific initiation of DNA replication at defined foci in isolated yeast nuclei. Genes Dev. *12*, 1504.

Pasero, P., Duncker, B. P., Schwob, E. and Gasser, S. M. (1999). A role for the Cdc7 kinase regulatory subunit Dbf4p in the formation of initiation-competent origins of replication. Genes Dev. *16*, 2159.

Pasero, P. and Schwob, E. (2000). Think global, act local--how to regulate S phase from individual replication origins. Curr. Opin. Genet. Dev. *2*, 178-186.

Pasero, P., Shimada, K. and Duncker, B. P. (2003). Multiple roles of replication forks in S phase checkpoints: sensors, effectors and targets. Cell. Cycle *6*, 568-572.

Pesin, J. A. and Orr-Weaver, T. L. (2008). Regulation of APC/C activators in mitosis and meiosis. Annu. Rev. Cell Dev. Biol., 475-499.

Raghuraman, M., Winzeler, E. A., Collingwood, D., Hunt, S., Wodicka, L., Conway, A., Lockhart, D. J., Davis, R. W., Brewer, B. J. and Fangman, W. L. (2001). Replication dynamics of the yeast genome. Science *5540*, 115.

Randell, J. C. W., Bowers, J. L., Rodríguez, H. K. and Bell, S. P. (2006). Sequential ATP hydrolysis by Cdc6 and ORC directs loading of the Mcm2-7 helicase. Mol. Cell *1*, 29-39.

Randell, J. C. W., Fan, A., Chan, C., Francis, L. I., Heller, R. C., Galani, K. and Bell, S. P. (2010). Mec1 is one of multiple kinases that prime the Mcm2-7 helicase for phosphorylation by Cdc7. Mol. Cell *3*, 353-363.

Remus, D., Beuron, F., Tolun, G., Griffith, J. D., Morris, E. P. and Diffley, J. F. X. (2009). Concerted loading of Mcm2-7 double hexamers around DNA during DNA replication origin licensing. Cell *4*, 719-730.

Rose, A.H. and Harrison, J.S. (1991) (eds). The Yeasts. 2nd ed. Vol.4: Yeast Cytology. Academic Press, London.

Sancar, A., Lindsey-Boltz, L. A., Ünsal-Kaçmaz, K. and Linn, S. (2004). Molecular mechanisms of mammalian DNA repair and the DNA damage checkpoints. Annu. Rev. Biochem. *1*, 39-85.

Santocanale, C. and Diffley, J. F. (1998). A Mec1- and Rad53-dependent checkpoint controls late-firing origins of DNA replication. Nature *6702*, 615-618.

Sato, M., Gotow, T., You, Z., Komamura-Kohno, Y., Uchiyama, Y., Yabuta, N., Nojima, H. and Ishimi, Y. (2000). Electron microscopic observation and single-stranded DNA binding activity of the Mcm4, 6, 7 complex 1. J. Mol. Biol. *3*, 421-431.

Schübeler, D., MacAlpine, D. M., Scalzo, D., Wirbelauer, C., Kooperberg, C., Van Leeuwen, F., Gottschling, D. E., O'Neill, L. P., Turner, B. M. and Delrow, J. (2004). The histone modification pattern of active genes revealed through genome-wide chromatin analysis of a higher eukaryote. Genes Dev. *11*, 1263.

Schwacha, A. and Bell, S. P. (2001). Interactions between two catalytically distinct MCM subgroups are essential for coordinated ATP hydrolysis and DNA replication. Mol. Cell *5*, 1093-1104.

Sclafani, R. A. (2000). Cdc7p-Dbf4p becomes famous in the cell cycle. J. Cell. Sci. *12*, 2111.

Sclafani, R. and Holzen, T. (2007). Cell cycle regulation of DNA replication. Annu. Rev. Genet., 237.

Semple, J. W., Da-Silva, L. F., Jervis, E. J., Ah-Kee, J., Al-Attar, H., Kummer, L., Heikkila, J. J., Pasero, P. and Duncker, B. P. (2006). An essential role for Orc6 in DNA replication through maintenance of pre-replicative complexes. EMBO J. *21*, 5150-5158.

Semple, J. W. and Duncker, B. P. (2004). ORC-associated replication factors as biomarkers for cancer. Biotechnol. Adv. *8*, 621-631.

SGD project. "Saccharomycese genome database" http://www.yeastgenome.org. (October 25th, 2011)

Shaner, N. C., Steinbach, P. A. and Tsien, R. Y. (2005). A guide to choosing fluorescent proteins. Nature Methods *12*, 905.

Sherman, F. (2002). Getting started with yeast. Methods Enzymol. *350*, 3-41.

Sheu, Y. J. and Stillman, B. (2010). The Dbf4–Cdc7 kinase promotes S phase by alleviating an inhibitory activity in Mcm4. Nature *7277*, 113-117.

Sheu, Y. J. and Stillman, B. (2006). Cdc7-Dbf4 phosphorylates MCM proteins via a docking site-mediated mechanism to promote S phase progression. Mol. Cell *1*, 101-113.

Shima, N., Alcaraz, A., Liachko, I., Buske, T. R., Andrews, C. A., Munroe, R. J., Hartford, S. A., Tye, B. K. and Schimenti, J. C. (2006). A viable allele of Mcm4 causes chromosome instability and mammary adenocarcinomas in mice. Nat. Genet. *1*, 93-98.

Shirahige, K., Hori, Y., Shiraishi, K., Yamashita, M., Takahashi, K., Obuse, C., Tsurimoto, T. and Yoshikawa, H. (1998). Regulation of DNA-replication origins during cell-cycle progression. Nature *6702*, 618-621.

Snaith, H. A., Brown, G. W. and Forsburg, S. L. (2000). Schizosaccharomyces pombe Hsk1p is a potential Cds1p target required for genome integrity. Mol. Cell. Biol. *21*, 7922.

Sogo, J. M., Lopes, M. and Foiani, M. (2002). Fork reversal and ssDNA accumulation at stalled replication forks owing to checkpoint defects. Science *5581*, 599.

Speck, C. and Stillman, B. (2007). Cdc6 ATPase activity regulates ORC· Cdc6 stability and the selection of specific DNA sequences as origins of DNA replication. J. Biol. Chem. *16*, 11705.

Stead, B. E., Brandl, C. J. and Davey, M. J. (2011). Phosphorylation of Mcm2 modulates Mcm2–7 activity and affects the cell's response to DNA damage. Nucleic Acids Res.

Stead, B. E., Sorbara, C. D., Brandl, C. J. and Davey, M. J. (2009). ATP binding and hydrolysis by Mcm2 regulate DNA binding by Mcm complexes. J. Mol. Biol. *2*, 301-313.

Sweeney, F. D., Yang, F., Chi, A., Shabanowitz, J., Hunt, D. F. and Durocher, D. (2005). Saccharomyces cerevisiae Rad9 acts as a Mec1 adaptor to allow Rad53 activation. Current biology *15*, 1364-1375.

Swords, R., Mahalingam, D., O'Dwyer, M., Santocanale, C., Kelly, K., Carew, J. and Giles, F. (2010). Cdc7 kinase-A new target for drug development. Eur. J. Cancer *1*, 33-40.

Tak, Y. S., Tanaka, Y., Endo, S., Kamimura, Y. and Araki, H. (2006). A CDK-catalysed regulatory phosphorylation for formation of the DNA replication complex Sld2–Dpb11. EMBO J. *9*, 1987-1996.

Takahashi, T.S., Wigley, D.B., and Walter, J.C. (2005). Pumps, paradoxes and plowshares: mechanism of the MCM2-7 DNA helicase. Trends Biochem. Sci. *30*, 437-444

Takahashi, K., Yamada, H., and Yanagida, M. (1994). Fission yeast minichromosome loss mutants mis cause lethal aneuploidy and replication abnormality. Mol. Biol. Cell. *5*, 1145-1158.

Tanaka, S. and Diffley, J. F. X. (2002). Interdependent nuclear accumulation of budding yeast Cdt1 and Mcm2-7 during G1 phase. Nat. Cell Biol. *3*, 198-207.

Tanaka, T. Chromatin immunoprecipitation in budding yeast.

Tanaka, S., Umemori, T., Hirai, K., Muramatsu, S., Kamimura, Y. and Araki, H. (2007). CDK-dependent phosphorylation of Sld2 and Sld3 initiates DNA replication in budding yeast. Nature *7125*, 328-332.

Tenca, P., Brotherton, D., Montagnoli, A., Rainoldi, S., Albanese, C. and Santocanale, C. (2007). Cdc7 is an active kinase in human cancer cells undergoing replication stress. J. Biol. Chem. *1*, 208.

Tercero, J. A., Longhese, M. P. and Diffley, J. F. X. (2003). A central role for DNA replication forks in checkpoint activation and response. Mol. Cell *5*, 1323-1336.

Toh, G. W. and Lowndes, N. F. (2003). Role of the Saccharomyces cerevisiae Rad9 protein in sensing and responding to DNA damage. Biochem. Soc. Trans. *Pt 1*, 242-246.

Tsuji, T., Lau, E., Chiang, G. G. and Jiang, W. (2008). The role of Dbf4/Drf1-dependent kinase Cdc7 in DNA-damage checkpoint control. Mol. Cell *6*, 862-869.

Varrin, A. E., Prasad, A. A., Scholz, R. P., Ramer, M. D. and Duncker, B. P. (2005). A mutation in Dbf4 motif M impairs interactions with DNA replication factors and confers increased resistance to genotoxic agents. Mol. Cell. Biol. *17*, 7494.

Versini, G., Comet, I., Wu, M., Hoopes, L., Schwob, E. and Pasero, P. (2003). The yeast Sgs1 helicase is differentially required for genomic and ribosomal DNA replication. EMBO J. *8*, 1939-1949.

Walker, G.M. (1998). Yeast physiology and biotechnology. Wiley Press, New York, NY.

Weinert, T. A., Kiser, G. L. and Hartwell, L. (1994). Mitotic checkpoint genes in budding yeast and the dependence of mitosis on DNA replication and repair. Genes Dev. *6*, 652.

Weinreich, M. and Stillman, B. (1999). Cdc7p–Dbf4p kinase binds to chromatin during S phase and is regulated by both the APC and the RAD53 checkpoint pathway. EMBO J. *19*, 5334-5346.

Winey, M. and O'Toole, E. T. (2001). The spindle cycle in budding yeast. Nat. Cell Biol., E23-E27.

Woodward, A. M., Göhler, T., Luciani, M. G., Oehlmann, M., Ge, X., Gartner, A., Jackson, D. A. and Blow, J. J. (2006). Excess Mcm2–7 license dormant origins of replication that can be used under conditions of replicative stress. J. Cell Biol. *5*, 673.

Xu, W., Aparicio, J., Aparicio, O. and Tavaré, S. (2006). Genome-wide mapping of ORC and Mcm2p binding sites on tiling arrays and identification of essential ARS consensus sequences in S. cerevisiae. BMC Genomics *1*, 276.

Xu, X., Vaithiyalingam, S., Glick, G. G., Mordes, D. A., Chazin, W. J. and Cortez, D. (2008). The basic cleft of RPA70N binds multiple checkpoint proteins, including RAD9, to regulate ATR signaling. Mol. Cell. Biol. *24*, 7345.

Ying, C. Y. and Gautier, J. (2005). The ATPase activity of MCM2–7 is dispensable for pre-RC assembly but is required for DNA unwinding. EMBO J. *24*, 4334-4344.

Zegerman, P. and Diffley, J. F. X. (2010). Checkpoint-dependent inhibition of DNA replication initiation by Sld3 and Dbf4 phosphorylation. Nature *7314*, 474-478.

Zegerman, P. and Diffley, J. F. X. (2006). Phosphorylation of Sld2 and Sld3 by cyclin-dependent kinases promotes DNA replication in budding yeast. Nature *7125*, 281-285.

Zhao, X., Chabes, A., Domkin, V., Thelander, L. and Rothstein, R. (2001). The ribonucleotide reductase inhibitor Sml1 is a new target of the Mec1/Rad53 kinase cascade during growth and in response to DNA damage. EMBO J. *13*, 3544-3553.

Zou, L. and Stillman, B. (2000). Assembly of a complex containing Cdc45p, replication protein A, and Mcm2p at replication origins controlled by S-phase cyclin-dependent kinases and Cdc7p-Dbf4p kinase. Mol. Cell. Biol. *9*, 3086.